PhD program in Chemical Process Engineering

Liquid-Liquid Membrane Contactors for Sustainable Ammonia recovery and Valorization: Experimental Insights, novel approaches and Applications.

Doctoral thesis by:

Miguel Aguilar i Moreno

Thesis Advisors:

Jose Luís Cortina Pallás

César Alberto Valderrama

KEYWORDS

Ammonia recovery; Wastewater treatment; Membrane contactors; Coagulation-flocculation; Aeration; Aluminum sulphate; Liquid-liquid membrane contactors (LLMC); Sustainable technology; Hollow fiber membrane contactors; Circular economy

AKNOWLEDGEMENTS

This study was conducted at Universitat Politècnica de Catalunya (UPC), Barcelona. The research received support from the R2MIT project (CTM2017-85346-R) funded by the Spanish Ministry of Economy and Competitiveness (MINECO) and the Govern de Catalunya (ref. 2017-SGR-312). I would like to express my sincere gratitude to all the institutions involved for providing me with the opportunity to carry out this doctoral thesis. Their support has been essential in the development of this research work.

I would like to express my sincere gratitude for the continuous support and dedication I have received over these four years from Elena Guillén Burrieza, Mònica Reig, and my thesis advisors, José Luis Cortina and Cesar Valderrama. Their commitment, guidance, and expertise have been fundamental pillars in my academic journey. I am deeply thankful for the opportunity to benefit from their mentorship, which has been invaluable to the development and completion of this research project.

Furthermore, I want to extend my gratitude to my fellow doctoral collegues who shared this academic journey with me. Their ideas, discussions, and camaraderie have enriched my experience and created an environment conducive to mutual learning.

En últim lloc, voldria agrair a la meva família tot l'esforç i dedicació que m'han lliurat durant aquests anys, als meus amics de tota la vida que m'han fet costat i acompanyat quan ho necessitava, i sobretot agraïr i possar de manifest la paciencia i ajuda de la Gisela que m'ha donat tot el suport tant a les dures com a les madures, t'estimo, a tots vosaltres moltes gràcies.

ABSTRACT

This comprehensive research wants to represent a significant stride in the exploration of innovative strategies aimed to enhance ammonia recovery within diverse wastewater streams. The study is structured into distinct phases, each addressing crucial aspects of the ammonia recovery process.

In the initial phase, the research focuses on augmenting membrane contactor performance, employing coagulation-flocculation (C/F) and aeration as preliminary treatments. The outcomes of this phase demonstrate substantial increases in both the mass transfer coefficient and overall efficiency of ammonia recovery, increasing of 7.80×10^{-7} to 1.04×10^{-5} $m \cdot s^{-1}$ and from 8 to 67%, respectively, particularly notable when treating the sidestream centrate. A pivotal finding underscores the efficacy of dosing aluminum sulfate ($Al_2(SO_4)_3$) at 30 mg $Al^{+} \cdot L^{-1}$ in the C/F process, yielding remarkable efficiencies (>50%) in the removal of chemical oxygen demand (COD), turbidity, and total suspended solids (TSS).

Into the second phase, the study delves into the application of liquid-liquid membrane contactors (LLMC) for ammonia recovery. An array of experimental conditions is meticulously explored, with the results illuminating the considerable impact of replacing the acid washing liquid between steps on the overall performance of the LLMC. Additionally, the study highlights the nuanced relationship between the initial ammonia concentration and the subsequent recovery, providing valuable insights. This phase effectively showcases the potential versatility and efficiency of LLMCs in the valorization of ammonia within wastewater streams.

The third and final phase introduces a novel asymmetric hollow fiber liquid-liquid membrane contactor (HF-LLMC) with distinctive selectivity for ammonia over water P_{NH3} = 87 - 180 L m^{-2} h^{-1} bar^{-1} and P_w = 1.2 -1.4·10^{-3} L m^{-2} h^{-1} bar^{-1} at NTP conditions. The investigation entails a comprehensive examination of various operational parameters, including feed and acid flow rates, mass transfer coefficients, and acid consumption. Notably, the results affirm the high selectivity of the HF-LLMC for ammonia, coupled with minimal water transfer. This establishes the HF-LLMC as a promising technology for the recovery and concentration of ammonium in diluted urban and industrial streams.

The combination of these findings, considered from a global perspective, significantly contributes not only to the advancement of sustainable nutrient recovery technologies but

also underscores their pragmatic feasibility for implementation within the context of the circular economy and efficient resource management.

LIST OF CONTENTS

List of Figures

CHAPTER 1

CHAPTER 2

CHAPTER 3

Figure 4. Removal of COD (%) and turbidity (%) from anaerobic centrate after $Fe_3O_4(s)/SiO_2(s)$ addition.

Figure 5. Variation of pH and the efficiency of HCO_3^- removal with time in the aeration stage.

Figure 6. Membrane contactor results during operation: (A) TAN concentration evolution in the feed tank for pre-treated and untreated centrate, (B) TAN recovery and pH variation and (C) TAN concentration evolution and concentration factor in the acid tank.

Figure 7. Gross cost, revenues and net present value for the nitrogen recovery scenario under study.

Figure 8. Gross cost contribution of the nitrogen recovery scenario under study for: (A) the different processes and (B) for the different capital and operating costs.

Figure 9. Sensitivity analysis for a ±30% variation of the main economic parameters**.**

Figure 10. Sensitivity analysis for the NH_4NO_3 prices and mass transfer coefficient (K_m).

CHAPTER 4

Figure 1. Ammonia concentration evolution over time in the feed tank when changing (**a**) the acid and (**b**) feed between steps (up). Nitrogen concentration achieved in the liquid fertilizer by changing the (**c**) acid or (**d**) feed solution between steps (down). Orange color implies one stage of LLMC (triangle for the feed side and circle referring to the fertilizer solution), while yellow color refers to experiments with two LLMC stages (triangle for the feed side and circle referring to the fertilizer solution).

Figure 2. Ammonia recovery after each step, and the global results changing the acid or the feed solution between steps.

Figure 3. Comparison between working with the sidestream (high NH_3 concentration) and mainstream wastewater (low NH_3 concentration): (**a**) ammonia concentration evolution in the feed tank, (**b**) ammonia recovery, (**c**) concentration factor and (**d**) %N-NH_4 concentration in the liquid fertilizer. High ammonia concentration is indicated by the color orange, while the color yellow implies working at low ammonia concentrations.

Figure 4. Temperature results comparison: (**a**) ammonia recovery and (**b**) concentration factor.

CHAPTER 5

Figure 1. The asymmetric membrane structure of the Separel® EF-010-Q-60 module adapted from (DIC Corporation, 2016; DiC, n.d.).

Figure 2. Left, Separel® MC module details on the locations of different in-let and out-let streams. Right, LLMC Experimental set-up used for the ammonia transfer reactions.

Figure 3. NH_3 concentration (mol L^{-1}) in the feed tank (shell) and percentage of ammonia recovery in the feed tank; (A) Experiment 30-250; (B) Experiment 100-250; (C) Experiment 500-180; (D) Experiment 100-50 (E) Experiment 180-500-A; (F) Experiment 180-500-B**.** Points: experimental data; Lines: model simulation. The bars indicate the absolute errors of the IC measurements. It is observed that the model is in good agreement with the experimental results.

Figure 4. NH_4^+ and SO_4^{2-} concentration (**mol L^{-1}**) in the acid stripping tank (lumen***;*** (A) Experiment 30-250; (B) Experiment 100-250; (C) Experiment 500-180; (D) Experiment 100-50 (E) Experiment 180-500-A; (F) Experiment 180-500-B**.** Points: experimental data; Lines: model simulation. The bars indicate the absolute errors associated with the NH_4^+ and SO_4^{2-} IC measurements. It is observed that the model is in good agreement with the experimental results in all the experiments with the exception of the SO_4^{2-} of experiment 100-250 (4.B**).**

Figure 5. Ammonia recovery (%) as a function of time for experiments 30-250, 100-250, 500-180 and 100-50. Points: experimental data; Lines: model simulation.

Figure 6. Experimental data of the evolution of pH in the feed tank; (A) Experiment 30-250; (B) Experiment 100-250; (C) Experiment 500-180; (D) Experiment 100-50.

Figure 7. Dissociation of the sulfuric acid and corresponding sulphate (SO_4^{2-}) bisulphate (HSO_4^-) molar fractions as a function of pH simulated with the Hydra/Medusa speciation software (Puigdomenech, 2001).

Figure 8. Results of experiments 30-250; 100-250; 500-180 and 100-50: A) ammonia flux over time. Experimental results (dots) and simulated results (lines). B) Simulated water flux over time.

Figure 9. Membrane permeabilities for ammonia (P_{NH3}) and water (P_w), modelled mathematically at NTP conditions (i.e., 1 bar and 25 °C temperature) for each experiment.

Figure 10. Comparison between experiments 500-180, 180-500-A and 180-500-B in terms of A) ammonia % removal and B) theoretical ammonia (J_{NH3}) and water (J_w) fluxes. Points: experimental data; Lines: model simulation.

Figure 11. Representation of the natural logarithm $\ln(c_{NH3,0}/c_{NH3,t})$ versus the time (t) a linear relationship is found which slope is $\frac{k_{ov} \cdot A_m}{V}$ and from which k_{ov} is calculated**.** Points: experimental data; lines: linear fit to eq. 1.

Figure 12. Maximum J_{NH3} (at time = 0h in graphs 12A and 12B) and normalized by the initial ammonia feed concentration in g L^{-1} versus k_{ov} and U_{NH3} calculated for all the experiments.

LIST OF TABLES

Table 3. Results of the study of the feed volume effect.

CHAPTER 5

Table 1. Main characteristics of the Separel® EF-010-Q-60 module. Information provided by Separel, DIC Corporation, Japan (DIC Corporation, 2016; DiC, n.d.)

Table 2. Operational parameters of the experimental design.

Table 3. Root mean squared error (RMSE) and coefficient of determination (R^2) of the mathematical model for the NH_4 permeate concentrations of each experiment.

Table 4. Chemical equilibrium reactions that take place in the acidic stripping solution.

Table 5. Membrane permeabilities to water (P_w) and ammonia (P_{NH3}) calculated via the mathematical model for experiments 500-180, 180-500-A and 180-500-B.

Table 6. Experimentally calculated k_{ov} values referred to the internal membrane area (Table 1) and modelled U_{NH_3}, $k_{NH3,f}$, $k_{NH3,m}$ and $k_{NH3,a}$ values for each experiment.

GLOSSARY

ABC - Ammonium Bicarbonate

AD - Anaerobic Digestion

ANOVA - Analysis of Variance

AS - Ammonium Sulphate

BNR - Biological Nitrogen Removal

CANON - Completely Autotrophic Nitrogen Removal Over Nitrite

CF - Concentration Factor

COD - Chemical Oxygen Demand

DAP/MAP - Di-Ammonium Phosphate/MonoAmmonium Phosphate

FAO - Food and Agriculture Organization of the United Nations

FO - Forward Osmosis

HF-LLMC - Hollow Fiber Liquid-Liquid Membrane Contactor

ICS - Ion Chromatography System

IX - Ion Exchange

K_m - Ammonia Mass Transfer Coefficient

LLMC - Liquid-Liquid Membrane Contactor

MC - Membrane Contactor

MD - Membrane Distillation

Mt – Million of Tonnes

MFC - Microbial Fuel Cells

MEC - Microbial Electrolysis Cells

NFK - Nanofiltration

NPV - Net Present Value

NTU - Nephelometric Turbidity Units

PAX - Poly-Aluminum Chloride

PE - Polyethylene

PP - Polypropylene

PFA - Poly(tetrafluoroethylene-co-perfluorovinyl ether)

PMP - Polytetramethylpentene

PPM - Parts Per Million

PVDF - Polyvinylidene Fluoride

Re - Reynolds Number

RO - Reverse Osmosis

RSME - Root Mean Squared Error

Sc - Schmidt Number

TOC - Total Organic Carbon

TSS - Total Suspended Solids

UF - Ultrafiltration

USD - United States Dollar

WRRF - Water Resource Recovery Facility

WWTP - Wastewater Treatment Plant

CHAPTER 1

Introduction

1.1. The Global Impact of Nitrogen Fertilizers: Haber-Bosch process

One of the most important challenges that developed societies face nowadays is to transform the economy to a efficient economic model with more restricted and selective access to the necessary natural resources aiming to avoid resource shortage and other related issues, and at the same time increasing competitiveness without generating externalities in the supply chain. In this context moving from linear thinking (cradle to grave) to a circular model by closing the material loops is a primary objective (Suzanne et al., 2020). Throughout urban and industrial cycles, waste process is considered potentially as secondary resources, especially when they contain elements included in the list of critical raw materials (European Commission, 2023). In the urban water cycle, wastewater has been identified as having great potential through different components: i) carbon present in organic matter in wastewater streams to transform wastewater treatment plants (WWTP) in energy self-sufficient (energy positive WWTP's), the carbon present in these wastewater streams serves as a food source for the microorganisms found in wastewater treatment plants. Through biological processes, these microorganisms break down the carbon-rich organic matter, producing biogas as a byproduct, ii) nitrogen and phosphorus for fertilizers production and/or direct soil applications, and iii) water to be recover using reuse schemes for industrial, agricultural, and environmental applications.

The role of nutrients, such as P or N, significantly influences the intensive farming industry, where fertilizers are extensively used, leading to a substantial demand for this type of fertilizer (Robles et al., 2020). Fertilizers are categorized into two groups: single-nutrient fertilizers and multi-nutrient fertilizers. The former consists of one essential nutrient, while the latter combines two or more essential nutrients (K, P, and N) (Vecino et al., 2019). Specifically, focusing on Nitrogen (N), the global reactive nitrogen cycle has doubled over the last century due largely to population growth. Ammonia is the second most produced chemical in the world (Beckinghausen et al., 2020; Lee et al., 2021; Razon, 2018).

Ammonia production plants, typically utilizing the Haber-Bosch process (Eq. 1) for the synthesis of industrial ammonia, play a pivotal role in fertilizer generation (Kirova-Yordanova, 2004). This method incurs an energy consumption of approximately 35-50 MJ/kg N. Producing one ton of N-fertilizer requires almost 1000 m^3 (NTP) of natural gas. Due to the high resource and energy costs, there is a growing exploration of alternative sources for ammonia (Beckinghausen et al., 2020). Globally, approximately 85% of ammonia production is allocated to fertilizers, with the remaining 15% used in various industrial applications, such as plastics and fibers, underscoring agriculture's predominant role in ammonia usage (Vecino et al., 2019).

$$N_{2(g)} + 3H_{2(g)} \rightarrow 2NH_{3(g)} \qquad (1)$$

In general terms, more than 100 million tons of fertilizer are generated throughout the globe from the Haber-Bosch process, out of a total of approximately 160 million tons of ammonia. Asia is the region where the largest ammount of ammonia is produced by the Haber-Bosch method, accounting for about 50% (80 Mt) of total production (González Montiel, 2008), which entails the consumption of 1-2% of all the worldwide energy annually. It is estimated that 50% of the natural gas used in the industry corresponds to the production of fertilizer with the Haber-Bosch method (Smith et al., 2020). In addition, the amount of CO_2(g) emitted when when natural gas is used as the primary source for NH_3 generation, is estimated to be 1.6 t of CO_2 /t NH_3, reaching 3.2t CO_2(g)/t NH_3 if the raw material is coal (Osorio-Tejada et al., 2022; Yüzbasıoglu et al., 2021). The direct emissions from ammonia production currently amount to 450 million tons of CO_2 (IEA 2021) about 1.8% of global carbon dioxide emissions (Bird et al., 2020). Additionally, the market predictions for fertilizers indicate a significant growth, with a Compound Annual Growth Rate (CAGR) of approximately 9.1% from 2023 to 2030 (Company et al., 2023). During this period, it is expected that NPK fertilizers will lead the market, occupying the largest share.

A breakdown of the nitrogen fertilizer supply, demand and balance worldwide is listed in Table 1. (FAO, 2019). In addition, in Table 2 is collected the nitrogen consumption by region (Yara International, 2022).

Table 1. World nitrogen supply (in milions of tonnes), demand and balance 2016-2022 (FAO, 2019).

	2016	2017	2018	2019	2020	2021	2022
			World				
Ammonia-capacity	180	184	187	189	187	189	190
Ammonia-supply capability	153	155	157	161	160	161	163
Nitrogen-other uses	36	37	38	39	39	40	40
Nitrogen-avalible for fertilizers	116	117	119	120	119	121	122
Nitrogen-fertilizer demand	105	105	180	107	108	110	111
Nitrogen-potential balance	11	12	13	15	12	11	11

Table 2. Nitrogen use by region (% en each region) (Yara International, 2022).

Fertilizer	% of nitrogen-based fertilizers used				
	USA	Brazil	West/Central Europe	India	China
Urea	24	57	20	79	34
Ammonia	27	-	-	-	-
Nitrates	2	13	41	-	-
UAN	26	-	12	-	-
NPK	6	1	12	3	54
DAP/MAP	6	13	4	11	7
Other	12	4	11	1	6
As	-	12	-	-	-
ABC	-	-	-	-	-
Total year 2020 (milion tonnes)	12.1	5.3	11.1	23.7	20.4

UAN: Urea Ammonium Nitrate, NPK: Nitrogen, Phosphorus, Potassium fertilizer, DAP/MAP: Di-Ammonium Phosphate/MonoAmmonium Phosphate, AS: Ammonium Sulfate, ABC: Ammonium BiCarbonate.

The most widespread fertilizer used is urea, but the other varieties of fertilizer vary according to the requirements of each region as it is clearly shown in Table 2. This emphasizes the importance of considering the target market of the product when defining recovery strategies. According to Beckinghausen et al. 2020, a potential solution would be the most appropriate as it would encourage a relationship between farmers and the WWTPs if N and P recovery options need to be implemented (Beckinghausen et al., 2020).

A critical review by Razon (Razon, 2018) delves into the reactive nitrogen cycle, encompassing its generation, emission into the environment, and its integral connection to food security, environmental degradation, climate change, and alternative energy, as illustrated in Figure 1.

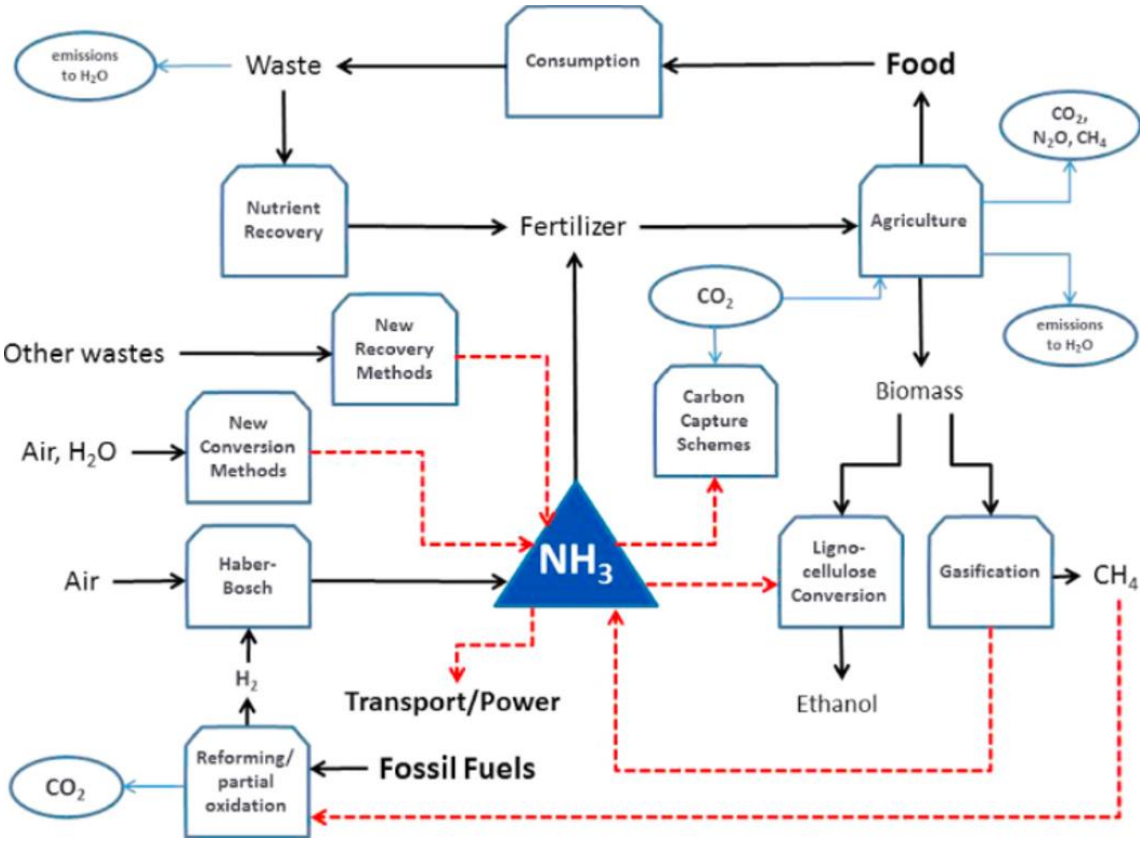

Figure 1. The relationship of ammonia to agriculture, energy and environmental emissions. Solid lines show existing relationships. Dashed lines show the possible future relationships. Only environmentally significant emissions are shown (Razon, 2018).

Figure 1 shows that the global food supply depends on anthropogenic nitrogen fertilizer and that its production and overuse has contributed to the deterioration of the environment through the different options identified in the N-cycle. It is being promoted from different regulatory bodies that biofuel production and carbon capture schemes may also increase demand for reactive nitrogen. In addition, ammonia is being proposed as an alternative fuel and new technologies to replace the Haber–Bosch process must be developed. (Kehrein et al., 2020).

Although the exact magnitude of future requirements is uncertain, a large demand for reactive nitrogen may be inevitable and recovery from waste must be pursued. This

recovery of reactive nitrogen from waste streams is imperfect because natural processes tend to return reactive nitrogen to the more stable state $N_2(g)$ and then in practice is lost. In this perspective, a change of paradigm on the waste water treatment cycles should be implemented: from N removal as $N_2(g)$ to N recovery. (Galloway et al., 2008; Geissdoerfer et al., 2017).

1.2. From nitrogen removal to nitrogen recovery in wastewater effluents

1.2.1. Conventional Nitrogen removal in WWTP's

Wastewater streams serve as significant sources of N, with raw urban wastewater containing nearly 60 to 80% of total nitrogen in the form of ammoniacal nitrogen. In industrial wastewater, the NH_3 content varies depending on the industry and specific processes, ranging approximately from 0.005 to 5 $g \cdot L^{-1}$. Urban wastewater streams, on the other hand, typically exhibits NH_3 concentrations around 0.01 to 1.20 $g \cdot L^{-1}$ depending on the WWTP configuration (Sheikh et al., 2023).

It is noteworthy that WWTPs are designed to mitigate NH_3 levels in waterways, primarily due to stringent total ammonia nitrogen content (TAN) discharge limits imposed to the discharge to environmental compartments. The main-stream and side-stream components have been identified as the major sources contributing to elevated NH_3 concentrations in WWTPs. (Azreen et al., 2017; Fowler et al., 2013; Salomon et al., 2016).

A prevalent technic employed for the mitigation of nitrogen in urban WWTP, where it predominantly exists in the form of ammoniacal nitrogen, in both inorganic and organic forms, is the Biological Nitrogen Removal (BNR) process (Ren et al., 2020). This involves the application of nitrification/denitrification techniques, including autotrophic oxygen-limited nitrification-denitrification, aerobic nitrification-denitrification using Bacillus, and decontamination techniques such as Anaerobic Ammonium Oxidation (anammox), Completely Autotrophic Nitrogen Removal Over Nitrite (CANON), as well as combinations like anammox and denitrification or bacterial consortiums involving algae and nitrification.

Nitrification involves the conversion of ammonium to nitrite and then to nitrate, while denitrification is the reduction of nitrate to gaseous nitrogen. The autotrophic process

refers to the ability of certain microorganisms to obtain energy from inorganic sources, such as ammonium or nitrite. Anaerobic Ammonium Oxidation (anammox) is a process where specific bacteria oxidize ammonium directly with nitrite, without the need for oxygen. CANON involves the autotrophic conversion of ammonium to nitrate over nitrite. (Mukarunyana et al., 2018; Thakur & Medhi, 2019; Yue et al., 2023).

A simplified urban WWTP is depicted in Figure 2. In the primary settling stage, which is part of the primary treatment in a WWTP, sedimentable solids from the mainstream are reduced. Subsequently, the mainstream moves to the biological treatment, where aerobic nitrogen removal takes place, following the stages previously described depending on the plant configuration. The most conventional process of carbon removal using conventional areared sludge (CAS) involves constant aeration to supply the necessary oxygen. During the biological stage, activated sludge (microbial biomass) is generated and then separated in the secondary settling. Advanced WWTPs where more restringing discharges of N are requested, biological removal processes need to be included.

In this phase, both the sludge from the primary settling and the secondary settling are treated in the absence of oxygen to produce biogas. The resulting liquid from this process, known as digestate, and the reject water from digestate is the remaining liquid phase after dehydrating anaerobically digested sludge, either through centrifugation or dewatering, are key aspects in the management of wastewater treatment. (Faragò et al., 2021; Fernández, 2008; Ma et al., 2020). If the WWTP does not have an AD stage, the centrate is the water from the solid-liquid separation. Thirty percent of the nitrogen load in the treatments can be provided by centrate water. (Beckinghausen et al., 2020; C. H. Guo et al., 2010). The streams resulting from these stages are known as side-streams to differentiate them from the mainstream. The properties of these types of streams can vary dramatically depending on the type of sludge handled and the methods employed for pre-treatment, digestion, and dewatering. Due to this complexity, categorizing the side-stream proves challenging (Aguilar-Moreno et al., 2022).

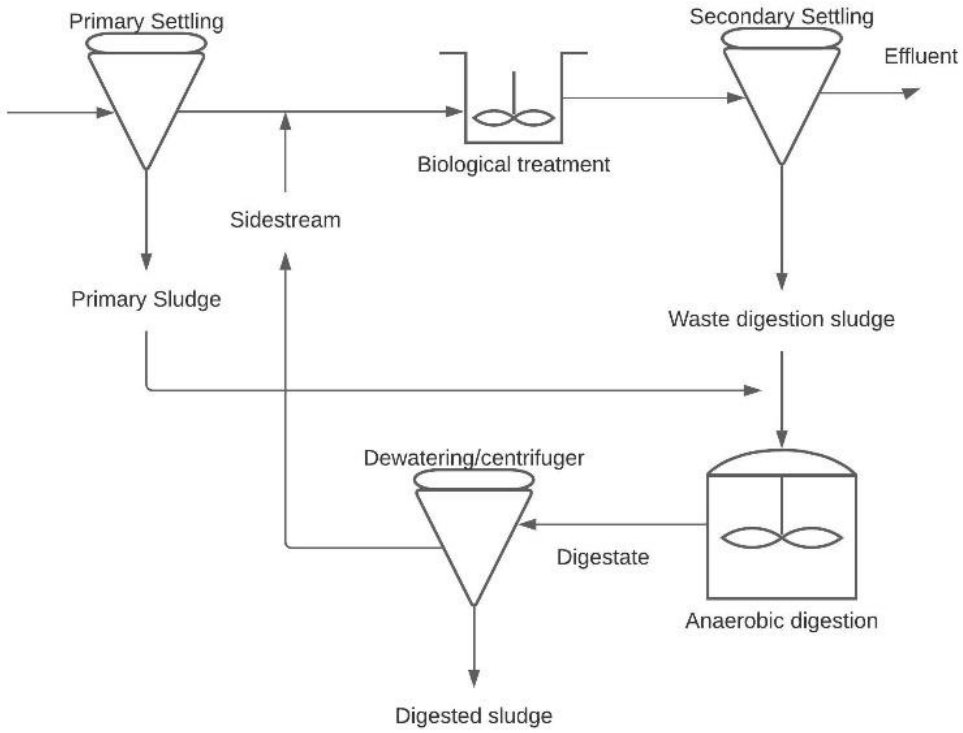

Figure 2. Schematic of typical wastewater treatment plant configuration with anaerobic digestion (AD) stage.

One of the greatest controversy and challenge of BNR processes is the high energy and resource demand to transform, for example, ammonia nitrogen into a low-valuable product such as N_2(g) (Ren et al., 2020). The aeration stage represents 50% of the usual energy consumption in WWTP wastewater treatment (Nowak, 2003). An extra 4% of electricity is used in the WWTP for the removal of nutrients in wastewater, i.e. 45 MJ/kg N, in addition, this leads to an emission of 0.9 kg CO_2/m^3 to the atmosphere, (Xie et al., 2016). Nowak 2003, quantified that the specific energy demand for aeration to remove nitrogen is 0.5 $kw \cdot h \cdot kg^{-1}$ O_2 consumed, which is equivalent to 40% of the O_2(g) consumption load for carbon disposal. (Nowak, 2003).

If the endeavours to recover NH_3 in WWTPs were strategically oriented towards a circular ecnomy, it could potentially yield significant energetic and economic benefits. For instance, if we take as case study the WWTP located at El Prat de Llobregat (Barcelona, Spain) one of the most modern and largest wastewater treatment plants in Europe (all the data in Table 3.), which treats 420.000 m^3/d, equivalent to 36% of all wastewater generated in the Barcelona metropolitan area, is a localized source of nitrogen.

Table 3. Metrics for Ammonia Recovery Potential at WWTP El Prat de Llobregat.

WWTP El Prat de Llobregat	Value
Volume treated by the WWTP	420,000 $m^3 \cdot d^{-1}$
Equivalent population served by the WWTP	1.26 million inhabitants
Nitrogen emission from the WWTP	2,500 ton $N \cdot year^{-1}$
Nitrogen production per inhabitant	5.5 g $N \cdot day^{-1}$
Price of one ton of ammonia	€180$\cdot ton^{-1}$
Total value of ammonia produced	€450,000$\cdot year^{-1}$

The WWTP of El Prat de Llobregat has an average input of 1.26 million equivalent inhabitants, with an emission of nitrogen into the environment of 2,500 t N/y (Àrea Metropolitana de Barcelona, 2002; Rufí-Salís et al., 2020). This implies that each inhabitant produces 5.5 g/N/d. According to data from the EC ((European Commission, 2019), the price of a ton of ammonia fluctuates around 180 €, which implies a value of 450,000 €/y considering only the WWTP of El Prat de Llobregat (Table 3).

1.2.2. Nutrients, Energy and Resources: From WWTPs to W&RRFs

The recovery of nutrients not only prevents their discharge into the environment but also facilitates their safe reintroduction into environmental compartments. This represents a significant step towards a circular economy (Robles et al., 2020). As a result, ammonium and phosphate are no longer viewed solely as pollutants to be eliminated but also as sustainable resources to be recovered (Darestani et al., 2017).

Water sources rich in ammonium can be used as a food source for both animals and humans, it can also be used for algae growth and/or bacteria that are used for the generation of biogas or biofuels or directly as fertilizers (Matassa et al., 2015; Thorin et al., 2018; WIDANARNI et al., 2012; Wuang et al., 2016). In the context of fertilizers, micro-organisms growing in wastewater cannot be directly applied due to the high concentration of metals and other pollutants that can appear in the biomass along with nitrogen. It is necessary to refine the biomass to guarantee a safe product. As an

alternative to this, direct application of nitrogen-rich recovery solutions to agricultural fields could be considered (Walsh et al., 2012).

It is still necessary to demonstrate the economic viability of this recovery, i.e. whether the value of the products recovered outweighs the economic effort involved (Perera et al., 2019).

WWTPs can be transformed into Water and Resource Recovery Facilities (W&RRFs) by recovering resources such as water, energy, biosolids, and nutrients, simultaneously reducing operating costs (Geissdoerfer et al., 2017; Lin et al., 2015).

The interconnection between water and energy has become an integral component of modern economies. In developed countries, WWTPs contribute to almost 3% of the total electrical energy load of a country (Capodaglio & Olsson, 2020).

Municipal wastewater contains approximately 5 to 10 times more energy (chemical and thermical) than is needed for wastewater treatment processes (Bauer, 2014; International Energy Agency, 2022; Tarallo, 2015). Wastewater is a highly concentrated source of organic matter (OM) and can be considered a carrier of chemical energy (Nasr Esfahani et al., 2022).

The total energy potential in wastewater is estimated at $898 \cdot 10^{15}$ J annually worldwide, with 80% being thermal energy and the remaining 20% chemical energy (Barnard & Stensel, 2014). According to data from the Water Environment Research Foundation (WERF) (Tarallo, 2015), it is possible to produce approximately $3.2 \cdot 10^{9}$ m^3 of biogas globally, equivalent to $72 \cdot 10^{15}$ J annually (Holmgren et al., 2016; Verstraete et al., 2009). However, biogas alone would only account for 8% of all the energy available in wastewater, highlighting the need to enhance current technologies and develop new and more efficient technologies that allow the recovery and use of the energy contained in wastewater.

Resource recovery poses a crucial challenge all the countries, particularly those lacking modern facilities. Taking the Macro Metropolis of Sao Paulo, Brazil, as an example, only 26% of wastewater treatment plants (WWTPs) implement resource recovery techniques (Chrispim et al., 2020). Another example is Italy, where a detailed analysis of 600 plants showed that over 60% exhibit no significant signs of resource recovery (Papa et al., 2017).

These results emphasize the need to transition towards more sustainable WWTPs globally. There is a substantial gap in the implementation of resource recovery practices worldwide, underscoring the urgency to adopt more sustainable practices such as Water and Resource Recovery Facilities (W&RRFs) (Coats & Wilson, 2017). These facilities not only align with circular economy objectives but also address fertilizer costs, generate energy, and produce purified water. The necessity for improvements in tertiary treatment and the advancement towards W&RRFs may lead to these facilities being considered innovative biofactories (self-sufficient or even energy-producing water treatment plants) producing materials like biomass, biofuels, biofertilizers, and bioplastics (Sheikh et al., 2023).

1.2.3. Alternative ammonia recovery techniques from wastewater

As previously mentioned, N (or the energy derivate) recovery is usually applied as a tertiary treatment divided into three categories: biological (BES, microalgae, duckweed and macrophyte westlands) (Zubair et al., 2020), physical-chemical and hybrid, a treatment train where two or more of these technologies would be combined (Cherif et al., 2023; Reig et al., 2022). Commonly, within physical-chemical, air stripping and chemical precipitation both could be regarded as the tertiary treatment technology with the greatest presence in WWTPs. New Alternative nitrogen recovery techniques are implemented with the aim of avoiding the use of air stripping stage given that this is an energy intensive technology and thus making the system very economically feasible as well as guaranteeing the generation of a valuable product from nitrogen (Yan et al., 2018).

Nutrient recovery is a promising strategy to reduce natural resource exploitation (Robles et al., 2020) in front of Biological Nitrogen Removal (BNR) (Mao et al., 2020) which focuses on the removal. During the past three decades, there has been a consistent rise in literature focusing on ammonia recovery, as depicted in Figure 3a and 3b. This surge in publications is driven by the necessity to explore alternative sources of ammonia. Urban wastewater streams, for instance, often exhibit low concentrations of nutrients but are present in substantial volumes, posing challenges for recovery. Consequently, there's a critical need to develop technologies that selectively target these nutrients or are capable of concentrating such streams (X. Guo et al., 2023; Tao et al., 2019).

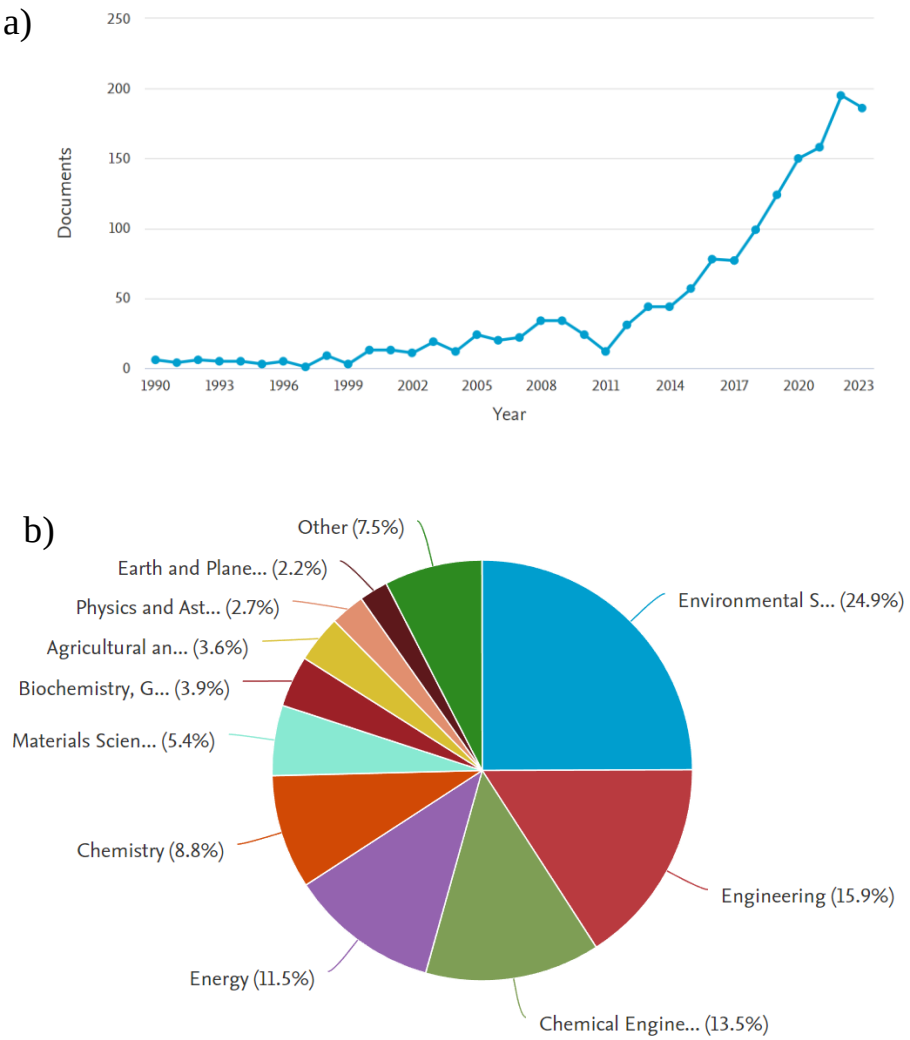

Figure 3. (a) Publications of peer-reviewed papers of "ammonia recovery technologies" [Scopus 2023] (b) Percentage of disciplines in total publications [Scopus 2023]

1.2.4. A chemical process for nitrogen recovery: recovery ammonium as struvite

Struvite ($NH_4MgPO_4 \cdot 6H_2O(s)$) precipitation is a methodology that allows indirect recovery of both nitrogen and phosphorus and even magnesium. However, struvite contains a low nitrogen content (6%), which reduces its effectiveness as a method for N recovery (Barros et al., 2022; Etter et al., 2011; Parsons & Doyle, 2002). Struvite is a crystalline material that precipitates stoichiometrically with the concentration ratio higher than 1:1:1 (Mg^{2+}: NH_4^+:PO_4^{3+}) (Bouropoulos & Koutsoukos, 2000) at a certain pH range 8-9. However, the precipitation needs input of magnesium due to its low content in the wastewater. This reagent addition stage is an extra cost in the whole process (Uludag-Demirer et al., 2005). It is possible to use struvite for phosphorus and nitrogen removal,

for example, from side-streams in WWTP's, besides it is considered a valuable slow release fertilizer optimal for grasslands and plantations (El Diwani et al., 2007; Kumar & Pal, 2015).

1.2.5. Physico-chemical processes for nitrogen recovery

The physico-chemical methods for nitrogen recovery include absorption, adsorption, ion exchange, membrane driven processes and stripping (e.g. vacuum or thermal).

1.2.5.1. Recovery by Ion-exchange (IEX)

A viable approach for ammonia recovery from wastewater involves adsorbing ammonium through ion exchange on an adsorbent, providing a swift process with the advantage of sorbent regeneration for subsequent cycles (Tarpeh et al., 2017). It is taking the benefit that in wastewaters the typical pH is usually below pH 9 and accordingly the ammoniacal inorganic nitrogen is mainly present as NH_4^+ (NH3 pKa =9.2). IEX processes have demonstrated their versatility, ease of control, straightforward design, and operational simplicity when compared to alternative processes (UF, NF, RO…) (Ahmadijokani et al., 2022; Pelalak et al., 2021). However, this technique faces challenges when treating water with large concentrations of competing ions typically present in waste water (e.g. Ca^{+2}, Mg^{+2}, Na^+ and K^+), which compete with ammonium during ion-exchange process (Eskicioglu et al., 2018). The effective implementation of this technology on fixed-bed configuration when the exchange material remains static while the liquid with the ions of interest flows through it, necessitates to ensure substantial recovery, along with the minimization of the potential issue of scaling formation in the process (Guida et al., 2021; Huang et al., 2020).

Natural zeolites, aluminium silicates with high sorption capacities, are particularly noteworthy in this context. The negative electrical charge carried by aluminium atoms in the crystalline lattice accounts for the natural ion exchange capacity of zeolites, making them effective for ammonium sorption, although the presence of other competing ions may limit the process (Burks et al., 2004). The regeneration of loaded zeolite using NaCl or NaOH solutions facilitates the formation of N-rich concentrates. Additionally, loaded zeolite can be directly applied to the soil (Guaya et al., 2018, 2020; Sancho et al., 2017).

1.2.5.2. Recovery by using vacuum and thermal stripping

Ammonia stripping is a simple desorption process to reduce and eliminate the ammonia content in a wastewater stream. (Laureni et al., 2013). The process is based on changing effluent conditions (increasing pH) that allow the transition from ammonium ion (NH_4^+) to ammonia (NH_3) and then ammonia gas ($NH_3(g)$) being transferred from the waste stream into the air, and then absorbed from the air into a strong acidic solution (typically sulphuric acid), thus producing an ammonium salt, which can be crystallized (Bonmatí & Flotats, 2003). On the other hand, thermal stripping involves the separation of ammonia through contact with hot air and a condensation column, while vacuum stripping, using a vacuum vessel, extracts ammonia with an acid solution.

The Veas WWTP in Oslo (Norway) has successfully employed ammonia stripping technique for over 20 years using nitric acid to produce ammonium nitrate (Ye et al., 2018). The thermal stripping is particularly efficient in anaerobic digestion effluents, as the generated biogas can be used to provide energy for the stripping process (Guštin & Marinšek-Logar, 2011). These methods offer different approaches to ammonia recovery, each with its advantages and specific applications (Eskicioglu et al., 2018; Sagberg et al., 2006; Tao et al., 2019).

1.2.5.3. Recovery by membrane-based processes

Various membrane-based processes that exhibit a good performance in transporting ammonia molecules have gained attention, particularly when utilizing hydrophobic porous membranes, such as hollow fiber membrane contactors or membrane distillation, as highlighted by Robles et al. 2020 (Robles et al., 2020) and Vecino et al. 2020 (Vecino et al., 2020). Additionally, ion exchange membranes, as employed in monopolar electrodialysis or bipolar electrodialysis (Jaroszek & Dydo, 2016), contribute to efficient ammonia transport. Non-porous membranes subjected to pressure or osmotic pressure, including Reverse Osmosis (RO), Forward Osmosis (FO), or Nanofiltration (NF), play a role in concentration or volume reduction stages. In the case of hydrophobic porous membranes, ammonia transport occurs through the membrane pores in the form of $NH_3(g)$ (Aguilar-Moreno et al., 2022). This membrane process transport is refer in the state of the art under different terms as: i) membrane gas extraction (Serra-Toro et al., 2022), ii) liquid-liquid membrane extraction (Rongwong & Goh, 2020), and iii) membrane distillation (MD) (Nthunya et al., 2019). The fact is, both sides of hydrophobic membranes facilitate the flow of liquid or gas/vapor through the membrane. These membranes typically are applied in the form of hollow fibers, spiral, or flat configuration.

Some membrane technologies have been integrated with chemical precipitation or biological processes in hybrid systems, as demonstrated by Yan et al. 2018 (Yan et al., 2018).

The use of membrane contactors technology, developed in the mid 1990's increasing year by year the amount of studies focused on the application to ammonia recovery (Zhu et al., 2024) (Figure 4). Membrane contactors facilitate mass transfer of gas/liquid or liquid/liquid without dispersion from one phase into another, this is achieved by passing the fluids through the opposite sides of a microporous membrane. (Agrahari et al., 2012; Gabelman & Hwang, 1999; Pabby & Sastre, 2013).

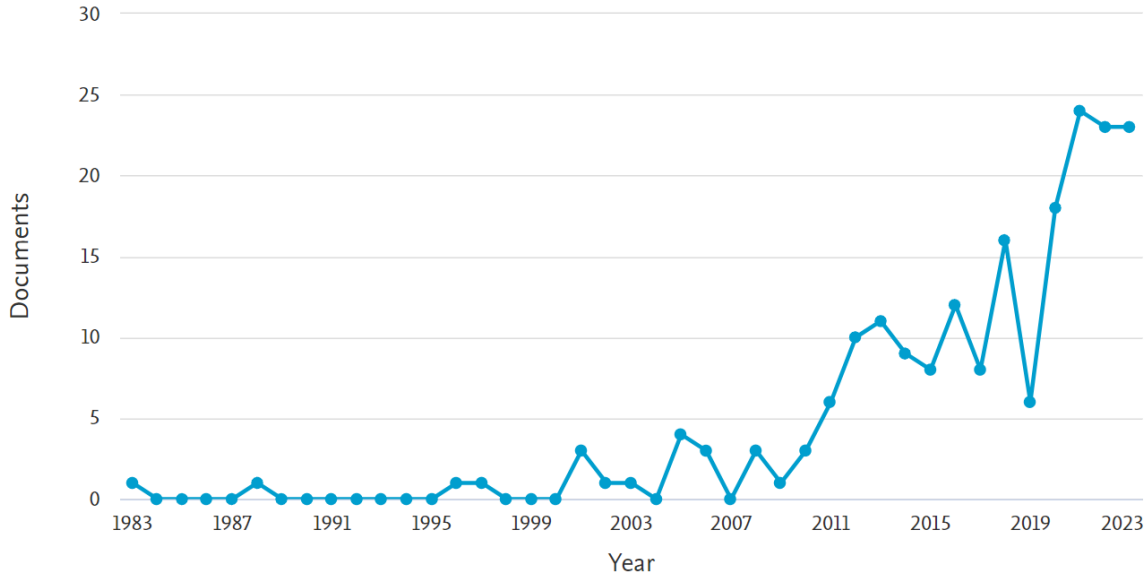

Figure 4. Publications of peer-reviewed papers of "Membrane contactors" and "ammonia".[Scopus 2023]

Membrane contactors have garnered considerable interest in industrial applications, particularly in the recovery and control of ammonia in wastewater effluents. This technology enables efficient treatment of these types of water, generating a nearly ammonia-free stream while producing a valuable product like ammonium sulphate or other ammonium salt, which serves as a suitable liquid fertilizer. Consequently, a waste stream containing ammonia is converted into a useful product (Ukwuani & Tao, 2016).

The utilization of hydrophobic membrane contactors presents an intriguing approach, allowing operation at room temperature. In this scenario, ammonia gas flows through the membrane driven by the concentration gradient, reacting with a stripping solution, typically an acid (e.g., H_3PO_4, HNO_3, H_2SO_4) or a combination of acids, as reported by

Vecino et al. 2019, using a mixture of H_3PO_4 and HNO_3. Liquid-liquid membrane contactors (LLMC), as employed by Licon et al. 2015 (Licon et al., 2015), achieved a 78% ammonia removal efficiency in a one-step configuration (Vecino et al., 2019). These studies indicated that an increase in pH and a decrease in flow rate significantly improved removal efficiency. This technology offers selective ammonia gas removal without incurring additional energy costs, such as feed temperature, and proves effective even in waters with very low ammonia levels (Darestani et al., 2017).

The transport of gases through porous membranes shows a high efficiency to degasify oxygen, carbon dioxide and other gaseous compounds in water (Mandowara & Bhattacharya, 2009) as shown in (Figure 5a) in this technique the liquid feed stream containing the ammonia is located on one side of the membrane (Feed side), it is essential to transform the NH_4^+(aq) into NH_3(g) in order to transport it through the pores of the membrane to the permeate side where the acid stripping solutions circulate (Gao et al., 2020).

A)

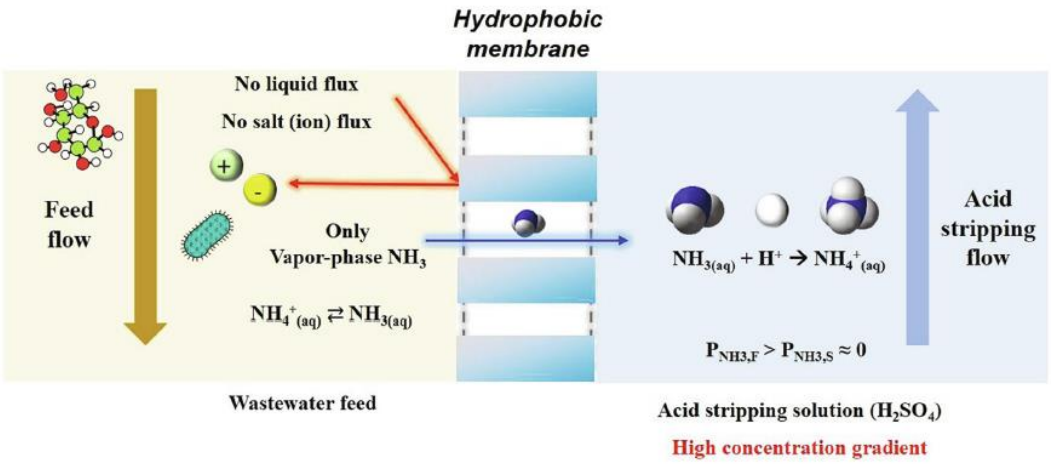

B)

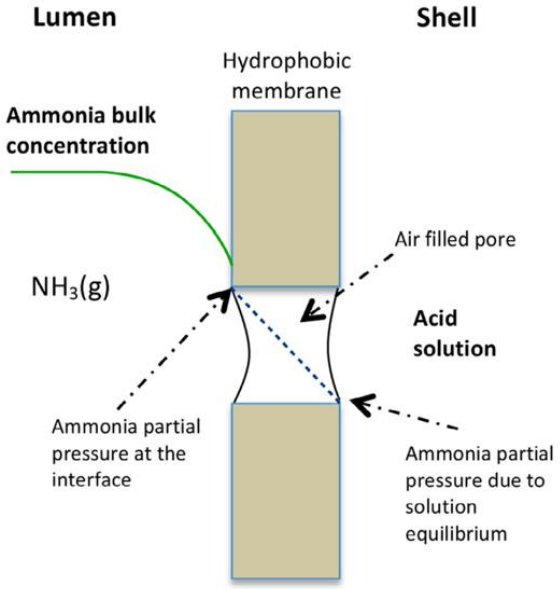

Figure 5. (a) Schematic representation of ammonia recovery by means gas permeable membrane (Lee et al., 2021). (b) Schematic description of ammonia transport through the hydrophobic membrane (E. E. Licon Bernal et al., 2016)

In this technology, the prevailing membranes commonly feature air-filled pores with hydrophobic surfaces, preventing membrane wetting (Mansourizadeh & Ismail, 2009). On the stripping side of the membrane, a vacuum pressure, stripping gas, or stripping liquid flow is applied, maintaining a partial pressure gradient across the membrane, facilitating the migration of molecules from the feed side, as illustrated in Figure 5a (Agrahari et al., 2012; Ulbricht et al., 2013).

Following the passage of ammonia through the hydrophobic membrane, the stripping solution, typically sulfuric acid, circulates in a counter-current configuration,

This implies that the feed flows in one direction, while the stripping solution flows in the opposite directionThe movement of ammonia toward the acid compartment is driven by the partial vapor pressure difference controlled by the pH (Gabelman & Hwang, 1999; Hasanoğlu et al., 2010). It is crucial to maintain a pH in the feed effluent above the pKa of ammonia (pKa = 9.25) to enable the flow of NH_3 in the gas phase through the pores of the membrane (Licon et al., 2015).

A critical aspect in membrane contactors is achieving affordable mass transfer and NH_3 flow through the membrane (Reig et al., 2021). For effective membrane performance, a deep understanding of membrane transport mechanism as illustrated in Figure 5b, becomes essential.

Membranes used are crafted from hydrophobic polymers, including materials such as polypropylene (PP), polyethylene (PE), polytetrafluoroethylene (PTFE), poly(tetrafluoroethylene-co-perfluorovinyl ether) (PFA), or polyvinylidene fluoride (PVDF). Notably, the innovative membranes from SEPAREL® are constructed from Polytetramethylpentene (PMP). In the presence of an polar liquid on one side of the hydrophobic microporous membrane, the membrane remains unwetted due to surface tension, and the liquid is unable to permeate the pores, a phenomenon dictated by the contact angle with the surface (Pabby & Sastre, 2013).

In aqueous mediums, the likelihood of pore wetting increases this occurs because polar liquids like water has the natural tendency to fill and occupy empty spaces on a surface, including the pores of a membrane. It is crucial to prevent membrane wetting, a challenge addressed through the control of surface tension facilitated by the chemical composition of the membrane surface and the pore geometry (Bavarella et al., 2022; McLeod et al., 2015).

Hydrophobic membranes are the basis of membrane contactors, with various configurations such as flat sheet, spiral-wound, rotary annular, and hollow fiber, among which the hollow fiber configuration is most commonly used (Bazhenov et al., 2018) (Figure 6). Typically arranged in a shell and lumen configuration, this design offers a robust structure, minimizing size and protecting the membranes. However, tubular configurations have been reported particularly useful in processes prone to fouling and requiring regular cleaning (Majd & Mukhtar, 2013).

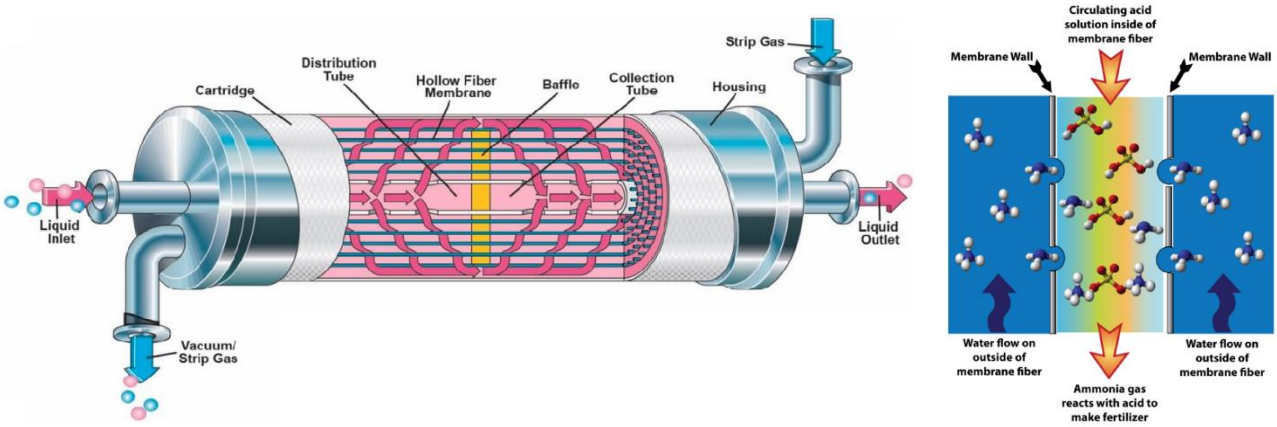

Figure 6. Schematic reproduction of Hollow Fiber Membrane Contactor (3M Liqui-cell)

Both flat sheet and hollow fiber configurations facilitate fluid exchange (gas/gas, gas/liquid, or liquid/liquid). Comparatively, the hollow fiber configuration boasts several advantages, including greater membrane area per unit volume, enhanced mechanical strength due to a more rugged and compact structure, and increased convenience in module manufacturing, repair, and membrane operation (Bazhenov et al., 2018).

In a patented method *(United States Patent, Patent No.: US 9,708,200 B2)* by Szogi et al. 2017, passive ammonia capture from liquid effluent is achieved by passing ammonia gas molecules through a gas-permeable membrane immersed in the effluent (Szogi et al., 2017). In some studies, Vanotti et al. 2017, configured a setup for ammonia recovery using gas-permeable membranes immersed in an effluent containing 2.3g $NH_4^+ \cdot L^{-1}$, transferring the recovered ammonia to a stripping stream to obtain an ammonium salt (Vanotti et al., 2017).

In terms of operation the membrane contactor configuration used should be considered, "open loop" configuration (Figure.7 (a)) where the feed passes through the contactor and is collected in a treated water tank, or if the feed solution is recirculated and recycled to the feed tank after passing through the membrane is named "closed loop" configuration (figure 7. (b)). It is possible to assemble a set up with one or more membrane contactors,

(Vecino et al., 2019) using Hollow fiber liquid-liquid membrane contactor in a two-step closed loop configuration with satisfactory results.

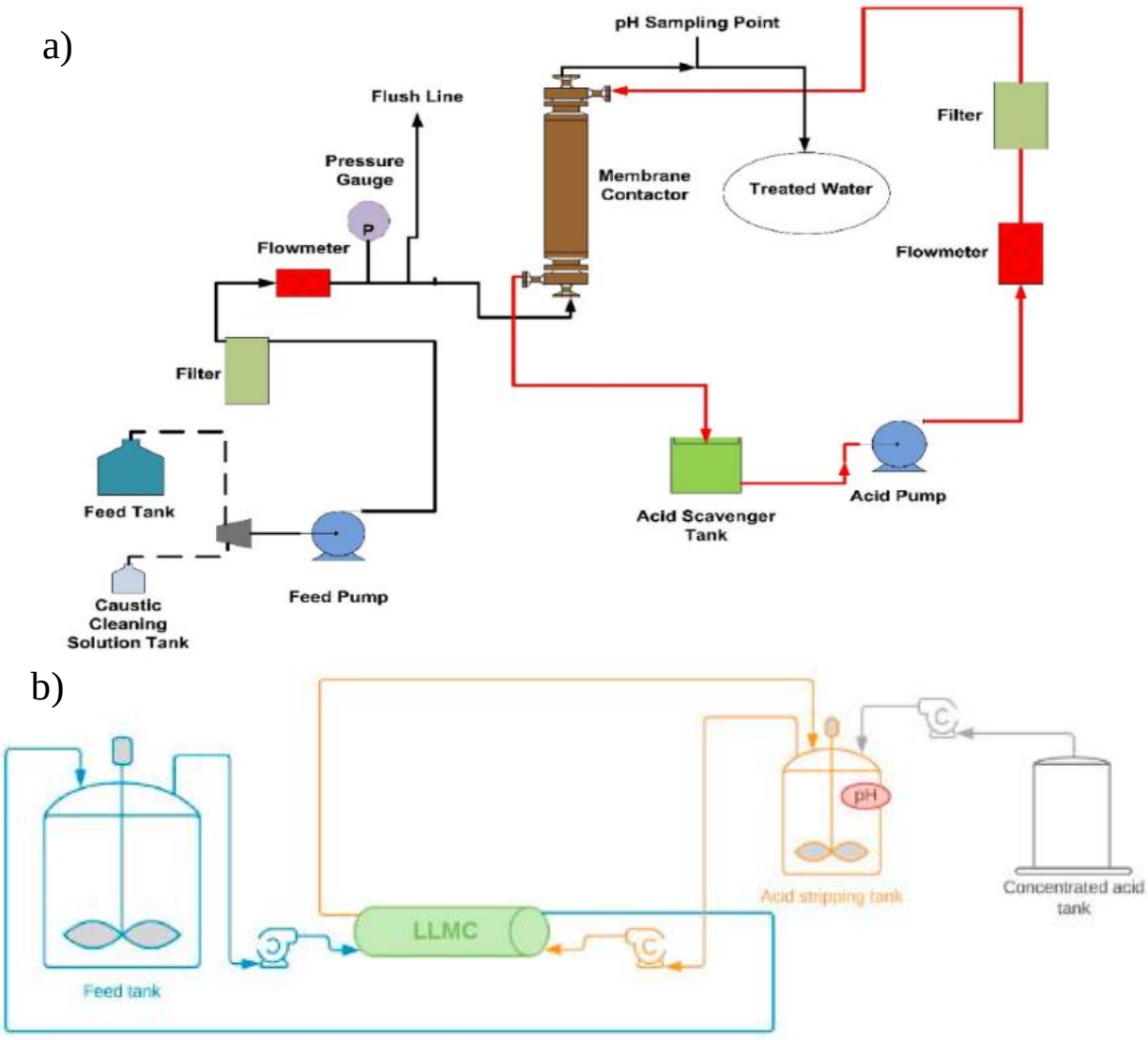

Figure 7. HFMC "open loop" set up (a) and HFMC "closed loop" set up (b) (Darestani et al., 2017; Vecino et al., 2019)

The advantages of ammonia recovery by means of membrane contactors are high selectivity, i.e., the pores of the membrane, being full of air, provide an optimum barrier for any other constituents contained in the feed water. This must always depend on the control of fouling and wetting.(Tan et al., 2006; Wang et al., 2023; Zarebska et al., 2014). For this reason, this leads to a series of advantages when it concerns the valorisation of

the collected product since it allows it to reach a very high level of purity. (Al-Juboori et al., 2022). In the case of membrane contactors, the control of the partial pressure for mass transfer is carried out by means of scrupulous control of the pH (Yu et al., 2021).

Recent developments in membrane technology have led to result a high density of membrane packingfor example 30 cm^2/cm^3 of density packing (Yang et al., 2013) thus optimising the space and a reduced portion of the membrane is a large effective area which results in a higher recovery. This allows Membrane Contactor Technology to be a suitable option at different levels, on a domestic as well as a metropolitan scale (Lee et al., 2021).

1.2.6. Biological process for nitrogen recovery

In recent years bioelectrochemical (BES) systems has been postulated as a potential reliable alternative for nutrient recovery in wastewater. In these systems the nitrogen is concentrated under the influence of an electrical current in the cathode area for further recovery (Kuntke et al., 2018), these systems are based on the use of microorganisms that function as catalysts for the reactions that take place in either the anode or the cathode by transforming chemical energy into electrical energy (or vice versa), just as a battery does (Rodríguez Arredondo et al., 2015). Within the BES there are mainly Microbial Electrolysis Cells (MEC) and Microbial Fuel Cells (MFC) (Jatoi et al., 2022; Kelly & He, 2014). The main difference between the both is the direction of the thermodynamic reaction, in the case of the MFC, the reaction is favoured in the anode producing energy when the oxygen is reduced, on the other hand, the MEC needs an extra energetic application due to the fact that the reaction is thermodynamically unfavourable in the cathode (Yan et al., 2018). Certainly, the most outstanding feature of this technology is the ability to generate energy (by producing electricity or hydrogen) while facilitating nutrient recovery. One of the main disadvantages of this technology is the fouling of the membrane, which generates a huge limitation (Mondor et al., 2009; Rahmani et al., 2020).

1.3. Research challenges and objectives

However, despite the relatively considerable amount of studies, and the number increasing each year, there is a certain gap in the knowledge of membrane contactors. This gap is not in the understanding of the operating mechanism but rather in the

application capabilities, such as the optimal type of influent for this technology, the operating conditions that contribute to higher performance, and the possibilities for scaling up. While the literature boasts an extensive repertoire of articles showcasing promising results with membrane contactors, these outcomes often pertain to very specific conditions that are not easily transferable to other scenarios, especially when dealing with real wastewater rather than synthetic water. The challenge lies in determining where to direct the recovery efforts whether to focus on the mainstream (0.1 $g \cdot L^{-1}$), the sides-tream or centrate from anaerobic digestion (1-3 g·L-1), agri-food wastewater effluents (>5 $g \cdot L^{-1}$), industrial streams (>5 g·L-1), or other waste streams sources of ammonia (Sheikh et al., 2023).

The successful application and integration of membrane contactors in these diverse streams require careful consideration of the water quality and pre-treatment requirements. This involves employing techniques like coagulation/flocculation, as well as implementing filtration stages such as Microfiltration (MF) and Ultrafiltration (UF) to reduce particulate material, suspended solids, and the dissolved and colloidal chemical demand of total oxygen (COD), thereby avoiding membrane fouling scenarios.

Additionally, the selection of membranes involves evaluating critical properties such as hydrophobicity, contact angle, and configuration. The question arises whether the commonly used symmetrical PP fibers are the most ideal solution, or if other polymers such as PMP would achieve similar performance. Moreover, exploring the potential benefits of an asymmetrical membrane structure adds another layer to this consideration.

Compounding these challenges is the absence of standardization in result representation within the literature. This lack of consistency in reporting methods poses difficulties in comparing findings across different articles, hindering the extrapolation of conclusions and the identification of best practices. Consequently, the establishment of standards in result presentation becomes crucial for enhancing the overall understanding and evaluation of the effectiveness of membrane contactors in ammonia recovery applications.

1.4. References

Agrahari, G. K., Shukla, S. K., Verma, N., & Bhattacharya, P. K. (2012). Model prediction and experimental studies on the removal of dissolved NH 3 from water applying hollow fiber membrane contactor. *Journal of Membrane Science*, *390–391*, 164–174. https://doi.org/10.1016/j.memsci.2011.11.033

Aguilar-Moreno, M., Vinardell, S., Reig, M., Vecino, X., Valderrama, C., & Cortina, J. L. (2022). Impact of Sidestream Pre-Treatment on Ammonia Recovery by Membrane Contactors: Experimental and Economic Evaluation. *Membranes*, *12*(12). https://doi.org/10.3390/membranes12121251

Ahmadijokani, F., Molavi, H., Peyghambari, A., Shojaei, A., Rezakazemi, M., Aminabhavi, T. M., & Arjmand, M. (2022). Efficient removal of heavy metal ions from aqueous media by unmodified and modified nanodiamonds. *Journal of Environmental Management*, *316*(April), 115214. https://doi.org/10.1016/j.jenvman.2022.115214

Al-Juboori, R. A., Uzkurt Kaljunen, J., Righetto, I., & Mikola, A. (2022). Membrane contactor onsite piloting for nutrient recovery from mesophilic digester reject water: The effect of process conditions and pre-treatment options. *Separation and Purification Technology*, *303*(September), 122250. https://doi.org/10.1016/j.seppur.2022.122250

Ammonia Technology Roadmap. (2021). *Ammonia Technology Roadmap*. https://doi.org/10.1787/f6daa4a0-en

Àrea Metropolitana de Barcelona. (2002). *Depuradora i estació de regeneració d ' aigua del Prat de Llobregat*.

Azreen, I., Lija, Y., & Zahrim, A. Y. (2017). Ammonia nitrogen removal from aqueous solution by local agricultural wastes. *IOP Conference Series: Materials Science and Engineering*, *206*(1). https://doi.org/10.1088/1757-899X/206/1/012077

Barnard, J. L., & Stensel, H. D. (2014). The activated sludge process in service of humanity. *DSD International Conference*, *Figure 1*. http://www.archive.org/details/cu31924005016419

Barros, A., Vecino, X., Reig, M., & Cortina, J. L. (2022). Coagulation and Flocculation Optimization Process Applied to the Sidestream of an Urban Wastewater Treatment Plant. *Water (Switzerland)*, *14*(24), 1–26. https://doi.org/10.3390/w14244024

Bauer, D. (2014). *Water-Energy Nexus : Challenges and Opportunities*.

Bavarella, S., Luqmani, B., Thomas, N., Brookes, A., Moore, A., Vale, P., Pidou, M., & McAdam, E. J. (2022). CO2 absorption into aqueous ammonia using membrane contactors: Role of solvent chemistry and pore size on solids formation for low energy solvent regeneration. *Separation and Purification Technology*, *290*(March), 120786. https://doi.org/10.1016/j.seppur.2022.120786

Bazhenov, S. D., Bildyukevich, A. V., & Volkov, A. V. (2018). Gas-liquid hollow fiber membrane contactors for different applications. *Fibers*, *6*(4). https://doi.org/10.3390/fib6040076

Beckinghausen, A., Odlare, M., Thorin, E., & Schwede, S. (2020). From removal to recovery: An evaluation of nitrogen recovery techniques from wastewater. *Applied Energy*, *263*(February), 114616. https://doi.org/10.1016/j.apenergy.2020.114616

Bird, F., Clarke, A., Davies, P., & Surkovic, E. (2020). Ammonia: zero-carbon fertiliser, fuel and energy store. In *The Royal Society*. https://royalsociety.org/-/media/policy/projects/green-ammonia/green-ammonia-policy-briefing.pdf

Bonmatí, A., & Flotats, X. (2003). Air stripping of ammonia from pig slurry: Characterisation and feasibility as a pre- or post-treatment to mesophilic anaerobic digestion. *Waste Management*, *23*(3), 261–272. https://doi.org/10.1016/S0956-053X(02)00144-7

Bouropoulos, N. C., & Koutsoukos, P. G. (2000). Spontaneous precipitation of struvite from aqueous solutions. *Journal of Crystal Growth*, *213*(3–4), 381–388. https://doi.org/10.1016/S0022-0248(00)00351-1

Burks, T. F., Shearer, S. a, Fulton, J. P., & Sobolik, C. J. (2004). *L Iterature R Eview*. *20*(3), 269–276. https://doi.org/10.1016/j.profnurs.2010.10.006

Capodaglio, A. G., & Olsson, G. (2020). Energy issues in sustainable urban wastewater management: Use, demand reduction and recovery in the urban water cycle. *Sustainability (Switzerland)*, *12*(1). https://doi.org/10.3390/su12010266

Cherif, H., Risse, H., Abda, M., Benmansour, I., Roth, J., & Elfil, H. (2023). Nanofiltration as an efficient tertiary wastewater treatment for reuse in the aquaponic system in Tunisia. *Journal of Water Process Engineering*, *52*(February), 103530. https://doi.org/10.1016/j.jwpe.2023.103530

Chrispim, M. C., Scholz, M., & Nolasco, M. A. (2020). A framework for resource recovery from wastewater treatment plants in megacities of developing countries. *Environmental Research*, *188*(June), 109745. https://doi.org/10.1016/j.envres.2020.109745

Coats, E. R., & Wilson, P. I. (2017). Toward Nucleating the Concept of the Water Resource Recovery Facility (WRRF): Perspective from the Principal Actors. *Environmental Science and Technology*, *51*(8), 4158–4164. https://doi.org/10.1021/acs.est.7b00363

Company, T. M., Group, H., Group, E., States, U., Fertilizers, P., Treatment, S., Overview, R. I., Intelligence, M., Analysis, C., & Data, H. (2023). *With 9 . 1 % CAGR , Chemical Fertilizers Market Size to Reach USD 23 . 1 Billion by 2030 | Global Chemical Fertilizers Industry Trends , Share , Value , Analysis & Forecast Report by Zion Market*.

Darestani, M., Haigh, V., Couperthwaite, S. J., Millar, G. J., & Nghiem, L. D. (2017). Hollow fibre membrane contactors for ammonia recovery: Current status and future developments. *Journal of Environmental Chemical Engineering*, *5*(2), 1349–1359. https://doi.org/10.1016/j.jece.2017.02.016

El Diwani, G., El Rafie, S., El Ibiari, N. N., & El-Aila, H. I. (2007). Recovery of ammonia nitrogen from industrial wastewater treatment as struvite slow releasing fertilizer. *Desalination*, *214*(1–3), 200–214. https://doi.org/10.1016/j.desal.2006.08.019

Eskicioglu, C., Galvagno, G., & Cimon, C. (2018a). Approaches and processes for ammonia removal from side-streams of municipal effluent treatment plants. *Bioresource Technology*, *268*(May), 797–810. https://doi.org/10.1016/j.biortech.2018.07.020

Eskicioglu, C., Galvagno, G., & Cimon, C. (2018b). Approaches and processes for ammonia removal from side-streams of municipal effluent treatment plants. *Bioresource Technology*, *268*(May), 797–810.

https://doi.org/10.1016/j.biortech.2018.07.020

Etter, B., Tilley, E., Khadka, R., & Udert, K. M. (2011). Low-cost struvite production using source-separated urine in Nepal. *Water Research*, *45*(2), 852–862. https://doi.org/10.1016/j.watres.2010.10.007

European Commission. (2019). Fertilisers in the EU - Prices, trade and use. *EU Agricultural Markets Briefs*, *15*(15), 1–8.

European Commission. (2023). Organic farming in the EU - A decade of organic growth. *Organic Farming in the EU - A Decade of Organic Growth*, *20*, 32. https://ec.europa.eu/info/sites/info/files/food-farming-fisheries/farming/documents/market-brief-organic-farming-in-the-eu_mar2019_en.pdf

FAO. (2019). *World fertilizer outlook and trends to 2022*.

Faragò, M., Damgaard, A., Madsen, J. A., Andersen, J. K., Thornberg, D., Andersen, M. H., & Rygaard, M. (2021). From wastewater treatment to water resource recovery: Environmental and economic impacts of full-scale implementation. *Water Research*, *204*(July). https://doi.org/10.1016/j.watres.2021.117554

Fernández, B. (2008). Tratamiento anaerobio de residuos de la industria alimentaria. *II Congreso Iberoamericano Sobre Seguridad Alimentaria. V Congreso Español de Ingeniería de Alimentos*, 1–8. https://upcommons.upc.edu/bitstream/handle/2117/97917/Flotats y Fernandez_CESIA2008.pdf

Fowler, D., Coyle, M., Skiba, U., Sutton, M. A., Cape, J. N., Reis, S., Sheppard, L. J., Jenkins, A., Grizzetti, B., Galloway, J. N., Vitousek, P., Leach, A., Bouwman, A. F., Butterbach-Bahl, K., Dentener, F., Stevenson, D., Amann, M., & Voss, M. (2013). The global nitrogen cycle in the Twentyfirst century. *Philosophical Transactions of the Royal Society B: Biological Sciences*, *368*(1621). https://doi.org/10.1098/rstb.2013.0164

Gabelman, A., & Hwang, S. T. (1999). Hollow fiber membrane contactors. *Journal of Membrane Science*, *159*(1–2), 61–106. https://doi.org/10.1016/S0376-7388(99)00040-X

Galloway, J. N., Townsend, A. R., Erisman, J. W., Bekunda, M., Cai, Z., Freney, J. R., Martinelli, L. A., Seitzinger, S. P., & Sutton, M. A. (2008). Transformation of the Nitrogen Cycle : *Science*, *320*(May), 889–892.

Gao, L., Li, J. De, Yang, G., Zhang, J., & Xie, Z. (2020). De-ammonification using direct contact membrane distillation – An experimental and simulation study. *Separation and Purification Technology*, *250*(February), 117158. https://doi.org/10.1016/j.seppur.2020.117158

Geissdoerfer, M., Savaget, P., Bocken, N. M. P., & Hultink, E. J. (2017). The Circular Economy – A new sustainability paradigm? *Journal of Cleaner Production*, *143*, 757–768. https://doi.org/10.1016/j.jclepro.2016.12.048

González Montiel, J. M. (2008). Acetato de etilo en la Industria. *Journal of Chemical Information and Modeling*, *53*(9), 287.

Guaya, D., Mendoza, A., Valderrama, C., Farran, A., Sauras-Yera, T., & Cortina, J. L. (2020). Use of nutrient-enriched zeolite (NEZ) from urban wastewaters in amended soils: Evaluation of plant availability of mineral elements. *Science of the Total Environment*, *727*, 138646. https://doi.org/10.1016/j.scitotenv.2020.138646

Guaya, D., Valderrama, C., Farran, A., Sauras, T., & Cortina, J. L. (2018). Valorisation of N and P from waste water by using natural reactive hybrid sorbents: Nutrients (N,P,K) release evaluation in amended soils by dynamic experiments. *Science of the Total Environment*, *612*, 728–738. https://doi.org/10.1016/j.scitotenv.2017.08.248

Guida, S., Van Peteghem, L., Luqmani, B., Sakarika, M., McLeod, A., McAdam, E. J., Jefferson, B., Rabaey, K., & Soares, A. (2021). Ammonia recovery from brines originating from a municipal wastewater ion exchange process and valorization of recovered nitrogen into microbial protein. *Chemical Engineering Journal*, *427*(April 2021), 130896. https://doi.org/10.1016/j.cej.2021.130896

Guo, C. H., Stabnikov, V., & Ivanov, V. (2010). The removal of nitrogen and phosphorus from reject water of municipal wastewater treatment plant using ferric and nitrate bioreductions. *Bioresource Technology*, *101*(11), 3992–3999. https://doi.org/10.1016/j.biortech.2010.01.039

Guo, X., Chen, J., Wang, X., Li, Y., Liu, Y., & Jiang, B. (2023). Sustainable ammonia

recovery from low strength wastewater by the integrated ion exchange and bipolar membrane electrodialysis with membrane contactor system. *Separation and Purification Technology*, *305*(August 2022), 122429. https://doi.org/10.1016/j.seppur.2022.122429

Guštin, S., & Marinšek-Logar, R. (2011). Effect of pH, temperature and air flow rate on the continuous ammonia stripping of the anaerobic digestion effluent. *Process Safety and Environmental Protection*, *89*(1), 61–66. https://doi.org/10.1016/j.psep.2010.11.001

Hasanoğlu, A., Romero, J., Pérez, B., & Plaza, A. (2010). Ammonia removal from wastewater streams through membrane contactors: Experimental and theoretical analysis of operation parameters and configuration. *Chemical Engineering Journal*, *160*(2), 530–537. https://doi.org/10.1016/j.cej.2010.03.064

Holmgren, K.E., Li, H.,Verstreete, W.,Cornal,P. (2016). State of the Art Compendium Report on Resource Recovery from Water Preface. *IWA Resource Recovery Cluster, The International Water Association (IWA), London, UK*, 49. http://www.iwa-network.org/publications/state-of-the-art-compendium-report-on-resource-recovery-from-water/

Huang, X., Guida, S., Jefferson, B., & Soares, A. (2020). Economic evaluation of ion-exchange processes for nutrient removal and recovery from municipal wastewater. *Npj Clean Water*, *3*(1). https://doi.org/10.1038/s41545-020-0054-x

International Energy Agency. (2022). International Energy Agency (IEA) World Energy Outlook 2022. *International Energy Agency*, 524. https://www.iea.org/reports/world-energy-outlook-2022

Jaroszek, H., & Dydo, P. (2016). Ion-exchange membranes in chemical synthesis-a review. *Open Chemistry*, *14*(1), 1–19. https://doi.org/10.1515/chem-2016-0002

Jatoi, A. S., Hashmi, Z., Mazari, S. A., Mubarak, N. M., Karri, R. R., Ramesh, S., & Rezakazemi, M. (2022). A comprehensive review of microbial desalination cells for present and future challenges. *Desalination*, *535*(April), 115808. https://doi.org/10.1016/j.desal.2022.115808

Kehrein, P., Van Loosdrecht, M., Osseweijer, P., Garfí, M., Dewulf, J., & Posada, J.

(2020). A critical review of resource recovery from municipal wastewater treatment plants-market supply potentials, technologies and bottlenecks. *Environmental Science: Water Research and Technology*, *6*(4), 877–910. https://doi.org/10.1039/c9ew00905a

Kelly, P. T., & He, Z. (2014). Nutrients removal and recovery in bioelectrochemical systems: A review. *Bioresource Technology*, *153*, 351–360. https://doi.org/10.1016/j.biortech.2013.12.046

Kirova-Yordanova, Z. (2004). Exergy analysis of industrial ammonia synthesis. *Energy*, *29*(12-15 SPEC. ISS.), 2373–2384. https://doi.org/10.1016/j.energy.2004.03.036

Kumar, R., & Pal, P. (2015). Assessing the feasibility of N and P recovery by struvite precipitation from nutrient-rich wastewater: a review. *Environmental Science and Pollution Research*, *22*(22), 17453–17464. https://doi.org/10.1007/s11356-015-5450-2

Kuntke, P., Sleutels, T. H. J. A., Rodríguez Arredondo, M., Georg, S., Barbosa, S. G., ter Heijne, A., Hamelers, H. V. M., & Buisman, C. J. N. (2018). (Bio)electrochemical ammonia recovery: progress and perspectives. *Applied Microbiology and Biotechnology*, *102*(9), 3865–3878. https://doi.org/10.1007/s00253-018-8888-6

Laureni, M., Palatsi, J., Llovera, M., & Bonmatí, A. (2013). Influence of pig slurry characteristics on ammonia stripping efficiencies and quality of the recovered ammonium-sulfate solution. *Journal of Chemical Technology and Biotechnology*, *88*(9), 1654–1662. https://doi.org/10.1002/jctb.4016

Lee, W., An, S., & Choi, Y. (2021). Ammonia harvesting via membrane gas extraction at moderately alkaline pH: A step toward net-profitable nitrogen recovery from domestic wastewater. *Chemical Engineering Journal*, *405*(May 2020), 126662. https://doi.org/10.1016/j.cej.2020.126662

Licon, E., Reig, M., Villanova, P., Valderrama, C., Gibert, O., & Cortina, J. L. (2015). Ammonium removal by liquid–liquid membrane contactors in water purification process for hydrogen production. *Desalination and Water Treatment*, *56*(13), 3607–3616. https://doi.org/10.1080/19443994.2014.974216

Lin, H., Liu, Q. L., Dong, Y. B., He, Y. H., & Wang, L. (2015). Physicochemical

properties and mechanism study of clinoptilolite modified by NaOH. *Microporous and Mesoporous Materials*, *218*, 174–179. https://doi.org/10.1016/j.micromeso.2015.07.017

Ma, B., Xu, X., Wei, Y., Ge, C., & Peng, Y. (2020). Recent advances in controlling denitritation for achieving denitratation/anammox in mainstream wastewater treatment plants. *Bioresource Technology*, *299*(December 2019), 122697. https://doi.org/10.1016/j.biortech.2019.122697

Majd, A. M. S., & Mukhtar, S. (2013). *AND FIELD-SCALE STUDIES*. *56*(Lm), 1951–1958.

Mandowara, A., & Bhattacharya, P. K. (2009). Membrane contactor as degasser operated under vacuum for ammonia removal from water: A numerical simulation of mass transfer under laminar flow conditions. *Computers and Chemical Engineering*, *33*(6), 1123–1131. https://doi.org/10.1016/j.compchemeng.2008.12.005

Mansourizadeh, A., & Ismail, A. F. (2009). Hollow fiber gas-liquid membrane contactors for acid gas capture: A review. *Journal of Hazardous Materials*, *171*(1–3), 38–53. https://doi.org/10.1016/j.jhazmat.2009.06.026

Matassa, S., Batstone, D. J., Hülsen, T., Schnoor, J., & Verstraete, W. (2015). Can direct conversion of used nitrogen to new feed and protein help feed the world? *Environmental Science and Technology*, *49*(9), 5247–5254. https://doi.org/10.1021/es505432w

McLeod, A., Buzatu, P., Autin, O., Jefferson, B., & McAdam, E. (2015). Controlling shell-side crystal nucleation in a gas-liquid membrane contactor for simultaneous ammonium bicarbonate recovery and biogas upgrading. *Journal of Membrane Science*, *473*, 146–156. https://doi.org/10.1016/j.memsci.2014.07.063

Mondor, M., Ippersiel, D., Lamarche, F., & Masse, L. (2009). Fouling characterization of electrodialysis membranes used for the recovery and concentration of ammonia from swine manure. *Bioresource Technology*, *100*(2), 566–571. https://doi.org/10.1016/j.biortech.2008.06.072

Mukarunyana, B., van de Vossenberg, J., van Lier, J. B., & van der Steen, P. (2018). Photo-oxygenation for nitritation and the effect of dissolved oxygen concentrations

on anaerobic ammonium oxidation. *Science of the Total Environment*, *634*, 868–874. https://doi.org/10.1016/j.scitotenv.2018.04.082

Nasr Esfahani, K., Pérez-Moya, M., & Graells, M. (2022). Modelling of the photo-Fenton process with flexible hydrogen peroxide dosage: Sensitivity analysis and experimental validation. *Science of the Total Environment*, *839*(March). https://doi.org/10.1016/j.scitotenv.2022.155941

Nowak, O. (2003). Benchmarks for the energy demand of nutrient removal plants. *Water Science and Technology*, *47*(12), 125–132. https://doi.org/10.2166/wst.2003.0637

Nthunya, L. N., Gutierrez, L., Derese, S., Nxumalo, E. N., Verliefde, A. R., Mamba, B. B., & Mhlanga, S. D. (2019). A review of nanoparticle-enhanced membrane distillation membranes: membrane synthesis and applications in water treatment. *Journal of Chemical Technology and Biotechnology*, *94*(9), 2757–2771. https://doi.org/10.1002/jctb.5977

Osorio-Tejada, J., Tran, N. N., & Hessel, V. (2022). Techno-environmental assessment of small-scale Haber-Bosch and plasma-assisted ammonia supply chains. *Science of the Total Environment*, *826*, 154162. https://doi.org/10.1016/j.scitotenv.2022.154162

Pabby, A. K., & Sastre, A. M. (2013). State-of-the-art review on hollow fibre contactor technology and membrane-based extraction processes. *Journal of Membrane Science*, *430*, 263–303. https://doi.org/10.1016/j.memsci.2012.11.060

Papa, M., Foladori, P., Guglielmi, L., & Bertanza, G. (2017). How far are we from closing the loop of sewage resource recovery? A real picture of municipal wastewater treatment plants in Italy. *Journal of Environmental Management*, *198*, 9–15. https://doi.org/10.1016/j.jenvman.2017.04.061

Parsons, S. A., & Doyle, J. D. (2002). Struvite formation, control and recovery. *Water Research*, *36*(16), 3925–3940.

Pelalak, R., Soltani, R., Heidari, Z., Malekshah, R. E., Aallaei, M., Marjani, A., Rezakazemi, M., Kurniawan, T. A., & Shirazian, S. (2021). Molecular dynamics simulation of novel diamino-functionalized hollow mesosilica spheres for adsorption of dyes from synthetic wastewater. *Journal of Molecular Liquids*, *322*,

114812. https://doi.org/10.1016/j.molliq.2020.114812

Perera, M. K., Englehardt, J. D., & Dvorak, A. C. (2019). Technologies for Recovering Nutrients from Wastewater: A Critical Review. *Environmental Engineering Science*, *36*(5), 511–529. https://doi.org/10.1089/ees.2018.0436

Rahmani, A. R., Navidjouy, N., Rahimnejad, M., Nematollahi, D., Leili, M., Samarghandi, M. R., & Alizadeh, S. (2020). Application of the eco-friendly bio-anode for ammonium removal and power generation from wastewater in bio-electrochemical systems. *Journal of Cleaner Production*, *243*, 118589. https://doi.org/10.1016/j.jclepro.2019.118589

Razon, L. F. (2018). Reactive nitrogen: A perspective on its global impact and prospects for its sustainable production. *Sustainable Production and Consumption*, *15*, 35–48. https://doi.org/10.1016/j.spc.2018.04.003

Reig, M., Vecino, X., Aguilar-moreno, M., & Valderrama, C. (2022). *Ammonia Valorization by Liquid – Liquid Membrane Contactors for Liquid Fertilizers Production : Experimental Conditions Evaluation*.

Reig, M., Vecino, X., Gibert, O., Valderrama, C., & Cortina, J. L. (2021). Study of the operational parameters in the hollow fibre liquid-liquid membrane contactors process for ammonia valorisation as liquid fertiliser. *Separation and Purification Technology*, *255*(July 2020), 117768. https://doi.org/10.1016/j.seppur.2020.117768

Ren, Y., Hao Ngo, H., Guo, W., Wang, D., Peng, L., Ni, B. J., Wei, W., & Liu, Y. (2020). New perspectives on microbial communities and biological nitrogen removal processes in wastewater treatment systems. *Bioresource Technology*, *297*(November 2019), 122491. https://doi.org/10.1016/j.biortech.2019.122491

Robles, Á., Aguado, D., Barat, R., Borrás, L., Bouzas, A., Giménez, J. B., Martí, N., Ribes, J., Ruano, M. V., Serralta, J., Ferrer, J., & Seco, A. (2020). New frontiers from removal to recycling of nitrogen and phosphorus from wastewater in the Circular Economy. *Bioresource Technology*, *300*(October 2019), 122673. https://doi.org/10.1016/j.biortech.2019.122673

Rodríguez Arredondo, M., Kuntke, P., Jeremiasse, A. W., Sleutels, T. H. J. A., Buisman, C. J. N., & Ter Heijne, A. (2015). Bioelectrochemical systems for nitrogen removal

and recovery from wastewater. *Environmental Science: Water Research and Technology*, *1*(1), 22–33. https://doi.org/10.1039/c4ew00066h

Rongwong, W., & Goh, K. (2020). Resource recovery from industrial wastewaters by hydrophobic membrane contactors: A review. *Journal of Environmental Chemical Engineering*, *8*(5), 104242. https://doi.org/10.1016/j.jece.2020.104242

Rufí-Salís, M., Brunnhofer, N., Petit-Boix, A., Gabarrell, X., Guisasola, A., & Villalba, G. (2020). Can wastewater feed cities? Determining the feasibility and environmental burdens of struvite recovery and reuse for urban regions. *Science of the Total Environment, 737*. https://doi.org/10.1016/j.scitotenv.2020.139783

Sagberg, P., Ryrfors, P., & Berg, K. G. (2006). 10 years of operation of an integrated nutrient removal treatment plant: Ups and down. Background and water treatment. *Water Science and Technology*, *53*(12), 83–90. https://doi.org/10.2166/wst.2006.409

Salomon, M., Schmid, E., Volkens, A., Hey, C., Holm-Müller, K., & Foth, H. (2016). Towards an integrated nitrogen strategy for Germany. *Environmental Science and Policy*, *55*, 158–166. https://doi.org/10.1016/j.envsci.2015.10.003

Sancho, I., Licon, E., Valderrama, C., de Arespacochaga, N., López-Palau, S., & Cortina, J. L. (2017). Recovery of ammonia from domestic wastewater effluents as liquid fertilizers by integration of natural zeolites and hollow fibre membrane contactors. *Science of the Total Environment*, *584–585*, 244–251. https://doi.org/10.1016/j.scitotenv.2017.01.123

Serra-Toro, A., Vinardell, S., Astals, S., Madurga, S., Llorens, J., Mata-Álvarez, J., Mas, F., & Dosta, J. (2022). Ammonia recovery from acidogenic fermentation effluents using a gas-permeable membrane contactor. *Bioresource Technology*, *356*(May), 127273. https://doi.org/10.1016/j.biortech.2022.127273

Sheikh, M., Harami, H. R., Rezakazemi, M., Cortina, J. L., Aminabhavi, T. M., & Valderrama, C. (2023). Towards a sustainable transformation of municipal wastewater treatment plants into biofactories using advanced NH3-N recovery technologies: A review. *Science of the Total Environment*, *904*(May), 166077. https://doi.org/10.1016/j.scitotenv.2023.166077

Smith, C., Hill, A. K., & Torrente-Murciano, L. (2020). Current and future role of Haber-Bosch ammonia in a carbon-free energy landscape. *Energy and Environmental Science*, *13*(2), 331–344. https://doi.org/10.1039/c9ee02873k

Suzanne, E., Absi, N., & Borodin, V. (2020). Towards circular economy in production planning: Challenges and opportunities. *European Journal of Operational Research*, *287*(March), 168–190. https://doi.org/10.1016/j.ejor.2020.04.043

Szogi, A. A., Data, R. U. S. A., & Ariel, L. (2017). *(12) United States Patent*. *2*(12).

Tan, X., Tan, S. P., Teo, W. K., & Li, K. (2006). Polyvinylidene fluoride (PVDF) hollow fibre membranes for ammonia removal from water. *Journal of Membrane Science*, *271*(1–2), 59–68. https://doi.org/10.1016/j.memsci.2005.06.057

Tao, W., Bayrakdar, A., Wang, Y., & Agyeman, F. (2019). Three-stage treatment for nitrogen and phosphorus recovery from human urine: Hydrolysis, precipitation and vacuum stripping. *Journal of Environmental Management*, *249*(July), 109435. https://doi.org/10.1016/j.jenvman.2019.109435

Tarallo, S. (2015). A Guide to Net-Zero Energy Solutions for Water Resource Recovery Facilities. In *Water Intelligence Online* (Vol. 14). https://doi.org/10.2166/9781780407685

Tarpeh, W. A., Udert, K. M., & Nelson, K. L. (2017). Comparing ion exchange adsorbents for nitrogen recovery from source-separated urine. *Environmental Science and Technology*, *51*(4), 2373–2381. https://doi.org/10.1021/acs.est.6b05816

Thakur, I. S., & Medhi, K. (2019). Nitrification and denitrification processes for mitigation of nitrous oxide from waste water treatment plants for biovalorization: Challenges and opportunities. *Bioresource Technology*, *282*(January), 502–513. https://doi.org/10.1016/j.biortech.2019.03.069

Thorin, E., Olsson, J., Schwede, S., & Nehrenheim, E. (2018). Co-digestion of sewage sludge and microalgae – Biogas production investigations. *Applied Energy*, *227*(January 2017), 64–72. https://doi.org/10.1016/j.apenergy.2017.08.085

Ukwuani, A. T., & Tao, W. (2016). Developing a vacuum thermal stripping – acid absorption process for ammonia recovery from anaerobic digester effluent. *Water Research*, *106*, 108–115. https://doi.org/10.1016/j.watres.2016.09.054

Ulbricht, M., Schneider, J., Stasiak, M., & Sengupta, A. (2013). Ammonia recovery from industrial wastewater by transMembranechemiSorption. *Chemie-Ingenieur-Technik*, *85*(8), 1259–1262. https://doi.org/10.1002/cite.201200237

Uludag-Demirer, S., Demirer, G. N., & Chen, S. (2005). Ammonia removal from anaerobically digested dairy manure by struvite precipitation. *Process Biochemistry*, *40*(12), 3667–3674. https://doi.org/10.1016/j.procbio.2005.02.028

Vanotti, M. B., Dube, P. J., Szogi, A. A., & García-González, M. C. (2017). Recovery of ammonia and phosphate minerals from swine wastewater using gas-permeable membranes. *Water Research*, *112*, 137–146. https://doi.org/10.1016/j.watres.2017.01.045

Vecino, X., Reig, M., Bhushan, B., Gibert, O., Valderrama, C., & Cortina, J. L. (2019). Liquid fertilizer production by ammonia recovery from treated ammonia-rich regenerated streams using liquid-liquid membrane contactors. *Chemical Engineering Journal*, *360*(December 2018), 890–899. https://doi.org/10.1016/j.cej.2018.12.004

Vecino, X., Reig, M., Gibert, O., Valderrama, C., & Cortina, J. L. (2020). Integration of liquid-liquid membrane contactors and electrodialysis for ammonium recovery and concentration as a liquid fertilizer. *Chemosphere*, *245*, 125606. https://doi.org/10.1016/j.chemosphere.2019.125606

Verstraete, W., Van de Caveye, P., & Diamantis, V. (2009). Maximum use of resources present in domestic "used water." *Bioresource Technology*, *100*(23), 5537–5545. https://doi.org/10.1016/j.biortech.2009.05.047

Walsh, J. J., Jones, D. L., Edwards-Jones, G., & Williams, A. P. (2012). Replacing inorganic fertilizer with anaerobic digestate may maintain agricultural productivity at less environmental cost. *Journal of Plant Nutrition and Soil Science*, *175*(6), 840–845. https://doi.org/10.1002/jpln.201200214

Wang, P., Cheng, W., Zhang, X., Li, J., Ma, J., & Zhang, T. (2023). Engineering a protective surface layer to resist membrane scaling and scale-induced wetting in membrane distillation for the treatment of hypersaline wastewater. *Chemical Engineering Journal*, *452*(July 2022), 1–10. https://doi.org/10.1016/j.cej.2022.139167

WIDANARNI, EKASARI, J., & MARYAM, S. I. T. I. (2012). Evaluation of Biofloc Technology Application on Water Quality and Production Performance of Red Tilapia Oreochromis sp. Cultured at Different Stocking Densities. *HAYATI Journal of Biosciences*, *19*(2), 73–80. https://doi.org/10.4308/hjb.19.2.73

Wuang, S. C., Khin, M. C., Chua, P. Q. D., & Luo, Y. D. (2016). Use of Spirulina biomass produced from treatment of aquaculture wastewater as agricultural fertilizers. *Algal Research*, *15*, 59–64. https://doi.org/10.1016/j.algal.2016.02.009

Xie, M., Shon, H. K., Gray, S. R., & Elimelech, M. (2016). Membrane-based processes for wastewater nutrient recovery: Technology, challenges, and future direction. *Water Research*, *89*, 210–221. https://doi.org/10.1016/j.watres.2015.11.045

Yan, T., Ye, Y., Ma, H., Zhang, Y., Guo, W., Du, B., Wei, Q., Wei, D., & Ngo, H. H. (2018). A critical review on membrane hybrid system for nutrient recovery from wastewater. *Chemical Engineering Journal*, *348*(December 2017), 143–156. https://doi.org/10.1016/j.cej.2018.04.166

Yang, D., Le, L., Martinez, R., & Morrison, M. (2013). Hollow fibers structured packings in olefin/paraffin distillation: Apparatus scale-up and long-term stability. *Industrial and Engineering Chemistry Research*, *52*(26), 9165–9179. https://doi.org/10.1021/ie400126y

Yara International. (2022). *Fertilizer Industry Handbook 2022*. *December*, 32. https://www.yara.com/siteassets/investors/057-reports-and-presentations/other/2022/fertilizer-industry-handbook-2022.pdf/

Ye, Y., Ngo, H. H., Guo, W., Liu, Y., Chang, S. W., Nguyen, D. D., Liang, H., & Wang, J. (2018). A critical review on ammonium recovery from wastewater for sustainable wastewater management. *Bioresource Technology*, *268*(June), 749–758. https://doi.org/10.1016/j.biortech.2018.07.111

Yu, S., Qin, Y., Zhao, Q., Li, M., Yu, H., Kang, G., & Cao, Y. (2021). Nafion-PTFE hollow fiber composite membranes for ammonia removal and recovery using an aqueous-organic membrane contactor. *Separation and Purification Technology*, *271*(April), 118856. https://doi.org/10.1016/j.seppur.2021.118856

Yue, X., You, A., Liu, Y., Lai, M., & Zhang, K. (2023). Low-concentration methanol

effect on the microorganisms, nitrogen removal, and recovery of the completely autotrophic nitrogen removal over nitrite. *Water Science and Technology*, *87*(1), 130–143. https://doi.org/10.2166/wst.2022.417

Yüzbasıoglu, A. E., Tatarhan, A. H., & Gezerman, A. O. (2021). Decarbonization in ammonia production, new technological methods in industrial scale ammonia production and critical evaluations. *Heliyon*, *7*(10). https://doi.org/10.1016/j.heliyon.2021.e08257

Zarebska, A., Nieto, D. R., Christensen, K. V., & Norddahl, B. (2014). Ammonia recovery from agricultural wastes by membrane distillation: Fouling characterization and mechanism. *Water Research*, *56*, 1–10. https://doi.org/10.1016/j.watres.2014.02.037

Zhu, Y., Chang, H., Yan, Z., Liu, C., Liang, Y., Qu, F., Liang, H., & Vidic, R. D. (2024). Review of ammonia recovery and removal from wastewater using hydrophobic membrane distillation and membrane contactor. *Separation and Purification Technology*, *328*(September 2023), 125094. https://doi.org/10.1016/j.seppur.2023.125094

Zubair, M., Wang, S., Zhang, P., Ye, J., Liang, J., Nabi, M., Zhou, Z., Tao, X., Chen, N., Sun, K., Xiao, J., & Cai, Y. (2020). Biological nutrient removal and recovery from solid and liquid livestock manure: Recent advance and perspective. *Bioresource Technology*, *301*(October 2019), 122823. https://doi.org/10.1016/j.biortech.2020.122823

CHAPTER 2

Objectives and Thesis overview

2.1. Objectives

The primary objective of this PhD thesis is to advance the development of a N recovery process aimed at producing a liquid fertilizer as a high valuable product, by leveraging the high selectivity of hydrophobic membrane contactors. These contactors facilitate the transport of solutes only in vapor or gas phases through the membrane. The study will focus on different types of streams: urban wastewater generated in sewage sludge anaerobic digesters (side-streams) with concentrations of up to 1.5 $g \cdot L^{-1}$, wastewater from the chemical industry, ranging from diluted streams (0.1 $g \cdot L^{-1}$) to concentrated ones (>10 $g \cdot L^{-1}$) containing ammonium/ammonia and digested effluents from the food industry with a NH_3 concentration between 3.5 and 10 $g \cdot L^{-1}$ and a very high organic load.

To achieve this goal, laboratory-scale tests for ammonia recovery will be conducted using membrane contactors (hollow fiber and flat sheet) and to a lesser extent membrane distillation. The experimental approach will be tailored to generate results that align with the initially defined objectives.

Specifically, the research will address the following key aspects:

- Identify sample pre-treatment needs to reduce suspended solids (SS), chemical oxygen demand (COD) and alkalinity to ensure safe operation, determination and optimization of pre-treatment trains: comparison of coagulation/sedimentation stages with sand filtration or UF/NF membrane technologies.

- To analyse the performance of novel hollow fiber membrane polymer; polypropylene and polymethylpentene (SEPAREL®), to quantify and compare in terms of nitrogen recovery and the transport of water, using synthetic and real solution to identify physical and chemical fouling and scaling events; to determine mass transfer parameters influencing membrane performance and compare with existing literature.

- To obtain and evaluate the purity, composition and concentration of liquid fertilizers as a pure product in the form of fertilizer that helps to mitigate the overwhelming demand for fertilizers due to the exploitation of extensive agriculture with commercial solutions and to quantify and economically evaluate the cost of the by-product.

- To estimate the economic feasibility to determine the potential role of proven technology as an effective alternative to the current fertilizer industry, reducing the depletion of raw materials, cost and impact on the environment, all within the framework of a circular economy.

2.2. Thesis overview

This section aims to give a more concrete view of the chapters of this PhD thesis in line with the objectives assigned to this work to provide a better understanding, monitoring, and ease of reading the manuscript.

- Chapter 3. Impact of side-stream pre-treatment on ammonia recovery by membrane contactors: Experimental and economic evaluation
- Chapter 4. Ammonia Valorization by Liquid–Liquid Membrane Contactors for Liquid Fertilizers Production: Experimental Conditions Evaluation
- Chapter 5. Ammonium recovery and concentration from synthetic wastewater using a poly(4-methyl-1-pentene) (PMP) liquid-liquid membrane contactor: flux performance and mass transport characterization

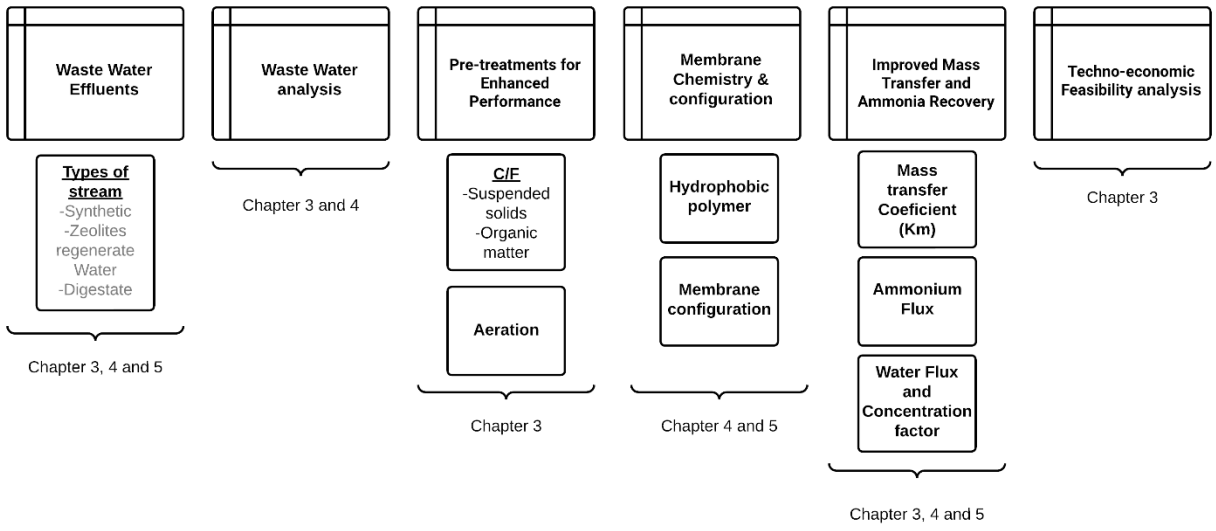

Figure 1. Graphical abstract of the project and how the chapters are interconnected in reference to the objectives. he six topics marked in this paper, along with their corresponding subtopics, appear in different chapters, outlining their relationships with each other.

CHAPTER 3

Impact of sidestream pre-treatment on ammonia recovery by membrane contactors: Experimental and economic evaluation

3.1. Abstract

Membrane contactor is a promising technology for ammonia recovery from anaerobic digestion centrate. However, high suspended solids and dissolved organic matter concentrations can reduce the effectiveness of the technology. In this study, coagulation-flocculation (C/F) and aeration pre-treatments were evaluated to reduce chemical oxygen demand (COD), turbidity, suspended solids and alkalinity before the ammonia recovery stage using a membrane contactor. The mass transfer coefficient (Km) and total ammonia (TAN) recovery efficiency of the membrane contactor increased from 7.80×10^{-7} to 1.04×10^{-5} $m \cdot s^{-1}$ and from 8 to 67%, respectively, after pre-treating the sidestream centrate. The pre-treatment results showed that dosing aluminium sulphate ($Al_2(SO_4)_3$) at 30 mg $Al^{+} \cdot L^{-1}$ was the best strategy for the C/F process, providing COD, turbidity and TSS removal efficiencies of 50±5, 95±3 and 90±4%, respectively. The aeration step reduced HCO_3^- content by 51±6% and allowed reducing alkaline consumption by increasing the pH before the membrane contactor. The techno-economic evaluation showed that the combination of C/F, aeration and membrane contactor can be economically feasible for ammonia recovery. Overall, the results of this study demonstrate that C/F and aeration are simple and effective techniques to improve membrane contactor performance for nitrogen recovery from the anaerobic digestion centrate.

Keywords: Gas permeable membrane; coagulation-flocculation; resource recovery; circular economy; techno-economic evaluation;

3.2. Introduction

Nutrient pollution is one of the major environmental problems due to excessive discharge of nitrogen and phosphorus into the environment. Anthropogenic activities and population growth have increased the amount of nitrogen contained in wastewater. The recovery of nitrogen is particularly important considering that ammonia is the second most produced chemical in the world (Beckinghausen et al., 2020; Lee et al., 2021; Razon, 2018). Ammoniacal-Nitrogen recovery has the potential (i) to reduce the dependency of Haber-Bosch process to obtain nitrogen-based fertilizers, (ii) to produce a fertilizer (e.g. NH_4NO_3, $(NH_4)_2HPO_4$, $(NH_4)_2SO_4$) suitable for commercialisation and (iii) to reintroduce

nitrogen into its cycle contributing to circular economy (Darestani et al., 2017; González Montiel, 2008). For this reason, it is important to develop efficient technologies for nitrogen recovery to support the transition of wastewater treatment plants (WWTPs) towards water resource recovery facilities (WRRF) (Puyol et al., 2017).

Several technologies have been proposed to recover nitrogen from wastewater treatment plants (WWTPs), such as ion exchange (IX) technologies (Kurniawan et al., 2006), membrane contactors (MC) (Hasanoğlu et al., 2010; Licon Bernal et al., 2016; Reig et al., 2021), or ultrafiltration (UF) (Hermassi et al., 2017). For instance, Wan et al. 2017, effectively recovered nutrients from the sludge fermentation liquor in a WWTP ($N\text{-}NH_4^+$ and $P\text{-}PO_4^{3-}$) using natural zeolites and proposed a model to predict that a maximum recovery of 94% ammonium and 98% phosphate could be achieved (Wan et al., 2017). Among them, ammoniacal nitrogen recovery through membrane contactors has been reported as a suitable technology to achieve high nitrogen recovery efficiencies with relatively low energy inputs (Darestani et al., 2017). By this technology, ammonia in gas form diffuses through a porous hydrophobic membrane from the feed solution to the acidic stripping solution. Subsequently, it can be recovered in ammonium form as a nitrogen-rich fertilizer. (Serra-Toro et al., 2022). Vecino et al. 2019, used a membrane contactor for ammonium recovery as a nutrient-based fertilizer product and achieved a maximum ammonium recovery of 94% using a regenerated stream with ion exchange from an initial sidestream wastewater (Vecino et al., 2019). Sheikh et al. 2022, also achieved similar values (>95%) of recovery using synthetic water and liquid-liquid hollow fibre MC (LL-HFMC) (Sheikh et al., 2022). Additionally, both membrane contactors and ion exchange technologies can be combined as proposed by Sancho et al. 2017. In that study, a concentrated ammonium stream was generated by means of liquid-liquid membrane contactors, by previously passing it through zeolites, achieving a recovery of 95% (Sancho et al., 2017). Thus, these publications highlight that membrane contactors have potential to achieve high recovery efficiencies and to obtain ammonium-free streams.

However, membrane contactors still need to overcome some challenges when using streams with high concentration of organic matter. Membrane fouling, caused by organic matter and/or suspended solids, can lead to the deposition of solids as a thin cake layer and increase pore clogging (Leiknes, 2009). This phenomenon generates a reduction of the flux during long-term operation. Thus, to maintain adequate flux levels, it is necessary

to increase energy and chemical consumption with a direct impact on the membrane lifetime and economic feasibility (Zarebska et al., 2014). In this regard, some pre-treatment strategies have been proposed to reduce fouling of membrane contactors, such as UF (Jiang, 2015), coagulation-flocculation (C/F) processes (Leiknes, 2009) or ion exchange (Rivadeneyra et al., 2007).

For example, Rivadeneyra et al. used ion exchange technology and observed a maximum chemical oxygen demand (COD) removal efficiency of 70% with an initial COD load of 4500 mg $O_2 \cdot L^{-1}$. Raghu et al. 2007, combined ion exchange with coagulation-flocculation and achieved a COD removal of 80% from an industrial wastewater effluent (Raghu & Ahmed Basha, 2007).

C/F consists of destabilization of colloids by surface modification. This reduces the electrostatic repulsive forces between the particles and leads to the formation of larger flocs with improved settling properties (Dosta et al., 2008). The most common coagulants and flocculants used are iron and aluminium salts because these chemicals have demonstrated their effectiveness to reduce the chemical oxygen demand (COD) of liquid streams (Krupińska, 2020; Postolachi et al., 2016). C/F has been widely applied in wastewater treatment applications as it allows removing organic and inorganic matter with relatively low costs (Jiang, 2015; Taboada-Santos et al., 2020). For instance, Al-Juboori et al. 2022 (Al-Juboori et al., 2022) evaluated the use of PAX/polymer or starch as a coagulant to pre-treat the centrate before a membrane contactor.

Besides C/F, aeration could also be a useful pre-treatment to reduce the amount of chemicals needed to increase the pH before the membrane contactor stage. Garcia-Gonzalez et al. 2015 applied low flow-rate aeration and increased the pH above 8.5 before the membrane contactor, which allowed reducing the operating costs of ammonia recovery by 57% (García-González et al., 2015). However, to the best of the authors' knowledge, the combination of C/F technology with aeration has not yet been used to pre-treat anaerobic digester centrate prior to a membrane contactor. Therefore, an experimental and economic study is needed to understand how C/F pre-treatment impacts the technical and economic competitiveness of implementing a membrane contactor system for nitrogen recovery.

The aim of this work is to evaluate the combination of C/F, aeration and membrane contactor processes to recover ammoniacal nitrogen from the effluent of an anaerobic digester (centrate). To this end, different operating conditions and chemical reagents were

evaluated for the C/F process. After the C/F process, an aeration stage was used to reduce the amount of bicarbonates in the centrate with a direct impact on the amount of chemicals needed for pH adjustment. Subsequently, the pre-treated centrate was fed to a membrane contactor system to understand how pre-treatment conditions impacted the performance of the membrane contactor and ammonium recovery efficiency. Finally, the economic potential of implementing these pre-treatment technologies before the membrane contactor was analysed.

3.3. Materials and Methods

3.3.1. Chemical reagent and wastewater source

Three types of coagulants were used for the coagulation-flocculation tests: (i) aluminium sulphate ($Al_2(SO_4)_3$ $18{\cdot}H_2O$) from Panreac®, Spain with a 96% of purity, (ii) iron chloride ($FeCl_3$) from Acros Organics®, Spain with a 98% of purity and (iii) a commercial coagulant HT20 from Derypol®, Spain. On the other hand, a mixture of Magnetite (Fe_3O_4) from Sigma-Aldrich®, USA with a 98% purity and silicon oxide (SiO_2) from Merck®, Germanywith a purity of 98% (relation of 30:70 %) was used as flocculant.

Different reagents were used for the chromatographic analysis: Methanesulfonic acid (CH_3SO_3H, 99%), sodium hydrogen carbonate ($NaHCO_3$, 99%), anhydrous sodium carbonate (Na_2CO_3, 99%), nitric acid (HNO_3 69%) and sodium hydroxide (NaOH 1 M). All these chemicals were analytical grade reagents and were supplied by Sigma-Aldrich®, USA.

The wastewater used in this study was the anaerobic digester centrate from a municipal WWTP located in the region of Barcelona (Spain). The centrate was decanted before the tests for 24h to reduce its concentration of COD, total suspended solids (TSS) and turbidity. The centrate used for the C/F tests contained COD and total ammonia nitrogen (TAN) concentrations of 786 mg $COD{\cdot}L^{-1}$ and 650 mg $N{\cdot}L^{-1}$, respectively measured by means photometry, which were within the range reported in the literature (Eskicioglu et al., 2018; Richter et al., 2020). It is worth mentioning that the water used for the flocculant tests came from the same location and had a similar ion concentration to that used in the other tests, although it contained a higher COD concentration (1650 mg $COD{\cdot}L^{-1}$).

3.3.2. Experimental design

The study was divided into two distinct stages (Figure 1). The first stage corresponded to the pre-treatment stage, selection of the optimum coagulant reagent and setting the optimum operating conditions with a specialized experimental design program. The specialized software Design Expert 11® (STAT-EASE, USA) allowed optimising mixing speed, mixing time and sedimentation time to maximize COD, TSS and turbidity removal efficiencies. Besides C/F, an aeration column for the removal of carbonate and the consequent increase of the pH was also considered. In the second stage, the performance of the membrane contactor (pH, ammonia concentration factor, ammonium recovery percentage) was tested with the untreated side-stream water and with the pre-treated water to evaluate the effectiveness of the pre-treatment on membrane contactor performance. Finally, an economic analysis was conducted to evaluate the feasibility of the application of this process train.

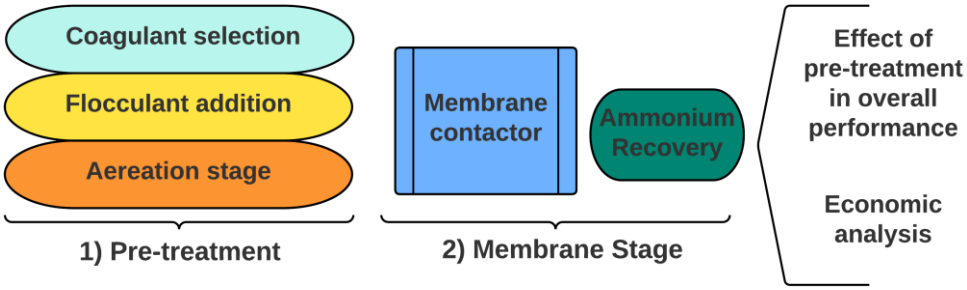

Figure 1. scheme of the different anaerobic side-stream treatment stages used in the present study.

3.3.3. Experimental set-up

3.3.3.1. Coagulant selection

The selection of the best coagulant reagent and dosage was based on combining literature screening and lab-scale tests. Initial literature research was carried out to determine the most common coagulants (Table 1) and it was observed that the most widely used coagulants were based on metals, such as aluminium or iron. After this initial screening, aluminium sulphate ($Al_2(SO_4)_3$), iron chloride ($FeCl_3$) and a commercial coagulant Derypol® HT20 (which is in the category of vegetable coagulants) were chosen.

Table 1. Most frequently used coagulants in water treatment according to bibliography.

Coagulant used	*Author*
Tanfloc POP	(Huang et al., 2019)
$Al_2(SO_4)_3$	(Fragoso et al., 2015)
$FeCl_3$	(Verma et al., 2010)
$FeCl_3$ + Clay Minerals	(Aygun & Yilmaz, 2010)
Lactic Acid	(Devesa-Rey et al., 2012)
$AlCl_3$	(Devesa-Rey et al., 2012)

The lab-scale tests were conducted in a Jar-test set-up (Jar-test *OVAN® JT60 E*), which consists of (i) six rotating stirring rods with adjustable speed and height and (ii) six beakers filled with 500 mL of the analysed centrate. Two set of experiments were conducted to determine the best coagulant and the dosage strategy for the C/F process.

The first set of experiments was designed to determine the two most favourable coagulants. In these tests, the type of coagulant was changed, while keeping the operating conditions constant. The dosage was set at 50 mg·L-1 and the mixing time was 5 minutes at a mixing speed of 200 rpm Table 2, which was based on available literature (Devesa-Rey et al., 2012; Fragoso et al., 2015; Hu et al., 2016; Wongcharee et al., 2020). The experiments were conducted in triplicate. The second set of experiments was designed (i) to determine the optimum dosage for the two flocculants selected in the previous experiments and (ii) to obtain the most favourable coagulant at this optimum dosage. All the coagulant dosages were referred to the quantity of metal added.

Table 2. Initial conditions for coagulant selection

Coagulant	*Dosage (mg·L-1)*	*Mixing time (min)*	*Mixing speed (rpm)*	*Settling time (min)*
$FeCl_3$				
$Al_2(SO_4)_3$	50	5	200	30

Derypol HT20

The impact of dosage on the efficiency of the C/F process was evaluated for the best coagulant. To this end, the dosage was varied from 10 to 800 mg·L-1 with the Jar-test conditions mentioned above. Table 3 lists the experimental conditions for these experiments. The experiments were conducted in triplicate.

Table 3. Experimental conditions for optimal dosage determination.

Coagulant	***Dosage (mg·L-1)***	***Mixing time (min)***	***Mixing speed (rpm)***	***Settling time (min)***
Optimal coagulant	10 30 50 100 200 400 800	5	200	30

3.3.3.2. Determination of the optimal operational conditions for the C/F process

Once the optimum coagulant chemical and dosage were selected, the most favourable operational parameters (i.e. mixing time, mixing speed and settling time) were determined by using the Jar-test equipment. For this purpose, a design programme was used to optimise the number of tests required and to determine the best operational conditions for the C/F process.

The Design Expert 11® (STAT-EASE, USA) software was used following the factorial design of Box-Behnken, which is based on dependent and independent variables (Ferreira et al., 2007). The dependent variables were those investigated and measured in the study, whereas the independent variables were modified to study their effect on the dependent variables (Vecino et al., 2021). Table 4 summarises the dependent variables studied in this work. The coded variables were assigned values of +1 (maximum), 0 (central) and -1 (minimum) depending on the variation of each variable.

Table 4. Individual dependent variables and their range of values.

Variable	Units	Studied range
Mixing time (MT)	min	5; 15; 25
Mixing velocity (MV)	Rpm	100; 175; 250
Resting time (RT)	min	15; 30; 45

The Box-Behnken design is a rotating or quasi-rotating second-order experimental design based on incomplete three-level factorial designs. The number of experiments (N) needed according to the Box-Behnken design can be obtained from Eq. 1.

$$N=2\cdot k(k-1)+C_0 \qquad \text{(Eq. 1)}$$

Where k is the number of variables, and C_0 is the number of central points (Apostol et al., 2011; Licon Bernal et al., 2016). In this case, three variables (MT, MV and RT) and five central points were studied resulting in seventeen experiments. The Box-Behnken experimental designs were applied by means of Eq. 3 and 4 (Licon Bernal et al., 2016).

$$y=\beta_0 \sum_{i=1}^{k} \beta_i X_i \sum_{i=1}^{k} \sum_{j\geq 1}^{k} \beta_{ij} X_i X_j+\varepsilon \qquad \text{(Eq.2)}$$

$$y=\beta_0 \sum_{i=1}^{k} \beta_i X_i +\beta_0 \sum_{i=1}^{k} \beta_{ii} X_i^2+ \sum_{i=1}^{k} \sum_{j\geq 1}^{k} \beta_{ij} X_i X_j+\varepsilon \qquad \text{(Eq.3)}$$

Where β_o is the constant factor, β_i represents the coefficients of the linear parameters, k is the number of variables, Xi and Xj represent the independent variables, ε is the residual factor associated with the experiments, y is the dependent variable, β_{ij} represents the coefficients of the interaction parameters and β_{ii} represents coefficients of the quadratic values.

Finally, the software allows analysing the obtained results to provide the optimal conditions (e.g., removal of each of COD, TSS and turbidity) through the analysis of figures and data.

3.3.3.3. Coagulation test for the optimal coagulant conditions and dosage

The optimal coagulant and dosage obtained from stage 1 and 2 were tested to determine the experimental COD, TSS and turbidity removal efficiencies under the most favourable conditions. In this assay, the optimal conditions determined by the two previous tests were

applied in the Jar-test equipment and it was verified if the theoretical results provided by the experimental design software were experimentally fulfilled. The experiments were conducted in triplicate.

3.3.3.4. Flocculation test

Flocculation tests were conducted to evaluate if combining coagulant and flocculant addition improves solids removal efficiency when compared with stand-alone coagulant addition. The flocculation experiments were carried out with the optimal conditions obtained from the previous experiments and adding different dosages (0-50 mg·L-1) of a flocculant clay-based (Fe_3O_4(s) and SiO_2(s)) that works effectively with metal-based coagulants for COD reduction (Aygun & Yilmaz, 2010). The flocculant was prepared by pulverizing and mixing Fe_3O_4 and SiO_2 with a relation of 30% Fe_3O_4 and 70% of SiO_2. Table 5 shows the operational parameters used for the flocculation tests.

Table 5. Flocculation parameters

Flocculation Parameters	
Mixing time	30 min
Mixing speed	30 rpm
Resting time	30 min
Dosage	10, 25, 30, 40 and 50 mg
Flocculant	Fe_3O_4 + SiO_2 (30-70%)

3.3.3.5. Aeration tests

The possibility of adding an aeration stage (Dube et al., 2016; García-González et al., 2015; Vanotti et al., 2017) was evaluated: i) to increase the pH of the centrate and ii) to reduce the concentration of carbonates present in the sample. The aeration tests were carried out in an open aeration column of 3.5 m height and 30 cm diameter with a capacity of 25 L. The air was introduced at the bottom of the tank through an electric compressor at a flow rate of 2 Nm^3/h. The column was filled with the centrate and a constant air flow rate (364 l/h) was applied for a period of time adequate to cause reactions described by Eqs. 4-6.

$$HCO^-_{3(aq)} + H^+_{(aq)} \leftrightarrow CO_{2(aq)} + H_2O_{(l)} \quad \text{(Eq.4)}$$

$$CO_{2(aq)} \leftrightarrow CO_{2(g)} \quad \text{(Eq.5)}$$

$$NH^+_{4(aq)} \leftrightarrow NH_{3(g)} + H^+_{(g)} \quad \text{(Eq.6)}$$

Thus, these experiments allowed bicarbonate conversion to $CO_2(g)$ (aq) (Eq 4) due to the aeration process promoting the removal of dissolved $CO_2(g)$ (aq) as $CO_2(g)$ (Eq. 5) and consequently increasing the pH. Subsequently, the pH increased at levels close to pKa. allowed the conversion of NH_4^+ into ammonia. (Eq. 6). The aeration experiments were performed in duplicate.

3.3.3.6. Flat-sheet membrane contactor

The different pre-treatment processes aimed at conditioning the centrate to reduce fouling and clogging in the membrane contactor. A flat-sheet membrane contactor similar to the one used by Hasanoğlu et al. 2010, was used in this study (Hasanoğlu et al., 2010). The polytetrafluoroethylene (PTFE) membrane had a surface area of 90 cm^2 and a pore size of 0.2 µm. The pH of the feed solution was increased up to 10.2 with NaOH 1 M, to shift the equilibrium towards NH_3. The feed solution was stored in a 5 L tank, whereas the acid stripping solution (Concentration of 0.4 M of nitric acid) was stored in a 1.5 L tank. Both tanks were continuously agitated, while nitric acid was continuously added to maintain the pH of the stripping solution in the acidic regime (pH < 2). The feed and stripping solutions were circulated at 450 ml/min in counter current mode towards both sides of the membrane. Further details of the membrane contactor set-up can be found elsewhere (Reig et al., 2021).

The ammonia flux through the membrane is driven by the difference between the partial pressure on both sides of the membrane, ($p_{NH_3,f}$-$p_{NH_3,s}$) and the mass transfer coefficient ($K_{m(NH_3)}$) (Eq. (7)).

$$J_{NH_3} = \frac{K_{m(NH_3)}(p_{NH_3,f} - p_{NH_3,s})}{RT} \quad (7)$$

Where $p_{NH_3,s}$ is the partial pressure of ammonia in the shell side (atm), $p_{NH_3,f}$ is the partial pressure in the feed side (atm), $K_{m(NH_3)}$ is the ammonia mass transfer coefficient ($m \cdot s^{-1}$), R is the universal gas constant coefficient (0.082 $atm \cdot m^3 \cdot K^{-1}$ mol·K) and T is the temperature of the system (K).

Subsequently, Eq. (7) can be expressed as Eq. (8) considering that: (i) the partial pressure of ammonia on both sides of the membrane can be assumed as the concentration of ammonia on either side, (ii) the pH does not vary during the experimental procedure, meaning that the concentration of ammonia is proportional to the TAN concentration in

the feed solution and (iii) the ammonia partial pressure in the stripping side is negligible (Licon Bernal et al., 2016; Vecino et al., 2019).

$$\ln \frac{C_{0(NH_3)f}}{C_{t(NH_3)f}} = \frac{K_{m(NH_3)} A_m}{V_f} t \quad (8)$$

Where A_m is the membrane area (m^2), $C_{0(NH_3)f}$ and $C_{t(NH_3)f}$ are the feed ammonia concentration ($mg \cdot L^{-1}$) at the initial time and at the experimental time, respectively, and V_f is the feed volume (m^3).

The tests were conducted for both untreated and pre-treated centrate to evaluate and compare the membrane contactor performance before and after pre-treatment implementation.

3.3.4. Analytical methods

The anions and cations were analysed by an ion chromatography system (Dionex ICS-1000 and ICS-1100 Thermo-Fisher Scientific, USA) equipped with a cationic detector (ICS-1000) and an anionic detector (ICS-1100) and controlled by Chromeleon® chromatographic software. A CS16 column (4 x 250 mm) and an AS23 column (4 x 250 mm) (Phenomenex, Barcelona, Spain) were used for cation and anion determination and quantification, respectively. The mobile phase was a 0.03 $mol \cdot L^{-1}$ CH_3SO_3H solution for the cation system, and a mixture of 0.8 $mmol \cdot L^{-1}$ $NaHCO_3$ and 4.5 $mmol \cdot L^{-1}$ Na_2CO3 for the anion system.

The COD was analysed through the Standard Method 5220C (Matthews, 2014) using a multiparametric photometer HI83224 (Hanna Instruments, Italy), whereas TSS were analysed through the Standard Method 2540D (APHA, 2012). A turbidimeter HI 93703 (Hanna instruments, Italy) was used to measure the turbidity. Total alkalinity was measured by titration following the Standard Method 2320B (APHA Method 2320, 1992)and using a T70 titrator (Mettler Toledo, United States).

3.3.5. Economic analysis

An economic analysis was conducted to evaluate the techno-economic implications of implementing a membrane contactor system for ammonia recovery from the anaerobic digester centrate. Figure 2 shows the configuration evaluated in the economic analysis,

which included four different stages: (i) C/F with $Al_2(SO_4)_3$ to enhance solids sedimentation, (ii) precipitation for suspended solids removal, (iii) aeration to desorb part of the solubilised CO_2 and reduce the alkalinity, and (iv) membrane contactor system for nitrogen recovery.

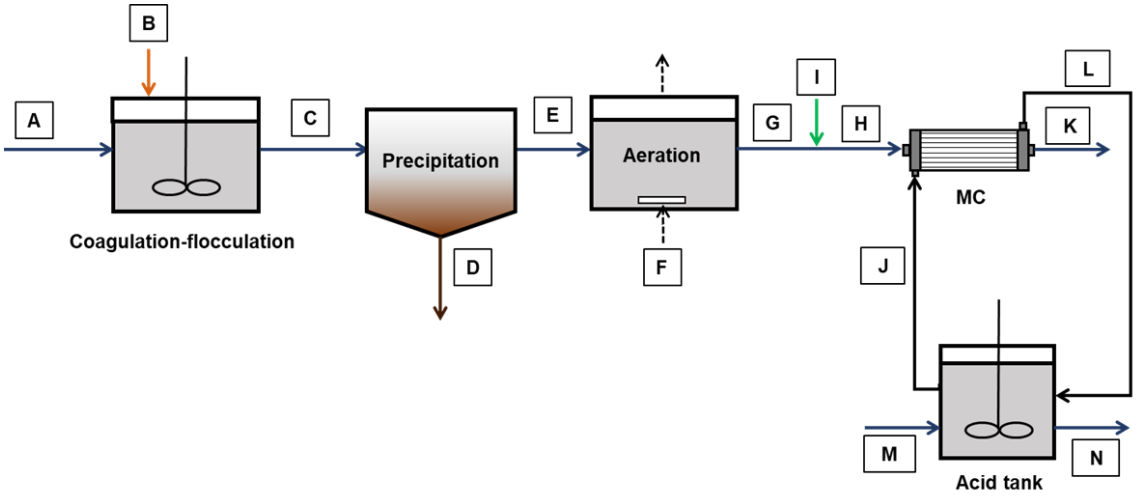

Figure 3. Schematic representation of the nitrogen recovery scheme.

The membrane contactor system was operated using a HNO_3 trapping solution and considering a relation between the feed and trapping solution flow rate of 1:1. The pH of the feed solution was adjusted to 10.2 with NaOH to shift the NH_4^+/NH_3 equilibrium towards NH_3. The trapping solution was continuously recirculated from the acid tank to the membrane contactor and replaced when the pH increased up to 6 (Richter et al., 2020). The mass balance was obtained considering that the WWTP generated 150 $m^3 \cdot day^{-1}$ of centrate, containing TAN and TSS concentrations of 0.71 g $N \cdot L^{-1}$ and 0.24 g $TSS \cdot L^{-1}$, respectively. Detailed information on the mass balance can be found in Table 5.

Table 5. Main flow data for the nitrogen recovery scenario under study.

(A) **Anaerobic digester centrate**	**Unit**	**Value**
Flow rate	$m^3 \cdot day^{-1}$	150
TSS	$g \cdot L^{-1}$	0.24
TAN	g $N \cdot L^{-1}$	0.71
pH	-	8.1
(B) $Al_2(SO_4)_3$ solution		
Flow rate	$m^3 \cdot day^{-1}$	9
$Al_2(SO_4)_3$	$mg \cdot L^{-1}$	500
(C) Coagulation-flocculation effluent		
Flow rate	$m^3 \cdot day^{-1}$	159

TSS	$g \cdot L^{-1}$	0.22
TAN	$g\ N \cdot L^{-1}$	0.67
pH	-	8.1
(D) Solid fraction precipitator		
Flow rate	$m^3 \cdot day^{-1}$	8
TSS	$g \cdot L^{-1}$	3.98
(E) Liquid fraction precipitator		
Flow rate	$m^3 \cdot day^{-1}$	151
TAN	$g\ N \cdot L^{-1}$	0.67
pH	-	7.9
(F) Air		
Flow rate	$m^3 \cdot day^{-1}$	2288
(G) Effluent aeration tank		
Flow rate	$m^3 \cdot day^{-1}$	151
TAN	$g\ N \cdot L^{-1}$	0.67
pH	-	8.9
(I) NaOH solution		
Flow rate	$m^3 \cdot day^{-1}$	0.3
NaOH	$mol \cdot L^{-1}$	1
(H) Feeding solution $MC_{t=0}$		
Flow rate	$m^3 \cdot day^{-1}$	151.3
TAN	$g\ N \cdot L^{-1}$	0.67
pH	-	10.3
(K) Feeding solution $MC_{t=F}$		
Flow rate	$m^3 \cdot day^{-1}$	151.3
TAN	$g\ N \cdot L^{-1}$	0.24
pH	-	8.42
(M) HNO_3 solution		
Volume/cycle	m^3/cycle	0.52
Number of cycles	cycles/day	22
HNO_3	$mol \cdot L^{-1}$	0.4
pH	-	0.4
(N) NH_4NO_3 solution		
Volume/cycle	m^3/cycle	0.52
Number of cycles	cycles/day	22
NH_4NO_3	$mol \cdot L^{-1}$	0.4
pH	-	6

The capital costs, operating costs and revenues were calculated using both lab-scale data and literature average values. The capital costs accounted for membrane contactor, tanks, stirrers, blowers and pumps, whereas the operating costs accounted for energy consumption, sludge disposal, equipment replacement and chemicals' purchase (i.e.,

$Al_2(SO_4)_3$, NaOH and HNO_3). Finally, the revenues were obtained considering (i) the commercialisation of the produced NH_4NO_3 and (ii) the lower nitrogen load to be treated in the mainstream of the WWTP. Table 6 and 7 of the summarise the main design and cost parameters used for the economic analysis.

The present value (PV) of the gross cost and revenues were calculated for the nitrogen recovery configuration by using Eq. (9) and Eq. (10), respectively. Subsequently, Eq. (11) was used to calculate the net present value (NPV):

$$PV_{GC}=CAPEX+\sum_{t=1}^{T}\frac{OPEX_t}{(1+i)^t} \quad (9)$$

$$PV_R=\sum_{t=1}^{T}\frac{R_t}{(1+i)^t} \quad (10)$$

$$NPV=\sum_{t=1}^{T}\frac{R_t\text{-}OPEX_t}{(1+i)^t}\text{-}CAPEX \quad (11)$$

Where CAPEX is the capital expenditure (€), $OPEX_t$ is the operating expenditure at year t (€), R_t is the revenue at year t (€), PV_{GC} is the PV of the gross cost (€), PV_R is the PV of the revenues (€), NPV is the net present value (€), i is the discount rate (5%) and T is the plant lifetime (20 years).

Table 6. Main design parameters used for the economic evaluation.

	Parameter	Value	Source
Coagulation-flocculation	Specific $Al_2(SO_4)_3$ consumption (g $Al_2(SO_4)_3 \cdot L^{-1}_{centrate}$)	0.19	Lab-scale data
	Retention time (h)	0.1	Lab-scale data
	Mixer revolutions (rpm)	100	Lab-scale data
Precipitation	Retention time (h)	0.5	Lab-scale data
	Q_0/Q_E (%)	95	Lab-scale data
Aeration	Retention time (h)	1	Lab-scale data
	Specific air consumption ($NL \cdot h^{-1} \cdot L^{-1}_{tank}$)	364	Lab-scale data
Membrane contactor	K_m ($m \cdot s^{-1}$)	1.04×10^{-5}	Lab-scale data
	TAN recovery (%)	64	Lab-scale data

Flow rate trapping solution:Flow rate feed solution	1:1	Lab-scale data
Specific NaOH consumption (mol NaOH·mol^{-1} $TAN_{recovered}$)	0.067	Lab-scale data
$pH_{t=0}$ HNO_3 trapping solution (-)	0.4	Lab-scale data
$pH_{t=F}$ HNO_3 trapping solution (-)	6	(Richter et al., 2020)

Table 7. Main economic parameters used for the economic evaluation.

Parameter	Value	Source
Tank cost (€/m^3)	220	(Verrecht et al., 2010)
Settler cost (€/m^3)	100	(Noriega-Hevia et al., 2021)
Pump cost (€/m^3/h)	12.1	(Verrecht et al., 2010)
Stirrer cost (€/m$^3_{Tank}$)	27.8	(Vinardell et al., 2020)
Blower cost (€/Nm^3/h)	4.15	(Verrecht et al., 2010)
Membrane cost (€/m^2)	49	(Noriega-Hevia et al., 2021)
$Al_2(SO_4)_3$ cost (€/kg)	0.16	(Vu et al., 2020)
NaOH cost (€/kg)	0.62	(Bouzas et al., 2019)
HNO_3 cost (€/kg)	0.38	(Das et al., 2018)
Electricity cost (€/kWh)	0.1445	(Eurostat, 2021)
Sludge disposal cost (€/t TS)	373	(Foladori et al., 2015)
Lifetime membrane (years)	10	(Noriega-Hevia et al., 2021)
Lifetime auxiliary equipment (years)	10	(Noriega-Hevia et al., 2021)
NH_4NO_3 price (€/kg)	0.43	(Ministerio de Agricultura Pesca y Alimentación, 2022)
Energy consumption mainstream N removal (kWh/kg N)	2.38	(Horstmeyer et al., 2018)

3.4. Results and discussion

The following sections discuss the results concerning the application of C/F and aeration pre-treatments before a membrane contactor. Table 8 shows the COD, TSS, turbidity and ions concentrations of the centrate wastewater used for these tests.

Table 8. Initial centrate characterization. The errors represent standard deviation (n=3).

Parameter	value	Units
Calcium	90.5±26.8	$mg \cdot L^{-1}$
Carbonates	3366.7±792.5	$mg \cdot L^{-1}$
Chlorine	348.0±15.4	$mg \cdot L^{-1}$
COD	786.0±126.7	$mg\ O_2 \cdot L^{-1}$
Magnesium	33.6±13.4	$mg \cdot L^{-1}$
Nitrate	30.7±8.8	$mg \cdot L^{-1}$
Phosphate	138.1±30.2	$mg \cdot L^{-1}$
Potassium	146.6±7.6	$mg \cdot L^{-1}$
pH	8.2 ± 0.1	--
Sodium	474.4±18.4	$mg \cdot L^{-1}$
Sulphate	37.5±10.8	$mg \cdot L^{-1}$
TAN	650 ±64.5	$mg \cdot L^{-1}$
TSS	235.0±104.7	$mg \cdot L^{-1}$
Turbidity	275.1±106.2	NTU

3.4.1. Coagulant and dosage selection for the C/F process

Table 9. Presents the COD and turbidity removal efficiencies for the three coagulants ($FeCl_3$, $Al_2(SO_4)_3$ and Derypol® HT20) analysed in this study. The $Al_2(SO_4)_3$ coagulant achieved the best COD removal efficiencies (50.2 ± 1.1%), followed by $FeCl_3$ (38.9 ± 0.3%) and Derypol HT20 (36.0 ± 0.3%). Thus, $Al_2(SO_4)_3$ and $FeCl_3$ were selected for the next set of experiments. The turbidity removal efficiencies ranged from 74.2 to 84.7 %. The lowest turbidity values were obtained by using $FeCl_3$ (74.2 $mg \cdot L^{-1}$) and they were similar to those achieved by Abdessemed et al. 2000, which achieved turbidity removal values of 66.1% using $FeCl_3$ (Abdessemed et al., 2000).

Table 9. Results obtained on COD removal (%) and Turbidity reduction for the coagulation assays coagulant test. The errors represent standard deviation (n=3).

Coagulant	*COD removal (%)*	*Turbidity reduction (%)*
$Al_2(SO_4)_3$	**50.2±1.1**	**82.3±1.1**
Derypol HT20	**36.0±0.3**	**84.7±0.4**
$FeCl_3$	**38.9±0.3**	**74.2±1.7**

Table 10. Results of water quality improvement for the coagulation experiments (COD removal (%), Turbidity reduction (%)) as a function of coagulant type and coagulant dose. The errors represent standard deviation (n=3).

Dosage	**$Al_2(SO_4)_3$**			**$FeCl_3$**		
($mg \cdot L^{-1}$)	COD removal	Turbidity reduction	pH	COD	Turbidity reduction	pH
10	51.5 ± 1.2	80.4 ± 2.8	8.0	42.5 ± 0.7	60.3 ± 1.2	8.0
30	56.2 ± 1.0	85.5 ± 4.4	7.7	48.0 ± 0.9	71.2 ± 1.2	7.9
50	50.1 ± 1.7	82.3 ± 3.5	7.4	38.9 ± 1.6	74.2 ± 2.4	7.7
100	41.1 ± 0.9	76.7 ± 1.2	7.1	41.5 ± 1.9	80.6 ± 3.4	7.4
200	62.1 ± 1.2	86.6 ± 4.0	6.9	45.1 ± 2.1	87.9 ± 3.3	7.1
400	66.7 ± 2.5	82.2 ± 1.7	6.1	50.0 ± 1.9	90.4 ± 4.1	6.7
600	64.7 ± 2.1	55.5 ± 2.4	4.3	52.5 ± 1.8	95.7 ± 3.4	6.4
800	66.9 ± 1.0	27.3 ± 3.3	4.1	51.8 ± 1.7	97.0 ±3.0	5.8

Table 10 lists the COD and turbidity removal efficiencies of $Al_2(SO_4)_3$ and $FeCl_3$ for concentrations ranging from 10-800 $mg \cdot L^{-1}$. The results showed that $Al_2(SO_4)_3$ provided better COD removal performance in comparison to $FeCl_3$, which reinforces the idea that $Al_2(SO_4)_3$ is the most favourable coagulant-flocculant to be used as a membrane contactor pre-treatment. On the one hand, the COD removal efficiency increased from 42.5 ± 0.7 to 51.8 ± 1.7% as the $FeCl_3$ concentration increased from 10 to 800 $mg \cdot L^{-1}$, respectively. On the other hand, the COD removal efficiency increased from 51.5 ± 1.2 to 62.1 ± 1.2% as the $Al_2(SO_4)_3$ concentration increased from 10 to 200 $mg \cdot L^{-1}$, respectively. However, in the case of $Al_2(SO_4)_3$, dosages above 200 $mg \cdot L^{-1}$ only led to minimal improvements in the COD removal efficiency. This behaviour is due to the fact that applying coagulant dosages above the optimal does not lead to considerable improvements (Duan & Gregory, 2003).

The results also showed that the pH progressively decreased as the coagulant dosage increased. In the case of$Al_2(SO_4)_3$, when the metal ion (Al^{+3}) hydrolyses in water, it reacts to form complexes ($Al(OH)_n^{+(n-3)}$) compounds. This leads to the formation of $CO_2(g)$, which increases the acidity of the solution (Krupińska, 2020). From the results of Table 6, it can be concluded that dosing 30 $mg \cdot L^{-1}$ of Al ($Al_2(SO_4)_3$) can be considered as the optimum strategy because this dosage achieved similar COD removal efficiencies than those achieved above 200 $mg \cdot L^{-1}$, while reducing the coagulant dosage more than seven times.

3.4.2. Optimisation of the operating conditions for the C/F process

After selecting the optimum coagulant and dosage ($Al_2(SO_4)_3$, 30 mg $Al^{+} \cdot L^{-1}$), the impact of the operational conditions (i.e. mixing time, mixing speed and settling time) on the C/F efficiency was evaluated. Seventeen experiments were tested based on the outputs provided by the Design Expert 11 software (Table 11).

Table 11. Experiments set of Design Expert 11 software.

Run	***M. Time (min)***	***M. Speed (rpm)***	***S. Time (min)***	***Run***	***M. Time (min)***	***M. Speed (rpm)***	***S. time (min)***
1	25	100	45	***10***	25	250	15

2	15	175	30	***11***	5	100	45
3	5	250	15	***12***	5	250	45
4	15	175	30	***13***	15	175	37.5
5	25	250	45	***14***	10	175	30
6	25	100	15	***15***	5	100	15
7	15	137.5	30	***16***	15	175	30
8	15	175	22.5	***17***	15	212.5	30
9	20	175	30				

These experiments were conducted changing the mixing time, the mixing speed and the settling time. Figure 3 shows the theoretical TSS, turbidity and COD removal values obtained from the Design Expert 11 software for the different mixing time and mixing speed conditions at a fixed settling time of 30 min. It is worth mentioning that only the results of 30 min settling time are illustrated because this condition provided the best results when compared with the other settling times. The results highlighted that reducing the mixing time to 5 minutes and the mixing speed to 100 rpm, would theoretically increase removal values up to 100% in turbidity and suspended solids and up to 70% in COD. Accordingly, the software revealed that there was better removal when mixing time and speed were reduced to the minimum tested values. This behaviour was in agreement with Kan et al. 2002, who reported that higher mixing speed did not give a better coagulation performance (Kan et al., 2002).

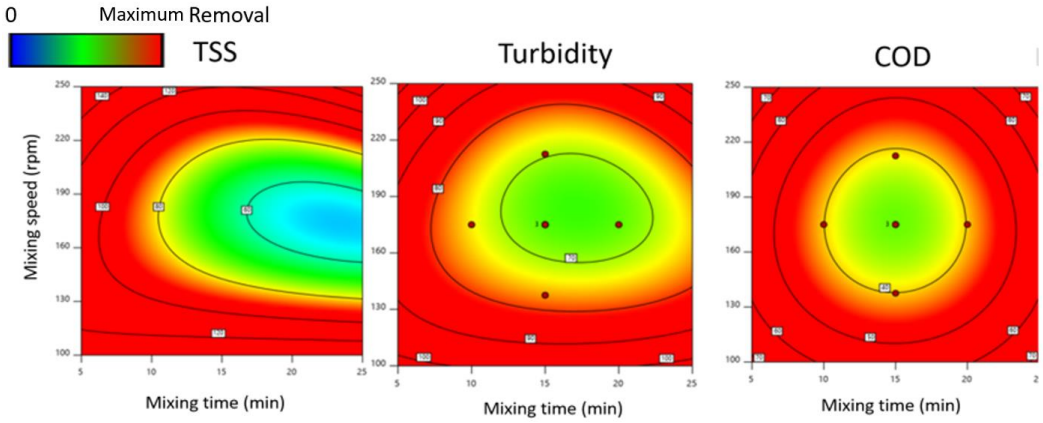

Figure 3. Theoretical TSS, turbidity and COD removal values for different mixing times and mixing speeds, at a fixed settling time of 30 min (graphics obtained from the Design Expert 11 software).

Subsequently, coagulation tests were carried out with the optimum conditions obtained from the software. Table 12 illustrates the results of these tests in terms of TSS, turbidity and COD removal values.

Table 12. Experimental COD, TSS and Turbidity removal using optimal conditions extracted from Design Expert 11. The errors represent standard deviation (n=3).

Variables	Studied conditions	Parameters	Experimental removal (%)
Mixing Time	5 min	COD	58.1 ± 0.3
Mixing Velocity	100 rpm	TSS	94.9 ± 0.2
Settling time	30 min	Turbidity	89.8 ± 0.8

The removal values showed an improvement compared with the previous test (58.1 ± 0.3 COD, 94.9 ± 0.2 TSS and 89.8 ± 0.8 turbidity), although the values predicted by the design software were not achieved. Guimarães et al. 2020, tested several coagulants (including aluminium sulphate at 40 $mg \cdot L^{-1}$ Al) and reached COD removal efficiencies (38%) below those achieved in this study (58%) (Guimarães et al., 2020). On the other hand, Salem et al. 2021 reported turbidity removal efficiencies of 86%, which were similar than those achieved in this study (90%)(Salem & AL-Musawi, 2021).

3.4.3. Flocculation stage

Figure 4 shows the obtained values of COD and turbidity removal for the different dosages of flocculant Fe_3O_4/SiO_2 (30-70% (w/w)) added. A test without flocculant was also conducted, which consisted in applying the optimum dosages and parameters obtained from the coagulant stage tests (Section 3.1). The results illustrated maximum COD removal (89.7 %) when the flocculant dosage was 10 $mg \cdot L^{-1}$ and maximum turbidity removal (83.6 %) when the dosage was increased up to 30 $mg \cdot L^{-1}$. In all the tests, the TSS removal values remained practically constant around 95%. Sultana et al. 2022, treated wastewater with an organic concentration (745 mg $O_2 \cdot L^{-1}$) similar to the present study water (786 mg $O_2 \cdot L^{-1}$) using aluminium sulphate coagulant and clay-based flocculant (Sultana et al., 2022). The authors obtained COD removal efficiencies of 46.7%, which are below those achieved in this study. On the other hand, Preston et al.

2010, worked with wastewater with a similar turbidity (300 NTU) than that of the present study (275 NTU), using aluminium sulphate as coagulant and Moringa as natural flocculant, and reached a similar turbidity removal of 96.2% (Preston et al., 2010). Overall, Figure 4 results revealed that the different doses addition of $Fe_3O_4(s)/SiO_2(s)$ only led to small improvements concerning removal values.

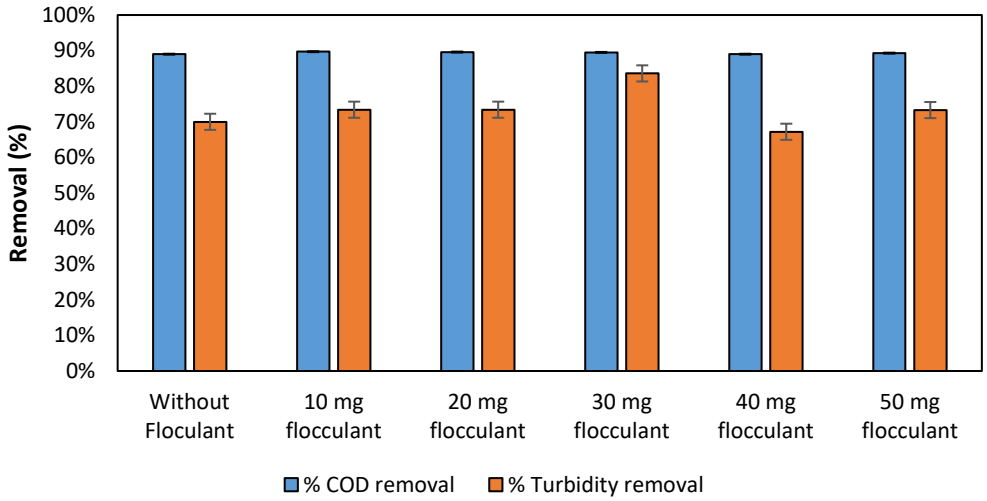

Figure 4. Removal of COD (%) and turbidity (%) from anaerobic centrate after $Fe_3O_4(s)/SiO_2(s)$ addition. The errors bars represent standard deviation (n=3).

According to the results obtained, it could be suggested that the addition of coagulant + flocculant did not necessarily yield a consistent positive improvement compared to the addition of only coagulant.

3.4.4. Aeration Stage

An aeration step was added after coagulation-flocculation to promote $CO_2(g)$ stripping to reduce alkalinity and increase the pH before the membrane contactor system (Dube et al., 2016). Figure 5 shows the evolution of HCO_3^- removal and pH over the aeration time. The HCO_3^- present in the centrate was reduced about 50% after 240 min of constant aeration, although almost 30% of elimination was reached after 15 minutes. The results showed that after 1h of operation time a compromise between carbonates removal (34%) and pH increase (8.83) was achieved, although higher removal values could be reached at expenses of higher times of operation. This agrees with the pH results, where a sudden

increase was observed after 15 minutes of aeration, reaching a constant value after 240 min. It is worth mentioning that the application of aeration could also lead to NH_3 losses due to volatilisation, although they did not account for more than 2% in our study (data not shown).

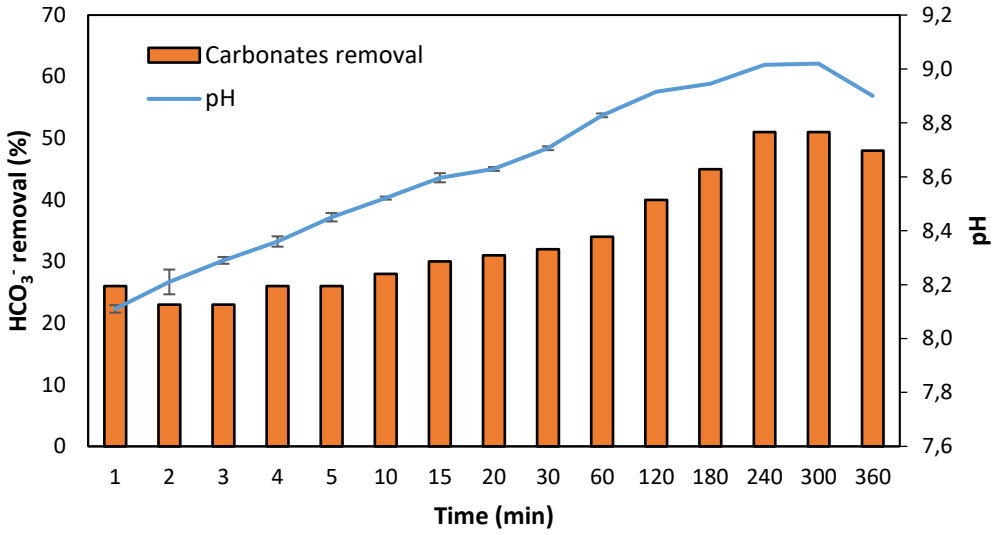

Figure 5. Variation of pH and the efficiency of HCO_3^- removal with time in the aeration stage. The errors bars represent standard deviation (n=3).

García-González et al. 2015, also used an aeration system as a membrane contactor pre-treatment stage. The aeration system increased the pH above 8.5, which allowed partially shifting NH_4^+/NH_3 equilibrium towards NH_3 without the addition of external chemicals (García-González et al., 2015). Besides technical aspects, aeration implementation has the potential to reduce the total cost of the process by 70% due to the reduction in alkaline purchasing cost (Dube et al., 2016). It is also relevant to mention that it is possible to use recycled chemicals to further reduce the operating cost of the system.

3.4.5. Flat-sheet membrane contactor stage

Figure 6 shows the membrane contactor results for the treated and untreated centrate during the experimental time. The results illustrated that the TAN recovery efficiency increased from 7.5 to 66.6% after implementing the pre-treatment train (C/F and Aereation) (Figure 6B). This highlighted that C/F and aeration pre-treatments are crucial to improve the TAN recovery efficiency from the anaerobic digester centrate using membrane contactors. In the case of the pre-treated centrate, the TAN concentration in

the feed solution decreased from 0.9 g·L^{-1} to 0.3 g·L-1 (Figure 6A), whereas the TAN concentration in the acid solution increased from 0 to 2.7 g·L^{-1} (Figure 6C). This is consistent with the outputs of other studies recovering TAN using membrane contactors (Hasanoğlu et al., 2010; Vecino et al., 2019). Similarly, the results obtained in terms of concentration factor are in line with the results of TAN in the acid tank. The concentration factor corresponded to 3.9 and was obtained from the relationship between the ammonium concentration in the acid tank (3.5 g·L^{-1}) and the initial ammonium concentration in the feed tank (0.9 g·L^{-1}).

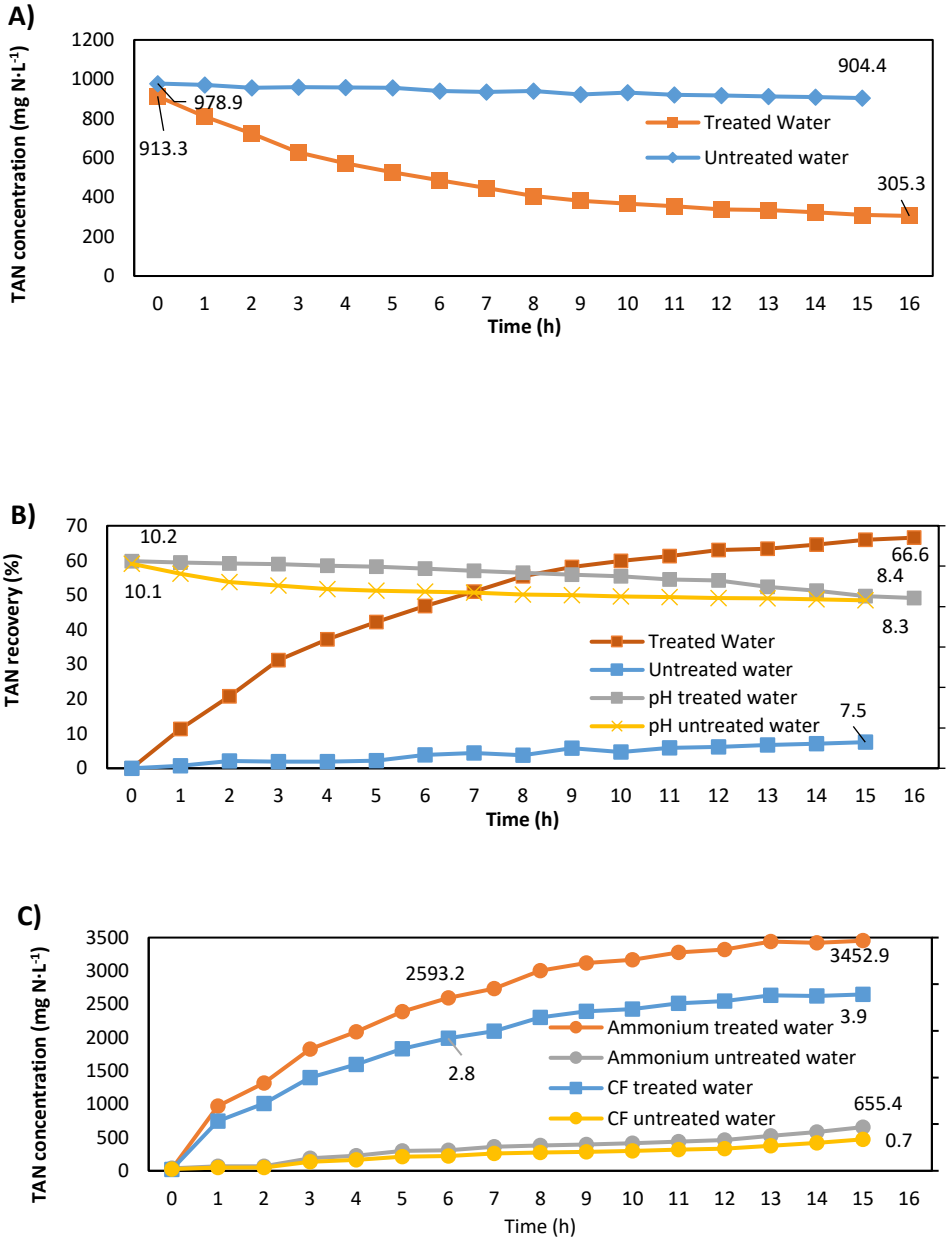

Figure 6. Membrane contactor results during operation: (A) TAN concentration evolution in the feed tank for pre-treated and untreated centrate, (B) TAN recovery and pH variation and (C) TAN concentration evolution and concentration factor in the acid tank.

Besides the TAN recovery efficiency, the ammonia mass transfer coefficient (K_m) was also calculated. The K_m of the pre-treated centrate (1.04×10^{-5} $m \cdot s^{-1}$) was almost two orders of magnitude higher than that achieved with the non-treated centrate (7.80×10^{-7} $m \cdot s^{-1}$). These results corroborate that the implementation of C/F and aeration before the membrane contactor is needed to achieve efficient TAN recoveries from the anaerobic digester centrate. Interestingly, the K_m achieved in the present study with the pre-treated centrate and flat-sheet membrane contactors was higher in comparison with K_m values reported in the literature using hollow fiber contactors (Table 13). The highest Km achieved in this study could be attributed to the high efficiency of the pretreatment process since COD, TSS and turbidity were substantially reduced. This led to almost negligible fouling, no clogging and no reduction in ammonia transfer during the operation of the membrane contactor for the pre-treated centrate.

Table 13. K_m values obtained in different studies with hollow fibre liquid-liquid membrane contactors.

Study	**Mass transfer K_m ($m \cdot s^{-1}$)**	**Flow rate (mL/min)**	**Type of contactor**	**Initial [NH_3] g·L-1**	**% removal**	**Pre-treatment**	**Water**
This study	1.04×10^{-5}	450	FS-LLMC (PTFE)	0.9	66.6	C/F and Aireation	Sidestream
(Vecino et al., 2019)	8.80×10^{-7}	450	HF-LLMC (PP)	3.9	76.1	Ion-exchange	Sidestream
(Liu & Wang, 2016)	8.91×10^{-6}	920	HF-LLMC (PVDF)	2-10	90.0	-	Synthetic
(Sheikh et al., 2022)	2.90×10^{-7}	770	HF-LLMC (PMP)	5.0	93.1	-	Synthetic
(Vecino et al., 2020)	1.89×10^{-6}	450	HF-LLMC (PP)	1.7	85	Sorption	Sidestream

The results of this study clearly suggest that, in the case of a centrate with a high concentration of organic matter and suspended solids, pre-treatment using C/F and aeration can improve the performance of the membrane contactor. The pre-treatment application could potentially help avoid operating problems, such as loss of hydrophobicity due to biofouling and clogging of the membrane, improving the membrane recovery performance and making it technically feasible.

3.4.6. Economic Analysis

3.4.6.1. Economic feasibility of membrane contactor implementation

Figure 7 illustrates the economic balance of implementing a membrane contactor system to recover ammonia from the anaerobic digester centrate. The results show that membrane contactor implementation in a WWTP led to a negative NPV. Ammoniacal nitrogen recovery from the anaerobic digester centrate allows (i) achieving revenues from the ammonium nitrate fertilizer produced and (ii) reducing the nitrogen load to the mainstream of the WWTP with a direct impact on energy consumption. However, these revenues did not offset the additional costs associated with the construction and operation of the different process units. From these results, it is conceivable to state that further improvements are still necessary to make nitrogen recovery through membrane contactors economically attractive. Besides economic considerations, ammonical nitrogen recovery from the anaerobic digester centrate has the potential to reduce disturbances in the mainstream nitrification-denitrification process and improve the WWTP effluent quality (Rodriguez-Garcia et al., 2014; Vinardell et al., 2021).

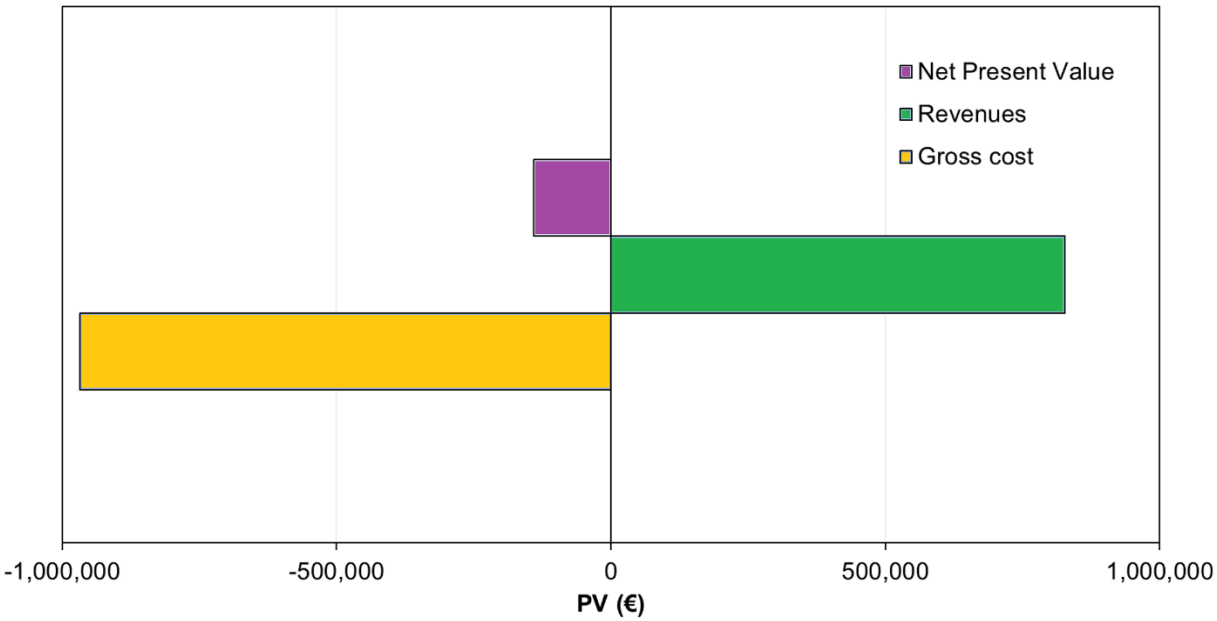

Figure 7. Gross cost, revenues, and net present value for the nitrogen recovery scenario under study.

The membrane contactor system represented the most expensive process (55%), followed by aeration (36%) and coagulation-flocculation (9%) (see Figure 8A). The high cost of the membrane contactor system is mainly associated with the intensive consumption of HNO_3 and, to a lesser extent, NaOH. In this regard, chemicals' consumption features the highest cost contribution, representing 57% of the gross cost (Figure 8B). Energy consumption also represents an important fraction of the gross cost (34.1%), which can be attributed to the high energy requirements of the air blower system. These results highlight that chemical consumption and aeration requirements are two important operational factors influencing the economic competitiveness of the system.

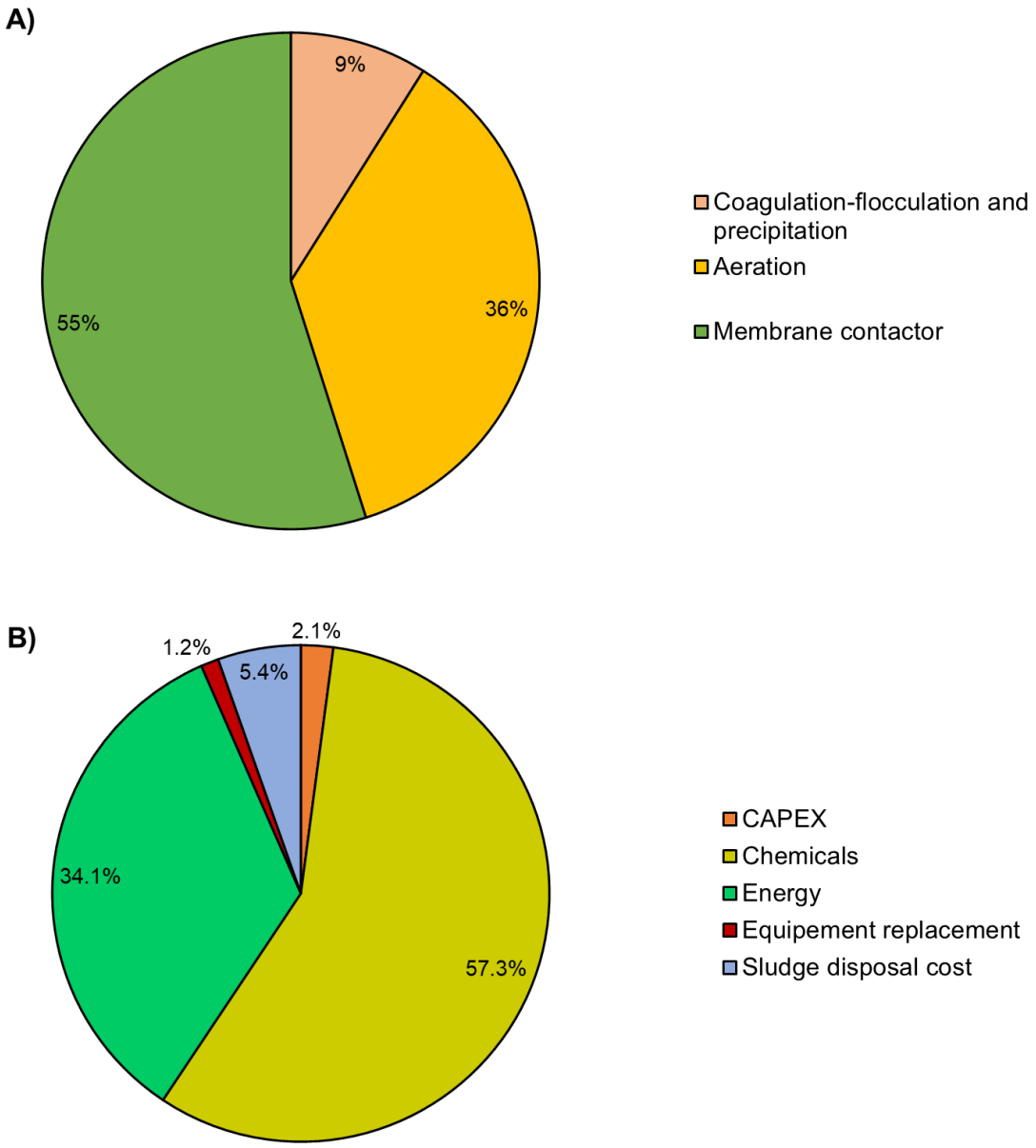

Figure 8. Gross cost contribution of the nitrogen recovery scenario under study for: (A) the different processes and (B) for the different capital and operating costs of all treatment train (C/F, aeration and Membrane contactor)

3.4.6.2. Sensitivity analysis

Figure 9 shows the sensitivity analysis for a ± 30% variation, this variation implies the effects of increasing or decreasing these economic parameters by 30% are being assessed to comprehend how this would impact the financial outcome of the system. The results illustrate that NH_4NO_3 price featured the highest impact on the NPV. This is particularly

important considering that the cost of fertilizers is expected to increase in the future due to the progressive increase in fuel and electricity costs according to Panos & Desing, 2019 (Panos & Densing, 2019). To better understand how NH_4NO_3 price impacts the economic balance of the system, a sensitivity analysis was conducted for NH_4NO_3 prices between 0.30 and 0.70 €/kg of dry weight (Figure 9). The results show that the NPV of ammoniacal nitrogen recovery increased from -350,000 to 300,000 € as the NH_4NO_3 price increased from 0.30 to 0.70 €/kg, respectively. This implies that a positive NPV was achieved at NH_4NO_3 prices above 0.52 €/kg. Overall, these results highlight that the commercialisation of the produced NH_4NO_3 fertilizer has the potential to make membrane contactor configuration economically feasible.

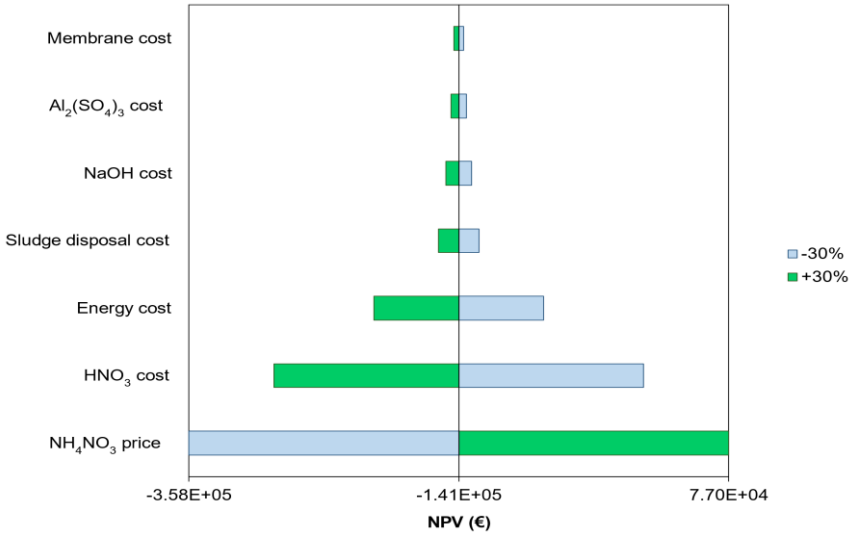

Figure 9. Sensitivity analysis for a ± 30% variation involves evaluating the consequences of both increasing and decreasing these economic parameters by 30%, aiming to understand how this would affect the financial outcome of the project.

Nitric acid and electricity costs also feature a noticeable impact on the NPV of the system (Figure 9). This reinforces the idea that chemicals consumption and aeration requirements are two important aspects influencing the economics of this configuration. Conversely, membrane purchase cost variation showed the least influence in the NPV compared with the others factors studied. The low impact of the membrane purchase cost on NPV can be attributed to the high K_m coefficient (1.04×10^{-5} $m\cdot s^{-1}$) achieved in this study, which is substantially higher than in other studies (Darestani et al., 2017; Noriega-Hevia et al., 2020) . However, it is worth mentioning that the K_m could be substantially lower during long-term membrane contactor operation due to organic and inorganic membrane fouling

development on the membrane surface. For this reason, a sensitivity analysis was conducted to evaluate the impact of K_m on the economic balance of the nitrogen recovery scheme under study (Figure 10).

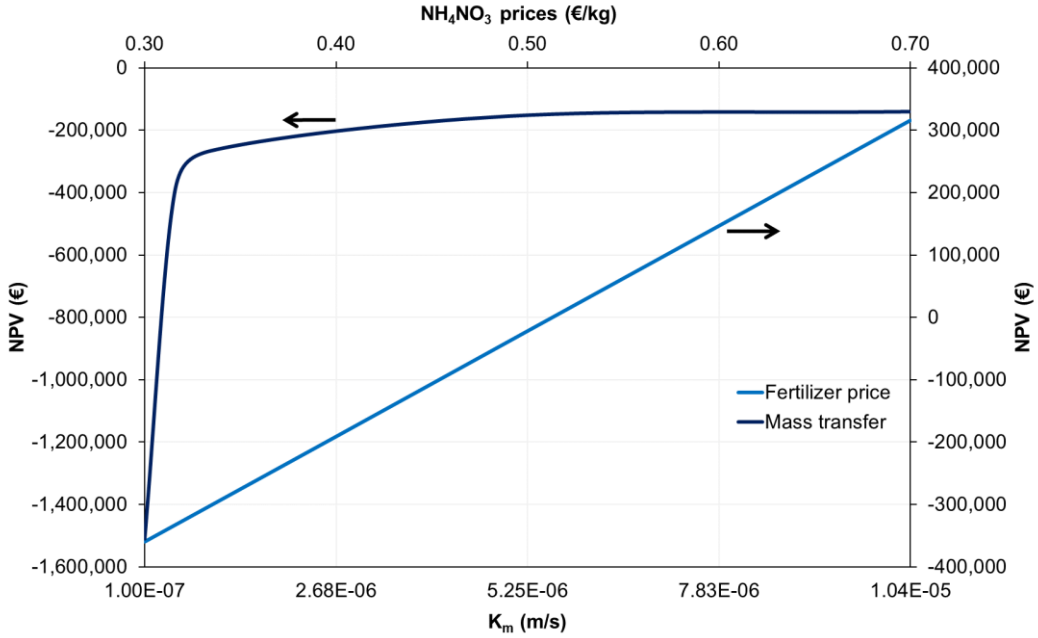

Figure 10. Sensitivity analysis illustrating the impact of mass transfer coefficient (K_m) variations and ammonium nitrate (NH_4NO_3) price on the net present value (NPV) of the nitrogen recovery scheme.

The results show that the NPV slightly decreased from -140,000 to -260,000 € as the K_m decreased from 1×10^{-5} to 1×10^{-6} $m\cdot s^{-1}$, respectively (Figure 10). However, a sharp decrease of the NPV was observed at K_m values below 1×10^{-6} $m\cdot s^{-1}$. These results highlight that K_m could have a large influence on the economic balance due to its impact on the membrane requirements of the system. For this reason, it is important to look for suitable physical and chemical cleaning strategies able to achieve effective control of long-term membrane fouling without excessive consumption of chemicals and energy.

3.5. Conclusions

This study evaluated the implementation of C/F and aeration pre-treatments prior to a membrane contactor stage to recover nitrogen from the anaerobic digester centrate. The results revealed that dosing $Al_2(SO_4)_3$ at 30 mg $Al^+\cdot L^{-1}$ was the best strategy for the coagulation process. The maximum COD, turbidity and TSS removals (58 and 95 and 90%, respectively) were achieved with a mixing speed of 100 rpm, a mixing time of 5

minutes and a settling time of 30 min. The flocculation stage using Fe_3O_4(s)/SiO_2(s) (30-70% (w/w)) according to our assessment, did not appear to introduce discernible improvements in the removal efficiencies. The aeration stage reduced HCO_3^- content up to 51% and increased the pH up to 9, without the addition of external chemicals. Subsequently, the effluent from the C/F and aeration stages was fed to the membrane contactor for nitrogen recovery. The membrane contactor recovered 67% of TAN and achieved a concentration factor of 3.8. in the acid solution Finally, although is highly depending on the market price the techno-economic evaluation showed that the combination of C/F, aeration and membrane contactor has potential to be an economically competitive alternative for nitrogen recovery.

3.6. References

Abdessemed, D., Nezzal, G., & Ben Aim, R. (2000). Coagulation-adsorption-ultrafiltration for wastewater treatment and reuse. *Desalination*, *131*(1–3), 307–314. https://doi.org/10.1016/S0011-9164(00)90029-8

Al-Juboori, R. A., Uzkurt Kaljunen, J., Righetto, I., & Mikola, A. (2022). Membrane contactor onsite piloting for nutrient recovery from mesophilic digester reject water: The effect of process conditions and pre-treatment options. *Separation and Purification Technology*, *303*(September), 122250. https://doi.org/10.1016/j.seppur.2022.122250

APHA. (2012). *Standard Methods for the Examination of Water and Wastewater*. 1496.

APHA Method 2320. (1992). Zigurat Roche.Pdf. *American Public Health Association*, *552*, 2–25 to 2–28. https://law.resource.org/pub/us/cfr/ibr/002/apha.method.2320.1992.pdf

Apostol, G., Kouachi, R., & Constantinescu, I. (2011). Optimization of coagulation-flocculation process with aluminum sulfate based on response surface methodology. *UPB Scientific Bulletin, Series B: Chemistry and Materials Science*, *73*(2), 77–84.

Aygun, a, & Yilmaz, T. (2010). Improvement of Coagulation-Flocculation Process for Treatment of Detergent Wastewaters Using Coagulant Aids. *International Journal of Chemical and Environmental Engineering*, *1*(2), 97–101.

Beckinghausen, A., Odlare, M., Thorin, E., & Schwede, S. (2020). From removal to recovery: An evaluation of nitrogen recovery techniques from wastewater. *Applied Energy*, *263*(February), 114616. https://doi.org/10.1016/j.apenergy.2020.114616

Bouzas, A., Martí, N., Grau, S., Barat, R., Mangin, D., & Pastor, L. (2019). Implementation of a global P-recovery system in urban wastewater treatment plants. *Journal of Cleaner Production*, *227*, 130–140. https://doi.org/10.1016/j.jclepro.2019.04.126

Darestani, M., Haigh, V., Couperthwaite, S. J., Millar, G. J., & Nghiem, L. D. (2017). Hollow fibre membrane contactors for ammonia recovery: Current status and future developments. *Journal of Environmental Chemical Engineering*, *5*(2), 1349–1359. https://doi.org/10.1016/j.jece.2017.02.016

Das, S., Gaustad, G., Sekar, A., & Williams, E. (2018). Techno-economic analysis of supercritical extraction of rare earth elements from coal ash. *Journal of Cleaner Production*, *189*, 539–551. https://doi.org/10.1016/j.jclepro.2018.03.252

Devesa-Rey, R., Bustos, G., Cruz, J. M., & Moldes, A. B. (2012). Evaluation of non-conventional coagulants to remove turbidity from water. *Water, Air, and Soil Pollution*, *223*(2), 591–598. https://doi.org/10.1007/s11270-011-0884-8

Dosta, J., Rovira, J., Galí, A., Macé, S., & Mata-Álvarez, J. (2008). Integration of a Coagulation/Flocculation step in a biological sequencing batch reactor for COD and nitrogen removal of supernatant of anaerobically digested piggery wastewater. *Bioresource Technology*, *99*(13), 5722–5730. https://doi.org/10.1016/j.biortech.2007.10.021

Duan, J., & Gregory, J. (2003). Coagulation by hydrolysing metal salts. *Advances in Colloid and Interface Science*, *100–102*(SUPPL.), 475–502. https://doi.org/10.1016/S0001-8686(02)00067-2

Dube, P. J., Vanotti, M. B., Szogi, A. A., & García-González, M. C. (2016). Enhancing recovery of ammonia from swine manure anaerobic digester effluent using gas-permeable membrane technology. *Waste Management*, *49*, 372–377. https://doi.org/10.1016/j.wasman.2015.12.011

Eskicioglu, C., Galvagno, G., & Cimon, C. (2018). Approaches and processes for ammonia removal from side-streams of municipal effluent treatment plants. *Bioresource Technology*, *268*(May), 797–810. https://doi.org/10.1016/j.biortech.2018.07.020

Eurostat. (2021). *Electricity price statistics*.

Ferreira, S. L. C., Bruns, R. E., Ferreira, H. S., Matos, G. D., David, J. M., Brandão, G. C., da Silva, E. G. P., Portugal, L. A., dos Reis, P. S., Souza, A. S., & dos Santos, W. N. L. (2007). Box-Behnken design: An alternative for the optimization of analytical methods. *Analytica Chimica Acta*, *597*(2), 179–186. https://doi.org/10.1016/j.aca.2007.07.011

Foladori, P., Andreottola, G., & Ziglio, G. (2015). Sludge Reduction Technologies in Wastewater Treatment Plants. In *Sludge Reduction Technologies in Wastewater Treatment Plants*. IWA Publishing. https://doi.org/10.2166/9781780401706

Fragoso, R. A., Duarte, E. A., & Paiva, J. (2015). Contribution of Coagulation-Flocculation Process for a More Sustainable Pig Slurry Management. *Water, Air, and Soil Pollution*, *226*(5), 4–9. https://doi.org/10.1007/s11270-015-2388-4

García-González, M. C., Vanotti, M. B., & Szogi, A. A. (2015). Recovery of ammonia from swine manure using gas-permeable membranes: Effect of aeration. *Journal of*

Environmental Management, *152*, 19–26. https://doi.org/10.1016/j.jenvman.2015.01.013

González Montiel, J. M. (2008). Acetato de etilo en la Industria. *Journal of Chemical Information and Modeling*, *53*(9), 287.

Guimarães, N. R., Dörr, F., Marques, R. de O., Pinto, E., & Ferreira Filho, S. S. (2020). Removal efficiency of dissolved organic matter from secondary effluent by coagulation-flocculation processes. *Journal of Environmental Science and Health - Part A Toxic/Hazardous Substances and Environmental Engineering*, *56*(2), 161–170. https://doi.org/10.1080/10934529.2020.1856580

Hasanoğlu, A., Romero, J., Pérez, B., & Plaza, A. (2010). Ammonia removal from wastewater streams through membrane contactors: Experimental and theoretical analysis of operation parameters and configuration. *Chemical Engineering Journal*, *160*(2), 530–537. https://doi.org/10.1016/j.cej.2010.03.064

Hermassi, M., Valderrama, C., Gibert, O., Moreno, N., Querol, X., Batis, N. H., & Cortina, J. L. (2017). Recovery of nutrients (N-P-K) from potassium-rich sludge anaerobic digestion side-streams by integration of a hybrid sorption-membrane ultrafiltration process: Use of powder reactive sorbents as nutrient carriers. *Science of the Total Environment*, *599–600*, 422–430. https://doi.org/10.1016/j.scitotenv.2017.04.140

Horstmeyer, N., Weißbach, M., Koch, K., & Drewes, J. E. (2018). A novel concept to integrate energy recovery into potable water reuse treatment schemes. *Journal of Water Reuse and Desalination*, *8*(4), 455–467. https://doi.org/10.2166/wrd.2017.051

Hu, H., Ding, L., Geng, J., Huang, H., Xu, K., & Ren, H. (2016). Effect of coagulation on dissolved organic nitrogen (DON) bioavailability in municipal wastewater effluents. *Journal of Environmental Chemical Engineering*, *4*(2), 2536–2544. https://doi.org/10.1016/j.jece.2016.04.036

Huang, A. K., Veit, M. T., Juchen, P. T., Gonçalves, G. D. C., Palácio, S. M., & Cardoso, C. D. O. (2019). Sequential process of coagulation/flocculation/sedimentation-adsorption - Microfiltration for laundry effluent treatment. *Journal of Environmental Chemical Engineering*, *7*(4), 103226. https://doi.org/10.1016/j.jece.2019.103226

Jiang, J. Q. (2015a). The role of coagulation in water treatment. *Current Opinion in Chemical Engineering*, *8*, 36–44. https://doi.org/10.1016/j.coche.2015.01.008

Jiang, J. Q. (2015b). The role of coagulation in water treatment. *Current Opinion in Chemical Engineering*, *8*, 36–44. https://doi.org/10.1016/j.coche.2015.01.008

Kan, C., Huang, C., & Pan, J. R. (2002). Time requirement for rapid-mixing in coagulation. *Colloids and Surfaces A: Physicochemical and Engineering Aspects*, *203*(1–3), 1–9. https://doi.org/10.1016/S0927-7757(01)01095-0

Krupińska, I. (2020). The effect of the type of hydrolysis of aluminum coagulants on the effectiveness of organic substances removal from water. *Desalination and Water Treatment*, *186*(September 2019), 171–180. https://doi.org/10.5004/dwt.2020.25248

Kurniawan, T. A., Lo, W. H., & Chan, G. Y. S. (2006). Physico-chemical treatments for removal of recalcitrant contaminants from landfill leachate. *Journal of Hazardous Materials*, *129*(1–3), 80–100. https://doi.org/10.1016/j.jhazmat.2005.08.010

Lee, W., An, S., & Choi, Y. (2021). Ammonia harvesting via membrane gas extraction at moderately alkaline pH: A step toward net-profitable nitrogen recovery from domestic wastewater. *Chemical Engineering Journal*, *405*(May 2020), 126662. https://doi.org/10.1016/j.cej.2020.126662

Leiknes, T. O. (2009). The effect of coupling coagulation and flocculation with membrane filtration in water treatment: A review. *Journal of Environmental Sciences*, *21*(1), 8–12. https://doi.org/10.1016/S1001-0742(09)60003-6

Licon Bernal, E. E., Maya, C., Valderrama, C., & Cortina, J. L. (2016). Valorization of ammonia concentrates from treated urban wastewater using liquid-liquid membrane contactors. *Chemical Engineering Journal*, *302*, 641–649. https://doi.org/10.1016/j.cej.2016.05.094

Liu, H., & Wang, J. (2016). Separation of ammonia from radioactive wastewater by hydrophobic membrane contactor. *Progress in Nuclear Energy*, *86*, 97–102. https://doi.org/10.1016/j.pnucene.2015.10.011

Matthews, J. A. (2014). Chemical Oxygen Demand (Cod). *Encyclopedia of Environmental Change*, *5000*, 14–19. https://doi.org/10.4135/9781446247501.n623

Ministerio de Agricultura Pesca y Alimentación. (2022). *Índices y Precios Pagados Agrarios*.

Noriega-Hevia, G., Serralta, J., Borrás, L., Seco, A., & Ferrer, J. (2020). Nitrogen recovery using a membrane contactor: Modelling nitrogen and pH evolution. *Journal of Environmental Chemical Engineering*, *8*(4), 103880.

https://doi.org/10.1016/j.jece.2020.103880

Noriega-Hevia, G., Serralta, J., Seco, A., & Ferrer, J. (2021). Economic analysis of the scale-up and implantation of a hollow fibre membrane contactor plant for nitrogen recovery in a full-scale wastewater treatment plant. *Separation and Purification Technology*, *275*(June), 119128. https://doi.org/10.1016/j.seppur.2021.119128

Panos, E., & Densing, M. (2019). The future developments of the electricity prices in view of the implementation of the Paris Agreements: Will the current trends prevail, or a reversal is ahead? *Energy Economics*, *84*. https://doi.org/10.1016/j.eneco.2019.104476

Postolachi, L., Rusu, V., & Lupascu, T. (2016). Effect of aluminium sulphate aging on coagulation process for the Prut river water treatment. *Chemistry Journal of Moldova*, *11*(1), 27–32. https://doi.org/10.19261/cjm.2016.11(1).03

Preston, K., Lantagne, D., Kotlarz, N., & Jellison, K. (2010). Turbidity and chlorine demand reduction using alum and moringa flocculation before household chlorination in developing countries. *Journal of Water and Health*, *8*(1), 60–70. https://doi.org/10.2166/wh.2009.210

Puyol, D., Batstone, D. J., Hülsen, T., Astals, S., Peces, M., & Krömer, J. O. (2017). Resource recovery from wastewater by biological technologies: Opportunities, challenges, and prospects. *Frontiers in Microbiology*, *7*(JAN), 1–23. https://doi.org/10.3389/fmicb.2016.02106

Raghu, S., & Ahmed Basha, C. (2007). Chemical or electrochemical techniques, followed by ion exchange, for recycle of textile dye wastewater. *Journal of Hazardous Materials*, *149*(2), 324–330. https://doi.org/10.1016/j.jhazmat.2007.03.087

Razon, L. F. (2018). Reactive nitrogen: A perspective on its global impact and prospects for its sustainable production. *Sustainable Production and Consumption*, *15*, 35–48. https://doi.org/10.1016/j.spc.2018.04.003

Reig, M., Vecino, X., Gibert, O., Valderrama, C., & Cortina, J. L. (2021). Study of the operational parameters in the hollow fibre liquid-liquid membrane contactors process for ammonia valorisation as liquid fertiliser. *Separation and Purification Technology*, *255*(July 2020), 117768. https://doi.org/10.1016/j.seppur.2020.117768

Richter, L., Wichern, M., Grömping, M., Robecke, U., & Haberkamp, J. (2020). Ammonium recovery from process water of digested sludge dewatering by membrane contactors. *Water Practice and Technology*, *15*(1), 84–91.

https://doi.org/10.2166/wpt.2020.002

Rivadeneyra, G., Ma, R., Carmen, D., Pérez, F., Alvarado, A., Norma, L., Cantú, A. V., Una, U. D. E., Intercambio, R. D. E., Para, I., Romero, G. R., Del, M., Flores, C., Lassman, A. A., & Vallejo, N. A. (2007). *Utilización de una Resina de Intercambio Iónico para el Desarrollo de Biopelícula Aerobia para el Tratamiento de Agua Residual Industrial Combinada*. 41–42.

Rodriguez-Garcia, G., Frison, N., Vázquez-Padín, J. R., Hospido, A., Garrido, J. M., Fatone, F., Bolzonella, D., Moreira, M. T., & Feijoo, G. (2014). Life cycle assessment of nutrient removal technologies for the treatment of anaerobic digestion supernatant and its integration in a wastewater treatment plant. *Science of the Total Environment*, *490*, 871–879. https://doi.org/10.1016/j.scitotenv.2014.05.077

Salem, A. T., & AL-Musawi, N. O. . (2021). Water Treatment With Conventional and Alternative Coagulants: A Review. *Journal of Engineering*, *27*(9), 20–28. https://doi.org/10.31026/j.eng.2021.09.02

Sancho, I., Licon, E., Valderrama, C., de Arespacochaga, N., López-Palau, S., & Cortina, J. L. (2017). Recovery of ammonia from domestic wastewater effluents as liquid fertilizers by integration of natural zeolites and hollow fibre membrane contactors. *Science of the Total Environment*, *584–585*, 244–251. https://doi.org/10.1016/j.scitotenv.2017.01.123

Serra-Toro, A., Vinardell, S., Astals, S., Madurga, S., Llorens, J., Mata-Álvarez, J., Mas, F., & Dosta, J. (2022). Ammonia recovery from acidogenic fermentation effluents using a gas-permeable membrane contactor. *Bioresource Technology*, *356*(May), 127273. https://doi.org/10.1016/j.biortech.2022.127273

Sheikh, M., Reig, M., Vecino, X., Lopez, J., Rezakazemi, M., Valderrama, C. A., & Cortina, J. L. (2022). Liquid–Liquid membrane contactors incorporating surface skin asymmetric hollow fibres of poly(4-methyl-1-pentene) for ammonium recovery as liquid fertilisers. *Separation and Purification Technology*, *283*, 120212. https://doi.org/10.1016/j.seppur.2021.120212

Sultana, S., Karmaker, B., Saifullah, A. S. M., Galal Uddin, M., & Moniruzzaman, M. (2022). Environment-friendly clay coagulant aid for wastewater treatment. *Applied Water Science*, *12*(1). https://doi.org/10.1007/s13201-021-01540-z

Taboada-Santos, A., Rivadulla, E., Paredes, L., Carballa, M., Romalde, J., & Lema, J. M. (2020). Comprehensive comparison of chemically enhanced primary treatment and

high-rate activated sludge in novel wastewater treatment plant configurations. *Water Research*, *169*, 115258. https://doi.org/10.1016/j.watres.2019.115258

Vanotti, M. B., Dube, P. J., Szogi, A. A., & García-González, M. C. (2017). Recovery of ammonia and phosphate minerals from swine wastewater using gas-permeable membranes. *Water Research*, *112*, 137–146. https://doi.org/10.1016/j.watres.2017.01.045

Vecino, X., Reig, M., Bhushan, B., Gibert, O., Valderrama, C., & Cortina, J. L. (2019). Liquid fertilizer production by ammonia recovery from treated ammonia-rich regenerated streams using liquid-liquid membrane contactors. *Chemical Engineering Journal*, *360*(December 2018), 890–899. https://doi.org/10.1016/j.cej.2018.12.004

Vecino, X., Reig, M., Gibert, O., Valderrama, C., & Cortina, J. L. (2020). Integration of liquid-liquid membrane contactors and electrodialysis for ammonium recovery and concentration as a liquid fertilizer. *Chemosphere*, *245*, 125606. https://doi.org/10.1016/j.chemosphere.2019.125606

Vecino, X., Reig, M., Valderrama, C., & Cortina, J. L. (2021). Ion-exchange technology for lactic acid recovery in downstream processing: Equilibrium and kinetic parameters. In *Water (Switzerland)* (Vol. 13, Issue 11). https://doi.org/10.3390/w13111572

Verma, S., Prasad, B., & Mishra, I. M. (2010). Pretreatment of petrochemical wastewater by coagulation and flocculation and the sludge characteristics. *Journal of Hazardous Materials*, *178*(1–3), 1055–1064. https://doi.org/10.1016/j.jhazmat.2010.02.047

Verrecht, B., Maere, T., Nopens, I., Brepols, C., & Judd, S. (2010). The cost of a large-scale hollow fibre MBR. *Water Research*, *44*, 5274–5283. https://doi.org/10.1016/j.watres.2010.06.054

Vinardell, S., Astals, S., Koch, K., Mata-Alvarez, J., & Dosta, J. (2021). Co-digestion of sewage sludge and food waste in a wastewater treatment plant based on mainstream anaerobic membrane bioreactor technology: A techno-economic evaluation. *Bioresource Technology*, *330*(March). https://doi.org/10.1016/j.biortech.2021.124978

Vinardell, S., Astals, S., Mata-Alvarez, J., & Dosta, J. (2020). Techno-economic analysis of combining forward osmosis-reverse osmosis and anaerobic membrane bioreactor technologies for municipal wastewater treatment and water production. *Bioresource*

Technology, *297*, 122395. https://doi.org/10.1016/j.biortech.2019.122395

Vu, H. P., Nguyen, L. N., Lesage, G., & Nghiem, L. D. (2020). Synergistic effect of dual flocculation between inorganic salts and chitosan on harvesting microalgae Chlorella vulgaris. *Environmental Technology and Innovation*, *17*, 100622. https://doi.org/10.1016/j.eti.2020.100622

Wan, C., Ding, S., Zhang, C., Tan, X., Zou, W., Liu, X., & Yang, X. (2017). Simultaneous recovery of nitrogen and phosphorus from sludge fermentation liquid by zeolite adsorption: Mechanism and application. *Separation and Purification Technology*, *180*, 1–12. https://doi.org/10.1016/j.seppur.2017.02.031

Wongcharee, S., Aravinthan, V., & Erdei, L. (2020). Removal of natural organic matter and ammonia from dam water by enhanced coagulation combined with adsorption on powdered composite nano-adsorbent. *Environmental Technology and Innovation*, *17*, 100557. https://doi.org/10.1016/j.eti.2019.100557

Zarebska, A., Nieto, D. R., Christensen, K. V., & Norddahl, B. (2014). Ammonia recovery from agricultural wastes by membrane distillation: Fouling characterization and mechanism. *Water Research*, *56*, 1–10. https://doi.org/10.1016/j.watres.2014.02.037

CHAPTER 4

Ammonia Valorization by Liquid–Liquid Membrane Contactors for Liquid Fertilizers Production: Experimental Conditions Evaluation

4.1. Abstract

Liquid–liquid membrane contactors (LLMCs) were studied as a sustainable technology for ammonia recovery from wastewater. Ammonia can be valorized by LLMCs as a potential nutrient and produce liquid fertilizers. Thus, this work aims for the study of different experimental LLMC conditions to produce ammonium salts by an acid stripping stream. The experiments were conducted using two 3M^{TM}Liqui-Cell^{TM} LLMC in a series, located in the vertical position and using HNO_3 as the acid stripping solution. The flow rates for the feed and stripping sides were fixed during the tests, and two steps were conducted based on previous works. However, different experimental conditions were evaluated to determine its effect on the overall performance: (i) replacing the feed or stripping solution between the steps, (ii) the initial ammonia concentration of the feed solution, (iii) feed volume and (iv) feed temperature. The results demonstrated that better recovery achievements were obtained replacing the acid stripping solution between steps, whereas the feed temperature did not substantially affect the overall performance. Additionally, a high initial ammonia concentration resulted in higher ammonia recovery compared to low concentrations. However, the concentration factor achieved was higher for the low initial ammonia concentration. Finally, a high feed volume afforded better results for the stripping side, whereas more NH_4^+ recovery was achieved using less feed volume.

Keywords: acid stripping; concentration; volume; temperature; ammonium salts; recovery

4.2. Introduction

Liquid–liquid membrane contactor (LLMC) is a promising and sustainable technology for nitrogen recovery from water or wastewater resources in comparison with other processes such as nutrient adsorption or biological oxidation, among others, where recovery is more difficult (Mayor et al., 2020). Regarding LLMCs, the use of hollow fibers (HF), which are usually hydrophobic and microporous, is common (Darestani et al., 2017; Moradihamedani, 2021), although there are some studies that used tubular

membranes can be beneficial in systems where a higher accumulation of solids or deposits on the membrane surface is expected, as they offer greater fouling resistance. (Majd & Mukhtar, 2013; Samani Majd & Mukhtar, 2013). Moreover, due to the hydrophobic feature of HF membranes, polytetrafluoroethylene (PTFE) and polypropylene (PP) materials are usually used, and more recently, polyvinylidene fluoride (PVDF) has been proposed (Naim et al., 2012). The former materials are symmetric membranes, and the latter is asymmetric, which provides less mass transfer resistance due to pore distribution and size (Li et al., 2000; Moradihamedani, 2021). In fact, a higher interfacial area per unit volume or the control of the flow rates are advantages for the use of hydrophobic HF-LLMCs in comparison with conventional processes (such as absorption) (Moradihamedani, 2021).

It is worth mentioning that, to recover nitrogen from wastewater streams by using HF-LLMCs, these streams should be at a pH above 9.25 (pKa) to assure that nitrogen is an ammonia gas form (Darestani et al., 2017). In fact, the driven force of HF-LLMCs is the chemical reaction of an acid stripping solution with ammonia gas due to the concentration or vapor pressure differences between the two sides of the membrane (Darestani et al., 2017; Mayor et al., 2020). Indeed, the ammonia gas passes through the hydrophobic membrane from the feed (named the shell side) to the acid stripping solution (called the lumen side) by diffusion phenomena. Thus, it is possible to transform the ammonia present in these resources into ammonium rich solutions, which could be used as liquid fertilizers (Darestani et al., 2017; Mayor et al., 2020). Sulfuric acid, nitric acid and phosphoric acid are acid stripping solutions used in HF-LLMC processes, the first acid being the most frequently applied (Darestani et al., 2017; Vecino et al., 2019). However, the bottleneck of the HF-LLMC processes is the control of the membrane wettability; if the liquid pressure exceeds the breakthrough pressure, the pores of the hydrophobic membrane get wet (Mayor et al., 2020). For that reason, there have been several studies where different operational parameters, configurations, membrane types, etc. were tested to maximize the ammonia recovery and minimize the water passage. For example, Zhu et al. 2005 (Z. Zhu et al., 2005) evaluated the effect of pH and the viscosity of the feed solution (containing 2 g $NH_3 \cdot L^{-1}$) on the mass transfer in two different PP HF-LLMCs. It was concluded that viscosity is not the main factor affecting the rate of mass transfer, while the pH of the feed had a significant effect on the rate of mass transfer, the removal efficiency, and the flux of ammonia. The authors suggested that the highest treating

efficiency was achieved when the initial pH value of the feed solution was adjusted above 11. Licon et al. 2016, studied the influence of various operational parameters (i.e., flow rate, initial ammonia concentration and stripping acid concentration) for ammonia recovery from tertiary effluents by zeolites that generate basic ammonia concentrates (up to 1–3 g $NH_3 \cdot L^{-1}$ in 1–2 g $NaOH \cdot L^{-1}$) by using PP HF-LLMC. It was concluded that the ammonia mass transfer did not vary substantially as a function of the initial ammonia concentration (0.3–1.7 g·L-1) and flow rate (7.59–11.06 $cm^3 \cdot s^{-1}$), and the reaction was only affected by the excess strong acid (nitric or phosphoric) used (Licon Bernal et al., 2016).

Reig et al. 2021, tested different parameters using PP HF-LLMC for ammonia valorization as follows: position (horizontal and vertical), feed and acid streams inputs (shell and lumen), type of acid stripping solution (H_3PO_4 and HNO_3), membrane drying, the flow rate for each stream (263–770 mL/min), number of steps (1 and 2) and number of membrane contactors (1 and 2 in a series). The treated urban wastewater stream contained high contents of ammonia (4.5-5 g $NH_3 \cdot L^{-1}$). The authors selected a one-step configuration using two vertical membrane contactors in a series, using the shell side for the feed stream and the lumen side for the acid stripping solution (HNO_3) at 450 mL/min and 770 mL/min flow rates for the feed and acid stripping solutions, respectively, to obtain the maximum ammonia recovery (>95%) (Reig et al., 2021). In the above mentioned works, the most commonly studied HF-LLMCs were those provided by 3M Company, USA under the tradename Liqui-Cell, which are made with PP membranes. However, recently, Sheikh et al. 2022, tested two novel HF-LLMCs modules containing S-type (named A60 with a skin layer with low porosity) and Q-type (called Q-A60 with a skin layer with high porosity) fibers supplied by Separel DIC Corporation (Japan). Both types of fibers, with asymmetric, porous, and hydrophobic membranes made from poly(4-methyl-1-pentene) (PMP), were used as an efficient technology for ammonia recovery by producing liquid fertilizers. The results showed that in terms of the N% recovered, the performance of the Q-type PMP-HF-LLMC module was better than the S-type, since it obtained a higher ammonia mass transfer in a shorter time. This could be because the Q-type module has a skin layer with higher porosity than the S-type (M. Sheikh et al., 2022).

Therefore, taking into account the aforementioned points, it remains interesting to study different operational parameters, such as (i) replacing the feed or the stripping solution between the steps, (ii) the initial ammonia concentration of the feed solution (1.0 and 4.5

$g \cdot L^{-1}$), (iii) feed volume (60 and 5 L) and (iv) feed temperature (25 and 35 °C) to evaluate the effects of them on the PP HF-LLMC efficiency of ammonium recovery from wastewater streams. In fact, to the best of our knowledge, some of these parameters have not been thoroughly studied previously, such as the feed volume effect on the PP HF-LLMC performance.

4.3. Materials and Methods

4.3.1. Reagents

Nitric acid (65%, HNO_3) was used as the acid stripping solution for ammonium salts production. Additionally, methanesulfonic acid (CH_3SO_3H, 99%), sodium hydrogen carbonate ($NaHCO_3$, 99%) and anhydrous sodium carbonate (Na_2CO_3, 99%) were used for the ionic chromatography analysis. All chemicals used in this work were analytical grade reagents and were supplied by Sigma-Aldrich®, Spain.

4.3.2. Wastewater Solution

Pretreated urban wastewater from the Vilanova i la Geltrú wastewater treatment plant (WWTP) in Barcelona, Spain, was utilized in this study. The wastewater subsequent treatment in a pilot plant situated within the same facility to decrease ammonium levels using zeolites (Reig et al., 2021; Sancho et al., 2017; Vecino et al., 2019). However, a notable drawback of this final treatment was the generation of a more concentrated stream with high ammonia content, resulting from the elevated pH (≈12). Consequently, this treated stream was employed as the feed solution for the present study.

4.3.3. Experimental Set-Up

Although the experimental setup has been described in other studies (Reig et al., 2021; Vecino et al., 2019, 2020), the most relevant details about the lab-scale LLMC experimental set-up are described in this section. A pair of Liqui-Cel® 2.5 × 8 Series Membrane Contactor X-50 polypropylene provided by 3M™, USA LLMC modules were used located in a series and the vertical position. The above mentioned modules and their characteristics (e.g., membrane configuration, active area, hydrophobicity, pore diameter or the number of fibers) have also been described previously (Licon Bernal et al., 2016), the configuration was hollow fibers with a membrane area of 1.4 m^2. Two tanks were used to introduce the feed solution (60 L) and the acid stripping solution (0.5 L) of 0.4 M of HNO_3, connected to the LLMC modules through PVC flexible tubes. All tests were

conducted under contra-current mode in a closed-loop (i.e., recirculating both streams and introducing the feed solution through the shell side and the acid stripping one through the lumen (inside the fibers). Furthermore, it should be noted that both flow rates were kept constant following the optimal results previously determined: 450 mL/min for the feed stream and 700 mL/min for the acid stripping side.

In summary, the hydrophobic LLMCs used in this work only allowed the passage of ammonia gas (pH > pKa(NH_4^+/NH_3) = 9.25) from the feed solution through the hollow fibers. Then, the NH_3 reacts with the acid stripping solution, producing ammonium salts, which can be used in agriculture as liquid fertilizers. In this case, HNO_3 was used as an acid stripping solution, keeping the stripping solution between pH 2 and 3 (Licon Bernal et al., 2016) by a concentrated HNO_3 (14M) addition. For that, 0.5 L of 0.4 M HNO_3 was prepared as the initial acid stripping solution, which, after the trials, was converted into ammonium nitrate salts, as follows in Equation 1.

$$NH_{3(g)} + HNO_3 \leftrightarrow NH_4NO_3 \qquad \text{(Eq.1)}$$

Moreover, to enhance ammonia recovery and fertilizer concentrations, the valorization process was conducted in two steps. Once the feed concentration reached a plateau, indicating no further ammonia transport to the stripping side, the experiment was halted, and either the acid or the feed solution was replaced with a fresh one. Previously, as per Reig et al. 2021, only the acid stripping solution was changed between steps to further decrease the ammonia concentration of the feed solution, albeit without increasing the ammonium salt concentration. However, in this study, changing the feed solution was also considered to increase fertilizer concentrations and determine which option would optimize overall performance. Furthermore, not only the replacing of the acid stripping or the feed solution between both stages was studied, but also other variables, such as the initial ammonia concentration in the feed solution (mainstream or side, around 1 or 4.5 g $NH_3 \cdot L^{-1}$, respectively), feed volume to be treated (60 or 5 L) and feed temperature (around 25 °C (room) or 35 °C (maximum allowed acoording to manufacturer (3M^{TM} LLMC)) (Reig et al., 2021).

During the experiments, 112 samples were collected from both tanks over time. Therefore, these samples were analyzed to determine their compositions (mainly the concentration of ammonia in the feed solution and the concentration of ammonium and

nitrate in the acid stripping solution). All experiments were replicated twice, and duplicate samples were taken at each experimental point, in order to report data with higher precision and confidence. Thus, data were reported as the mean ± standard deviation of replicate determinations.

4.3.4. Experimental Design

Five experiments were designed to study the effects of the abovementioned parameters. Table 1 summarizes the experimental design, where one parameter was varied trial after trial.

Table 1. Experimental Design of the Five Conducted Experiments, detailing which tank is changed if acid or feed tank before the plateau. Initial theoric Concentrations, Feed Volume, and Feed Temperature.

	Exp. 1	**Exp. 2**	**Exp. 3**	**Exp. 4**	**Exp. 5**
Tank change after plateau	acid	feed	acid	acid	acid
Feed [NH_3] ($g \cdot L^{-1}$)	4.5	4.5	1	1	1
Volume (L)	60	60	60	5	5
Temperature (°C)	25	25	25	25	35

As can be seen in Table 1, the initial experiments (1 and 2) were designed to study the effect of changing the acid or feed solution after the plateau stage. In this case, 60 L of sidestream wastewater at room temperature were used (4.5-5 g $NH_3 \cdot L^{-1}$) following the already published conditions (Reig et al., 2021; Vecino et al., 2019). Once the best option was found, the next experiment (Exp. 3) was conducted to study the effect of the initial ammonia concentration by using mainstream wastewater (≈ 1 g $NH_3 \cdot L^{-1}$), keeping the other parameters as in the first experiments. Next, the feed volume was varied from 60 to 5 L (Exp. 4) to determine its effect on the overall performance. Finally, the feed temperature was studied by increasing the feed solution temperature up to 35 °C (Exp. 5).

4.3.5. Data Analysis

Several main (measured and calculated) parameters were determined to analyze the LLMC efficiency, depending on the analyzed parameters, to valorize ammonia from wastewater and recover it as liquid fertilizers: two for the feed side and two more for the acid stripping side.

Thus, the final ammonia concentration and the ammonia recovery were the analyzed parameters for the feed side. The former was directly analyzed by analytical methodologies, and the latter was calculated by Equation 2.:

$$\text{Ammonia recovery (\%)} = \frac{C_{feed,0} - C_{feed,final}}{C_{feed,0}} \cdot 100 \qquad \text{(Eq.2)}$$

where $C_{feed,0}$ and $C_{feed,final}$ are the initial and final ammonia concentrations ($mg \cdot L^{-1}$), respectively, in the feed tank (Vecino et al., 2019).

On the other hand, the ammonia concentration factor (CF) and the final nitrogen concentration in the stripping side were also determined. Thus, the CF was calculated following Equation 3.:

$$CF\ (-) = \frac{C_{f(NH_3,\text{acid tank})}}{C_{0(NH_3,\text{feed tank})}} \qquad \text{(Eq.3)}$$

where $C_{0(NH3,feed\ tank)}$ and $C_{f(NH3,acid\ tank)}$ are the initial and final NH_3 concentrations ($mg \cdot L^{-1}$) in the feed and acid stripping tanks, respectively (Vecino et al., 2019).

The ammonium salt composition was expressed by the percentage of $N\text{-}NH_4$ present in the liquid fertilizer solution, as described by Equation 4.:

$$N\text{-}NH_4 \text{ concentration (\%, w/w)} = C_{acid\ stripping,final} \qquad \text{(Eq.4)}$$

where $C_{acid\ stripping,final}$ is the final ammonium concentration in the acid stripping tank (g $N\text{-}NH_4$/g solution (%, *w/w*)) (Vecino et al., 2019).

The %N in the liquid fertilizer is a common parameter that fertilizer companies consider when describing the composition of their liquid fertilizers instead of ammonium salt amount or concentration. Thus, this parameter was used to determine the composition of the obtained ammonium salts (fertilizer).

Finally, analysis of variance (ANOVA) is a statistical test that evaluates the hypothesis that the means of two or more populations are equal. Therefore, the null hypothesis

establishes that all the analyzed measures are identical, while the alternative hypothesis confirms that at least one value is different from the rest. The result of this test provides the statistical significance value, *p*; if this value is lower than the established significance level of 0.05 (<95%), it is concluded that at least one mean of the analyzed values is different from the rest of the values. (Barros et al., 2022).

4.3.5.1. Analytical Methodology

During the experiments, the pH was monitored and measured online by a GLP 22 pH meter (Crison®, Spain) which has a pH measuring range of 0-14, and the conductivity was measured by an EC-Metro GLP 31 (Crison®, Spain) (Vecino et al., 2019). The total carbon (TC) was determined by a TOC-V_{CPH} meter (Shimadzu®, Japan).

Moreover, the sample compositions were determined by ionic chromatography (IC). In this case, two apparatuses from Thermo-Fisher Scientific, USA were used for cation and anion quantifications: (i) Dionex ICS-1000 equipped with a CS16 column (5 × 250 mm), a pre-column CG16 (5 × 50 mm) and cationic detector ICS-1000 and (ii) Dionex ICS-1100 equipped with a AS23 column (4 × 250 mm), pre-column AG23 (4 × 50 mm) and an anionic detector ICS-1100. Thus, 0.03 $mol \cdot L^{-1}$ of the CH_3SO_3H solution was used as the mobile phase for the cations equipment and a mixture of 0.8 $mmol \cdot L^{-1}$ of $NaHCO_3$ and 4.5 $mmol \cdot L^{-1}$ of Na_2CO_3 for the anions system. Both devices were controlled by Chromeleon® chromatographic software.

4.4. Results and Discussion

First of all, pretreated wastewater from the WWTP was analyzed by ionic chromatography to determine the ions concentration and other parameters, such as pH or conductivity (Table 2).

Parameter	Value	Units
Ammonium (NH4+)	4.60 ± 0.14	mg·L-1
Calcium (Ca2+)	0.04 ± 0.02	
Chloride (Cl−)	0.35 ± 0.14	
Magnesium (Mg2+)	0.03 ± 0.01	

Nitrate (NO3−)	0.33 ± 0.11	
Phosphate (PO43−)	0.05 ± 0.02	
Potassium (K+)	0.46 ± 0.05	
Sodium (Na+)	12.70 ± 0.01	
Sulphate (SO42−)	0.38 ± 0.11	
Conductivity (25ºC)	66.30 ± 0.99	mS/cm
pH (25ºC)	13.13±0.24	-
Total carbon (C)	57.93 ± 0.87	mg·L-1

Table 2. Initial sidestream wastewater composition

As can be seen in Table 2, the sidestream wastewater used as the feed solution in this work was mainly composed of sodium and ammonium ions mixed with dissolved organic matter at a high pH, in this scenario, N is predominantly present in the form of NH_3(>pKa = 9.25). Then, ammonium was present as ammonia in gas form. Moreover, other elements were found, such as potassium, chloride, nitrate or sulphate, but at trace levels. On the other hand, apart from the sidestream wastewater, mainstream wastewater was also used in this work. In this case, the major difference between wastewaters was the ammonium concentration, being approximately 1 $g \cdot L^{-1}$ for the mainstream.

After each experiment, the remaining feed solution and, also, the ammonium salt produced were both analyzed to corroborate that only ammonium passed through the LLMC but not other elements (data not shown).

4.4.1. Effect of Changing Feed or Acid Stripping Solution between LLMC Process Steps to Increase Ammonia Recovery

As previously mentioned, two scenarios were studied: (i) changing the acid solution between steps and (ii) replacing the feed solution with a new one between steps. In the first case, the idea was to further decrease the final ammonia concentration of the feed solution while obtaining two liquid fertilizer solutions of a similar concentration. In the second scenario, the aim was to achieve a more concentrated liquid fertilized in the acid stripping side, although not able to decrease the ammonia concentration of the feed solution so much. Figure 1 shows the ammonia evolution in the feed solution and the

nitrogen concentration evolution in the ammonium salts solution over time for both scenarios.

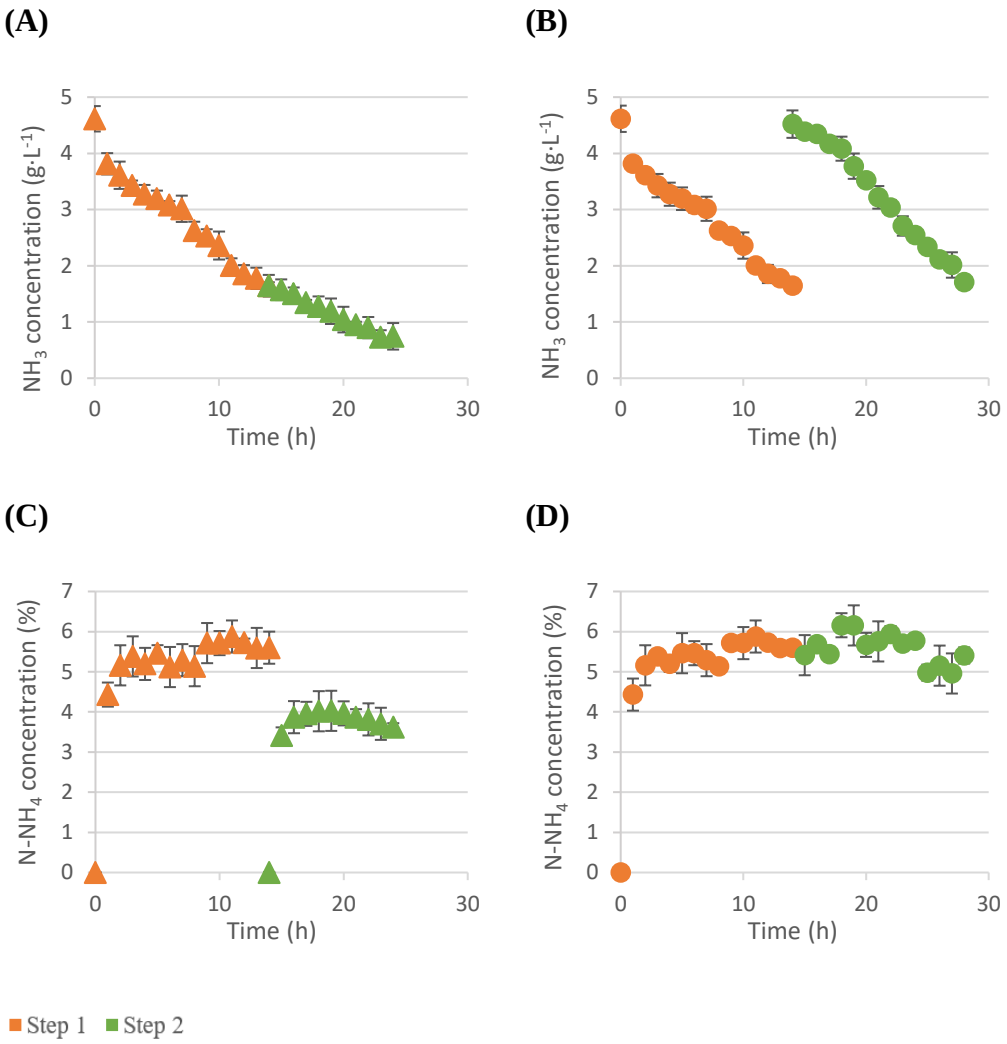

Figure 1. Ammonia concentration evolution over time in the feed tank when changing (**a**) the acid and (**b**) feed between steps (up). Nitrogen concentration achieved in the liquid fertilizer by changing the (**c**) acid or (**d**) feed solution between steps (down). Orange color implies one stage of LLMC (triangle for the feed side and circle referring to the fertilizer solution), while green color refers to experiments with two LLMC stages (triangle for the feed side and circle referring to the fertilizer solution). The errors bars represent standard deviation (n=4).

As can be seen in Figure 1, the ammonia concentration in the feed solution decreased over time from around 4.5 to 1.6 g $NH_3 \cdot L^{-1}$ during the first step (Figure 1 a,b). Afterwards, replacing the fertilizer for a new acid solution (0.4 M HNO_3) in the stripping side, it was

possible to further decrease the ammonia concentration down to 0.7 g·L-1 (Figure 1a), whereas a similar behaviour to that observed in step 1 was achieved when changing the feed solution for a new one with approximately 4.5 g $NH_3 \cdot L^{-1}$, reducing its concentration to 1.6 g $NH_3 \cdot L^{-1}$ (Figure 1b).

On the other hand, comparing the nitrogen concentration evolution in the stripping side (Figure 1c,d), it can be seen that two ammonium salt solutions (around 5.4% N-NH_4 and 3.9% N-NH_4) were produced when changing the acid between steps (Figure 1c), whereas just one liquid fertilizer was produced when changing the feed solution, although its concentration was almost not even increased (from around 5.5 to 5.6% N-NH_4) (Figure 1d).

Additionally, the ammonia recovery was calculated after each step and was also determined for the overall process, taking into account both steps (Figure 2).

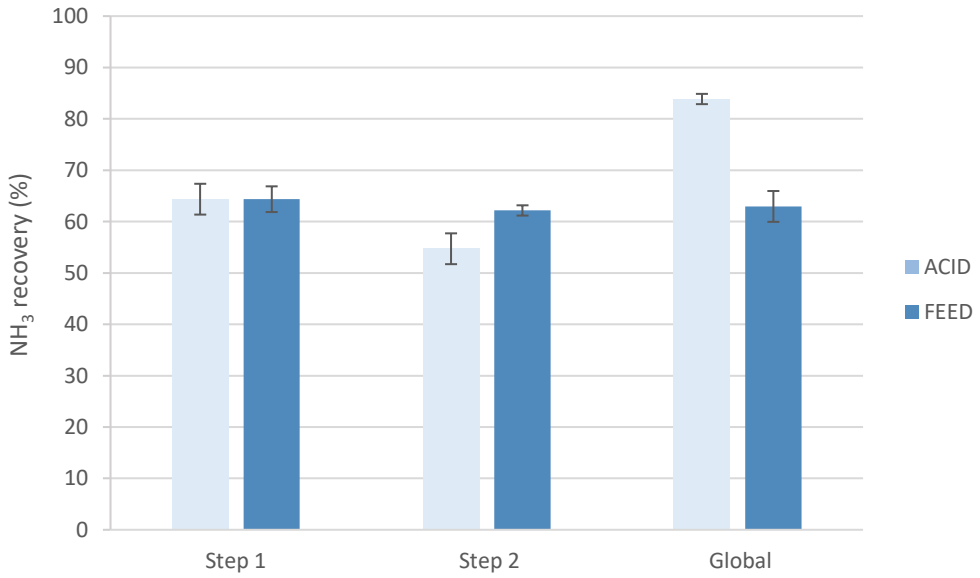

Figure 2. Ammonia recovery after each step, and the global results changing the acid or the feed solution between steps. The errors bars represent standard deviation (n=4).

Figure 2 illustrates, the first step for both experiments had the same performance, achieving ammonia recovery values of around 64.4%. The results for the second step demonstrated that the NH_3 recovery obtained was better when changing the feed solution after reaching a plateau (62.2±1.3% vs. 54.7±3.2% N-NH_4) since the initial ammonia concentration was again the same as in the beginning, so more ammonia ions could react with the remaining nitric acid of the stripping side. Nevertheless, the overall and

maximum ammonia recovery achieved was higher (≈83.9±0.7%) when changing the acid stripping solution between steps. The difference between both cases can be attributed to the fact that during operation, the saline concentration on the stripping side is practically zero or very low, which eliminates the effect of osmotic distillation. However, as the saline concentration on the stripping side increases, this phenomenon begins to occur, leading to a greater water passage and reducing the concentration capacity on the acid side. By changing the stripping solution, the saline concentration essentially returns to nearly zero, allowing for greater selectivity towards ammonia and therefore higher concentration capacity. On the other hand, when replacing the feed tank with a new one, a gradient in saline concentration is also generated, but it is lesser. This is why the ammonia concentration in the feed decreases, but it does not increase on the acid side. This is because the acidic solution already contains a high presence of salts from the previous feed tank that were transported, resulting in higher water transport due to osmotic distillation, preventing higher concentration on that side.

Few papers can be found in the literature studying the effects of working with different steps of LLMCs. Indeed, preliminary experiments by two-stage LLMC changing the acid stream were previously done by our research group (Reig et al., 2021). The results demonstrated that similar results were obtained by one or two steps. For this reason, in the present work, the feed solution was changed between steps to try to enhance the overall performance. However, changing the acid solution between steps was selected as optimal regarding the results. In fact, it allowed to obtain a feed solution with less ammonia concentration and two liquid fertilizer solutions with a similar nitrogen concentration, and also, a higher ammonia recovery (around 25% more) could be reached.

Furthermore, Zhang et al. 2021, proposed a three-stage LLMC process, changing the acid stripping solution by passing the feed stream through the three LLMC in the series. The main objective was to recover ammonia from human urine as ammonium nitrogen (J. Zhang et al., 2021). The results are in agreement with the one found in this article Zhang et al. 2021, since the average ammonia removal percentage was much higher as a global value (over 99%), than taking into account LLMC by LLMC (between 80 and 83%). Additionally, Yan et al. 2018, studied a four-stage LLMC system, recirculating both streams, feed and acid between steps. Again, the results demonstrated that the ammonia recovery could be increased by including more LLMC stages, being able to enhance the recovery value from 65 up to >98% (H. Yan et al., 2018).

4.4.2. Initial Ammonia Concentration Effect on the Overall LLMC Performance

Sidestream wastewater (4.5-5 g $NH_3 \cdot L^{-1}$) and mainstream wastewater (≈1 g $NH_3 \cdot L^{-1}$) were used as the feed solution in the LLMC. The results indicated that both wastewaters could be treated by LLMC, although several parameters were determined to establish the optimal performance. Figure 3 shows the ammonia concentration evolution over time and its recovery on the feed tank (up) and, also, the concentration factor and the nitrogen concentration achieved in the ammonium salt solution (down).

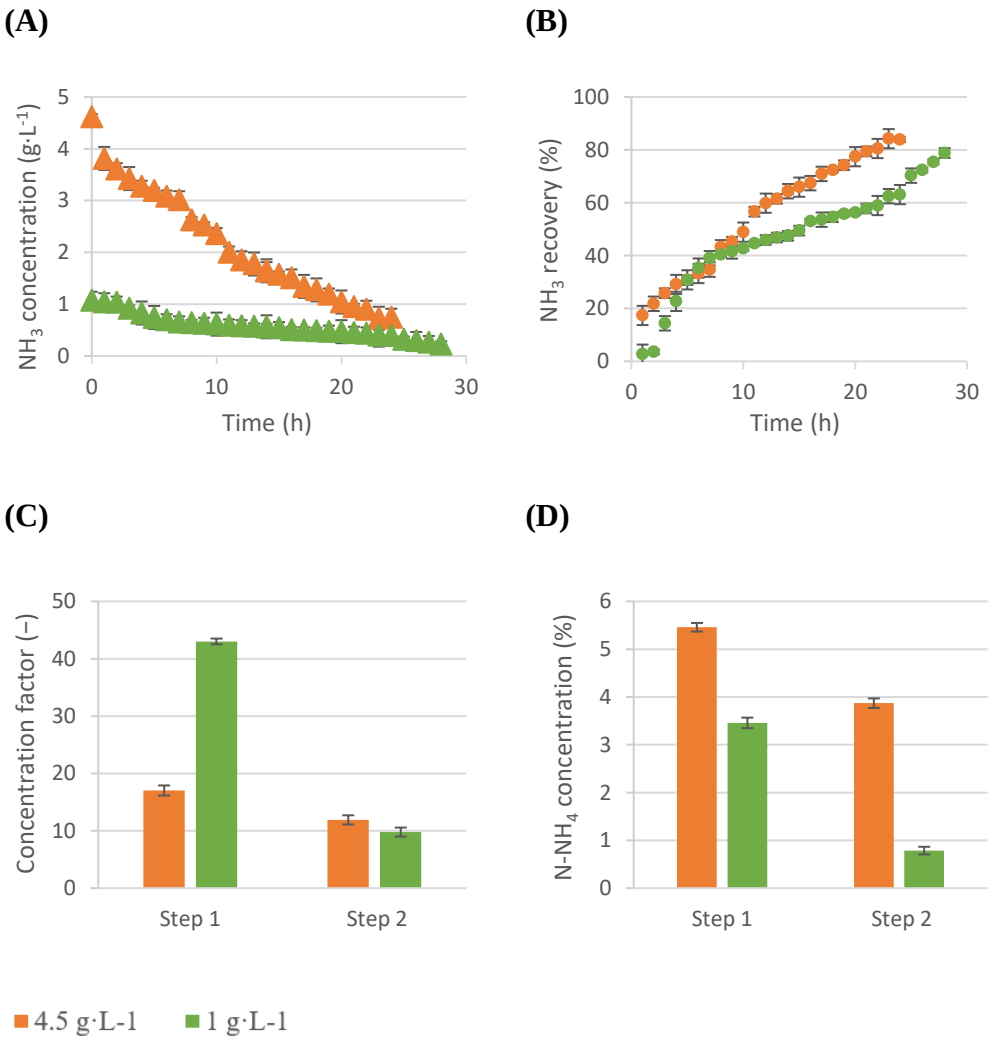

Figure 3. Comparison between working with the sidestream (high NH_3 concentration) and mainstream wastewater (low NH_3 concentration): (**a**) ammonia concentration evolution in the feed tank, (**b**) ammonia recovery, (**c**) concentration factor and (**d**) %N-NH_4 concentration in the liquid fertilizer. High ammonia concentration is indicated by the color orange, while the color yellow implies working at low ammonia concentrations. The errors bars represent standard deviation (n=4).

As shown in Figure 3a, the final ammonia concentration was lower when working with the mainstream wastewater, being able to achieve values lower than around 200 mg $NH_3 \cdot L^{-1}$. In this case, this stream (ammonia-free) could be reused in the zeolites process (Reig et al., 2021). Moreover, not only lower levels of ammonia were achieved by mainstream wastewater but, also, a similar recovery percentage (almost 80%) in comparison when using sidestream solutions (Figure 3b).

On the other hand, since the initial ammonia concentration in the feed solution was lower, when using the mainstream (1 $g \cdot L^{-1}$), the concentration factor was much higher (CF=43) during the first step of this experiment (Figure 3c). Nonetheless, the obtained nitrogen concentration values in the ammonium salt solution were higher when using the sidestream wastewater (around 5.5 and 3.9% $N\text{-}NH_4$ in the first and second steps, respectively) (Figure 3d). Thus, if the main purpose is to obtain a more concentrated liquid fertilizer, it would be better to use sidestream wastewater. However, evaluating the feed side of the LLMC, the difference between the ammonia recovery achieved using both wastewaters was around 6%, whereas the difference between the final ammonia concentration in both cases was almost 70%. Thus, the less-concentrated wastewater had a more efficient ammonia recovery performance by LLMC, although it obtained a less-concentrated liquid fertilizer.

The initial ammonia concentration influence on LLMC experiments has previously been studied, although there is not a concluding resolution. Some authors reported that the initial concentration did not influence the ammonia mass transfer through LLMC, whereas other authors, such as in our case, concluded that a lower ammonia initial concentration allowed a better LLMC performance.

For instance, the results obtained in this work agree with the published results by Ahn et al. 2011. In that case, a PTFE (pore size of 0.4 μm) tubular membrane was employed with 205.5 cm^2 of effective surface. Amongst the other parameters such as pH, feed and stripping flow rate, the influence of the initial ammonia concentration (250–1000 $mg \cdot L^{-1}$) was studied. The experiments were evaluated during 10 h of operating time, and the results obtained were the following: when 1000 $mg \cdot L^{-1}$ was used, the ammonia concentration decreased until reaching a concentration of approximately 300 $mg \cdot L^{-1}$, whilst 250 $mg \cdot L^{-1}$ showed a lower, steep decreasing trend over time and, thus, worse removal efficiency. Nevertheless, it was possible to achieve lower concentrations at 10 h

(from 250 to 100 mg·L^{-1}) than working with the 1000 mg·L^{-1} solution (down to 300 mg·L^{-1}). Furthermore, the results indicated a lessening in the mass transfer coefficient as the ammonia concentration was increased (8.9×10^{-3} m·h^{-1} to 7.0×10^{-3} m·h^{-1}) (Ahn et al., 2011).

On the other hand, Ashrafizadeh and Khorasani 2010, simulated different scenarios of ammonia recovery through LLMCs, assessing the parameters such as pH, initial ammonia concentration and solution flow velocity. Regarding the influence of the ammonia concentration on the recovery efficiency, several experiments were performed testing the feed solutions with ammonia concentrations lower than the ones tested in this study (between 50 mg·L^{-1} and 800 mg·L^{-1}). In that case, the authors concluded that the ammonia removal had a non-dependent behavior on the feed initial concentration (Ashrafizadeh & Khorasani, 2010). However, Kartohardjono et al. 2015 , also tested lower initial ammonia concentrations than the ones used in this work (from around 100–800 mg·L^{-1}) to determine the influence of the initial ammonia concentration in the feed solution. The results indicated that a slightly less ammonia recovery efficiency was achieved when increasing the initial ammonia concentration. In other words, the results showed that the lower the initial ammonia concentration, the more efficient the ammonia recovery. Furthermore, the overall mass transfer coefficient decreased as the initial ammonia concentration rose (Kartohardjono, Damaiati, et al., 2015; Kartohardjono, Fermi, et al., 2015).

Later, Moradihamedani 2021, published a review paper reporting that neither the ammonia removal nor the ammonia mass transfer coefficient were dependent on the initial ammonia concentration of the feed stream (Moradihamedani, 2021). Contrarily, Uzkurt Kaljunen et al. 2021, concluded that a higher initial nitrogen concentration had a negative impact on the mass transfer coefficient (Uzkurt Kaljunen et al., 2021). Additionally, Yu et al. 2021, recently made a comparison between the influence of the initial ammonia concentration (from 100 to 2000 mg·L^{-1}) when using a conventional LLMC or an aqueous–organic membrane contactor. They postulated that the initial ammonia concentration was not influenced when using conventional LLMCs, although the best results were achieved when treating feed streams with a low ammonia concentration through an aqueous–organic membrane contactor. In fact, they concluded that lower mass transfer coefficients were reached by increasing the initial ammonia concentration (Yu et al., 2021).

4.4.3. Study of the Effect of Initial Feed Volume on the LLMC Trials

The acid stripping side volume during the trials was kept constant at 0.5 L. However, two feed volumes (60 and 5 L) were tested to determine the best feed/acid stripping volume ratio (120 or 10) for the LLMC performance. The results (see Table 3) indicated that a lower feed volume (5 L) resulted in a better performance on the feed side, whereas a higher feed solution volume (60 L) implied a better evolution in the fertilizer side results.

Table 3. Results of the study on the effect of feed volume, with error bars representing the standard deviation (n=4).

		60 L			**5 L**		
		Step 1	**Step 2**	**Global**	**Step 1**	**Step 2**	**Global**
Feed side	**NH_3 recovery (%)**	47.5 ± 0.9	59.7 ± 1.1	78.8 ± 1.8	93.5 ± 3.2	48.6 ± 0.8	96.7 ± 2.9
	Final [NH_3] ($mg \cdot L^{-1}$)	564 ± 55.6	227.5 ± 49.9		74.4 ± 8.2	38.2 ± 5.3	
Acid stripping side	**CF (-)**	35.0 ± 0.8	9.8 ± 0.8	-	10.2 ± 0.6	43.0 ± 0.8	9.8 ± 0.8
	%N-NH_4 (%)	3.5 ± 0.1	0.9 ± 0.1	-	0.9 ± 0.1	3.5 ± 0.1	0.8 ± 0.1

For all these experiments, mainstream wastewater was used (initial NH_3 concentration around 1 $g \cdot L^{-1}$). As can be seen in Table 3, although the initial ammonia concentration was the same, more NH_3 recovery (96.7 vs. 78.8%) and less final ammonia concentration in the feed solution (38.2 vs. 227.5 mg $NH_3 \cdot L^{-1}$) were achieved by working with the 5-L feed solution in comparison with the 60-L wastewater stream. Thus, it can be concluded that lees feed water permitted to remove more ammonia from the mainstream wastewater, as well as to obtain a more ammonia-free stream at a high pH, could be reused in the regeneration stage of the zeolites process. On the other hand, if the main objective is to achieve a more concentrated liquid fertilizer, better results were obtained when treating the greater volume (60 L). In this case, higher CF values (one order of magnitude higher) and more %N-NH_4 (3.5 vs. 0.9% during the first step) were obtained in comparison to the results achieved by the lower volume experiments. Thus, more feed volume could be used if more concentrated fertilizer is required.

To the best of our knowledge, only one work was found in the literature studying the feed volume effect working with LLMCs. Indeed, the results of this work are in concordance with the results obtained by Mayor et al. 2020. In that case, three different feed volumes were tested: 5, 30 and 60 L. The results showed that the lower feed volume increased the ammonia recovery (from 85.0 to 96.3%) and also decreased the experimental time, obtaining the lower fertilizer concentration (Mayor et al., 2020).

4.4.4. Wastewater Temperature Effect on the LLMC Process

Lastly, the effect of the temperature of the feed wastewater was studied as a variable of the LLMC performance. In this case, room temperature (25 °C) and 10 °C more (35 °C) were tested. Again, the employed feed solution was the mainstream, with an initial concentration of about 1 g $NH_3 \cdot L^{-1}$. Moreover, 5 L of feed solution were used.

Figure 4 shows the ammonia recovery over time and the final concentration factor achieved working with the feed solution at 25 °C or 35 °C.

A)

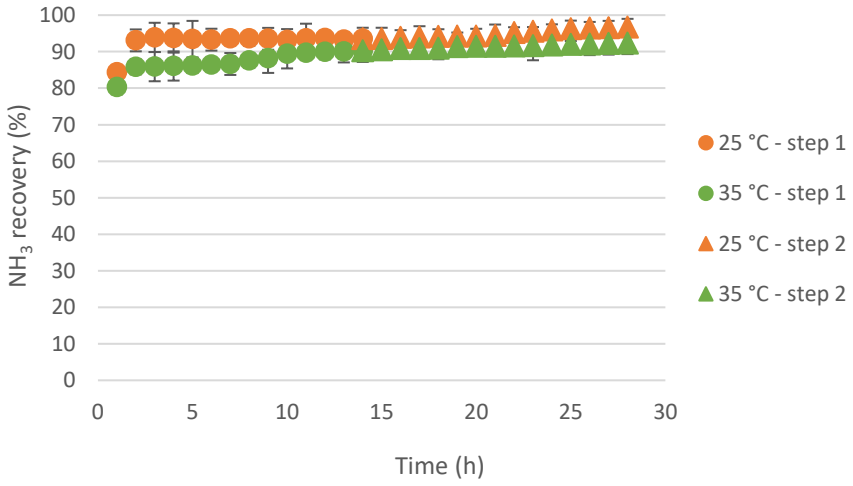

B)

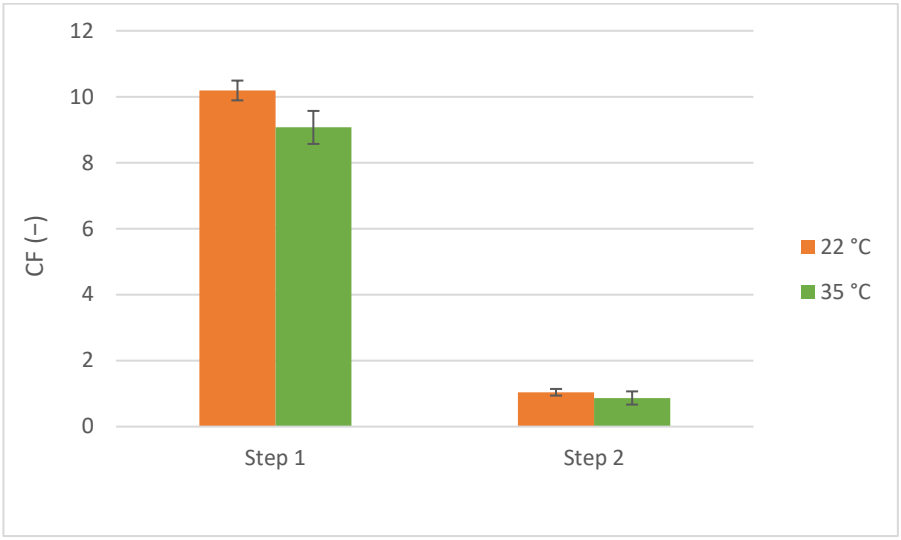

Figure 4. Temperature results comparison: (**a**) ammonia recovery and (**b**) concentration factor. The errors bars represent standard deviation (n=4).

As can be seen in Figure 4a, high ammonia recovery values were obtained in both cases (about 92%). An ANOVA test was done to determine if the obtained differences were significant, obtaining a *p*-value higher than 0.05, which determined that no significant differences occurred during NH_3 recovery when testing the LLMC with a feed solution at 25 or 35 °C. On the other hand, Figure 4b shows the concentration values achieved. As can be seen, higher concentration values (10.2 ± 0.3 and 9.1 ± 0.5 working at 25 and 35 °C, respectively) were obtained during the first step of the LLMC performance in comparison with the second step (1.0 ± 0.1 and 0.9 ± 0.2 for the 25 °C and the 35 °C experiments, respectively). Again, the concentration factors comparison between the different temperatures tested was done with an ANOVA test, obtaining a *p*-value > 0.05 for each step, indicating that the influence of the feed temperature was not significant on the overall LLMC performance.

Moradihamedani 2021, recently published a review article indicating that a higher feed temperature had a positive influence on the ammonia recovery by LLMC, improving the ammonia removal. However, it was concluded that this impact was significant at

temperature values higher than 40 °C. High temperatures (>40 °C) increased the ammonia partial pressure, improving the ammonia mass transfer due to the increased pressure different (Moradihamedani, 2021). However, when the temperature was lower than 40 °C, it seemed that there was no influence on the overall performance. In fact, Ahn et al. 2011, tested several LLMC operation parameters, such as flow rate, stripping solution, feed wastewater pH and temperature. In that case, the temperatures tested varied by 13 °C, being 22 °C and 35 °C. The results demonstrated that, although the ammonia removal percentage slightly increased (by 4.4%) with the temperature, its effect was not significant (Ahn et al., 2011). On the other hand, the maximum temperature allowed regarding the Design & Operational Guidelines of the LLMC Manufacturer Company (3M^{TM}) was 35 °C, which did not damage the membrane contactor (Guidelines, n.d.). Regarding the results of this work and, also, the obtained results in the already published literature, it would be better to work at room temperature (22–25 °C) instead of increasing the feed wastewater temperature. Thus, similar results will be obtained, although lower operational costs will be required without heating the feed solution. If not, based on the published literature, higher temperatures than 40 °C would be recommended.

4.5. Conclusions

This work studied the effect of several operational conditions during the LLMC performance. For instance, feed or acid solution replacement between the steps was evaluated, concluding that more than 20% improvement was achieved in the ammonia removal percentage when changing the acid stripping solution. Regarding the initial ammonia concentration, considering a sidestream (4.5 g $NH_3 \cdot L^{-1}$) or a mainstream (1 g $NH_3 \cdot L^{-1}$), both streams could be used with good LLMC results, depending on their purpose. A sidestream could be useful when the maximum ammonia recovery (6% difference) and more %N-NH_4 is required, whereas the mainstream would be better able to decrease the feed ammonia concentration to a lower value and, at the same time, to reach a higher concentration factor (60% of the difference in the first step). Additionally, the feed volume also has an impact on the LLMC technique. In fact, it has been observed that a larger volume has a more notable positive impact on the fertilizer side, as it increases the concentration factor and the percentage of N-NH_4. On the other hand, a smaller volume seems to yield more favorable results on the feed side, facilitating greater ammonia recovery and reducing the final concentration of ammonia in the feed. This summary could be considered limited, as it does not capture all the complexity and

nuances of the observed results. Finally, the differences in temperature tested were not enough to have significant improvements in the LLMC performance. All in all, LLMC proved to be a versatile technique to treat wastewater with low (1 $g \cdot L^{-1}$) and high (4.5 $g \cdot L^{-1}$) initial ammonia concentrations, where the most influential parameter was the change of the stripping solution in the formulation of ammonium salts. Therefore, LLMC could be an easy technique to be implemented in biofactories for the recovery of nutrients from main or side wastewater streams.

4.6. References

Ahn, Y. T., Hwang, Y. H., & Shin, H. S. (2011). Application of PTFE membrane for ammonia removal in a membrane contactor. *Water Science and Technology*, *63*(12), 2944–2948. https://doi.org/10.2166/wst.2011.141

Ashrafizadeh, S. N., & Khorasani, Z. (2010). Ammonia removal from aqueous solutions using hollow-fiber membrane contactors. *Chemical Engineering Journal*, *162*(1), 242–249. https://doi.org/10.1016/j.cej.2010.05.036

Barros, A., Vecino, X., Reig, M., & Cortina, J. L. (2022). Coagulation and Flocculation Optimization Process Applied to the Sidestream of an Urban Wastewater Treatment Plant. *Water (Switzerland)*, *14*(24), 1–26. https://doi.org/10.3390/w14244024

Darestani, M., Haigh, V., Couperthwaite, S. J., Millar, G. J., & Nghiem, L. D. (2017). Hollow fibre membrane contactors for ammonia recovery: Current status and future developments. *Journal of Environmental Chemical Engineering*, *5*(2), 1349–1359. https://doi.org/10.1016/j.jece.2017.02.016

Guidelines, S. (n.d.). *3M ™ Liqui-Cel ™ EXF Series Membrane Contactors*.

Kartohardjono, S., Damaiati, G. M., & Rama, C. T. (2015). Effects of absorbents on ammonia removal from wastewater through hollow fiber membrane contactor. *Journal of Environmental Science and Technology*, *8*(5), 225–231. https://doi.org/10.3923/jest.2015.225.231

Kartohardjono, S., Fermi, M. I., Yuliusman, Elkardiana, K., Sangaji, A. P., & Ramadhan, A. M. (2015). The removal of dissolved ammonia from wastewater through a polypropylene hollow fiber membrane contactor. *International Journal of Technology*, *6*(7), 1146–1152. https://doi.org/10.14716/ijtech.v6i7.1845

Li, K., Kong, J., & Tan, X. (2000). Design of hollow fibre membrane modules for soluble gas removal. *Chemical Engineering Science*, *55*(23), 5579–5588. https://doi.org/10.1016/S0009-2509(00)00193-7

Licon Bernal, E. E., Maya, C., Valderrama, C., & Cortina, J. L. (2016). Valorization of ammonia concentrates from treated urban wastewater using liquid-liquid membrane contactors. *Chemical Engineering Journal*, *302*, 641–649. https://doi.org/10.1016/j.cej.2016.05.094

Majd, A. M. S., & Mukhtar, S. (2013). *AND FIELD-SCALE STUDIES*. *56*(Lm), 1951–1958.

Moradihamedani, P. (2021). Recent developments in membrane technology for the elimination of ammonia from wastewater: A review. *Polymer Bulletin*, *78*(9), 5399–5425. https://doi.org/10.1007/s00289-020-03386-y

Naim, R., Ismail, A. F., & Mansourizadeh, A. (2012). Effect of non-solvent additives on the structure and performance of PVDF hollow fiber membrane contactor for CO 2 stripping. *Journal of Membrane Science*, *423–424*, 503–513. https://doi.org/10.1016/j.memsci.2012.08.052

Reig, M., Vecino, X., Gibert, O., Valderrama, C., & Cortina, J. L. (2021). Study of the operational parameters in the hollow fibre liquid-liquid membrane contactors process for ammonia valorisation as liquid fertiliser. *Separation and Purification Technology*, *255*(July 2020), 117768. https://doi.org/10.1016/j.seppur.2020.117768

Samani Majd, A. M., & Mukhtar, S. (2013). Ammonia diffusion and capture into a tubular gas-permeable membrane using diluted acids. *Transactions of the ASABE*, *56*(5), 1943–1950. https://doi.org/10.13031/trans.56.10218

Sheikh, M., Reig, M., Vecino, X., Lopez, J., Rezakazemi, M., Valderrama, C. A., & Cortina, J. L. (2022). Liquid–Liquid membrane contactors incorporating surface skin asymmetric hollow fibres of poly(4-methyl-1-pentene) for ammonium recovery as liquid fertilisers. *Separation and Purification Technology*, *283*, 120212. https://doi.org/10.1016/j.seppur.2021.120212

Uzkurt Kaljunen, J., Al-Juboori, R. A., Mikola, A., Righetto, I., & Konola, I. (2021). Newly developed membrane contactor-based N and P recovery process: Pilot-scale field experiments and cost analysis. *Journal of Cleaner Production*, *281*, 125288. https://doi.org/10.1016/j.jclepro.2020.125288

Vecino, X., Reig, M., Bhushan, B., Gibert, O., Valderrama, C., & Cortina, J. L. (2019). Liquid fertilizer production by ammonia recovery from treated ammonia-rich regenerated streams using liquid-liquid membrane contactors. *Chemical Engineering Journal*, *360*(December 2018), 890–899. https://doi.org/10.1016/j.cej.2018.12.004

Vecino, X., Reig, M., Gibert, O., Valderrama, C., & Cortina, J. L. (2020). Integration of liquid-liquid membrane contactors and electrodialysis for ammonium recovery and concentration as a liquid fertilizer. *Chemosphere*, *245*, 125606. https://doi.org/10.1016/j.chemosphere.2019.125606

Yan, H., Wu, L., Wang, Y., Shehzad, M. A., & Xu, T. (2018). Ammonia capture by water splitting and hollow fiber extraction. *Chemical Engineering Science*, *192*, 211–217. https://doi.org/10.1016/j.ces.2018.07.040

Yu, S., Qin, Y., Zhao, Q., Li, M., Yu, H., Kang, G., & Cao, Y. (2021). Nafion-PTFE hollow fiber composite membranes for ammonia removal and recovery using an aqueous-organic membrane contactor. *Separation and Purification Technology*, *271*(April), 118856. https://doi.org/10.1016/j.seppur.2021.118856

Zhang, J., Xie, M., Yang, D., Tong, X., Qu, D., Feng, L., & Zhang, L. (2021). The design of multi-stage open-loop hollow fiber membrane contactor and its application in ammonia capture from hydrolyzed human urine. *Water Research*, *207*(October), 117811. https://doi.org/10.1016/j.watres.2021.117811

Zhu, Z., Hao, Z., Shen, Z., & Chen, J. (2005). Modified modeling of the effect of pH and viscosity on the mass transfer in hydrophobic hollow fiber membrane contactors. *Journal of Membrane Science*, *250*(1–2), 269–276. https://doi.org/10.1016/j.memsci.2004.10.031

CHAPTER 5

Ammonium recovery and concentration from synthetic wastewater using a poly(4-methyl-1-pentene) (PMP) liquid-liquid membrane contactor: flux performance and mass transport characterization

5.1. Abstract

Hollow fiber membrane contactors are a promising technology for the removal and recovery of ammonia from liquid effluents. However, a better understanding of the process engineering (e.g. mass transport of ammonia over water) and performance optimization is required. In this study, the performance of a hollow fibre liquid-liquid membrane contactor (HF-LLMC), incorporating a new polymer chemistry (i.e., poly (4-methyl-1-pentene (PMP) and an asymmetric fibre structure, for the recovery and concentration of ammonium from synthetic aqueous solutions, was investigated. The influence of the feed and acid flow rates was evaluated experimentally by determining the overall mass transfer coefficient (k_{ov}), the ammonium recovery as a function of time and the acid consumption. In addition, the experimental results were fitted to a mathematical model to determine the membrane permeabilities to ammonia (P_{NH3}) and water (P_w) and identify the mass transfer resistance regime. The highest k_{ov} values experimentally obtained were in the range of $3 \cdot 10^{-3}$ to $3.51 \cdot 10^{-3}$ m h^{-1} with corresponding ammonia recovery rates of 94 to 96.2% after 10h, operating at a feed and acid flow rates of 180 L h^{-1} and 500 L h^{-1}, respectively, which are in the upper range of the HF-LLMC literature. The overall results of this study a much-lower water transport was confirmed indirectly by the concentration factor (CF) values obtained experimentally. The remarkable selectivity of the membrane towards ammonia over water (i.e., P_{NH3} = 87 - 180 L m^{-2} h^{-1} bar^{-1} and P_w = 1.2 -1.4·10^{-3} L m^{-2} h^{-1} bar^{-1} at NTP conditions) could be attributed to the asymmetrical membrane structure and the polymer chemistry (i.e., PMP). The proven high ammonia selectivity of the HF-LLMC renders it a promising technology for the recovery and concentration of ammonium from urban (e.g. wastewaters) and industrial (e.g. soda ash and fertilizers production) diluted streams.

Keywords: Asymmetric membrane; Ammonia recovery and concentration; Ammonia membrane permeability.

5.2. Introduction

The growing world population results in increase demand for food, leading to an increased need for fertilizer production (Chagas et al., 2023; W. Lee et al., 2021; Mayor et al., 2023), and consequently an increase in energy consumption due to an almost exclusive dependence on the Haber-Bosch process (HB) for the synthesis of nitrogenous fertilizers (Silva & Quesada, 2010). The HB process consumes approximately 35-50 MJ kg^{-1} N (i.e., 1000 m^3 of natural gas per ton of N-based fertilizers) which represents approximately 1-2% of the global energy consumption and 50% of the total natural gas used in the chemical industry (Beckinghausen et al., 2020). Approximately, 85% of the worldwide synthesized ammonia is employed in fertilizer production (PotashCorp, 2014) and out of the 160 Mt of fertilisers used annually worldwide, 100 Mt come from the HB process (González Montiel, 2008). It is therefore necessary to identify alternative sources of ammonia in order to reduce the energy impact of fertilizer production (Razon, 2018).

On the other hand, nitrogenous fertilizers (N-fertilizers) have very low application efficiencies and only 16% of the applied quantity is converted into proteins usefull por animals/humans while the rest is lost into water bodies and the atmosphere aggravating phenomena such as eutrophication (Deng et al., 2021). About 10 - 40% of the lost N-fertilizers ends up denitrified (i.e., released as N_2) by the vegetation or in wastewater treatment plants (WWTPs) (Matassa et al., 2015; Mayor et al., 2023). Nitrogen is traditionally removed in WWTPs during the secondary treatment using biological nutrient removal methods, and although the annamox technology has gained much interest recently (Beckinghausen et al., 2020; Vineyard et al., 2020), the nitrification-denitrification (N/DN) process remains the most widely. The N/DN is an energy intensive process (i.e., 45 MJ per kg^{-1} N eliminated) (Ledezma et al., 2015) whose aeration requirements represent 50% of the total energy consumption of a WWTP (Nowak, 2003). For instance, WWTPs in the United States account for 4% of the nation's yearly electricity consumption and generate a carbon footprint of 0.9 kg CO_2 per m^3 of treated water (Xie et al., 2016).

In the new circular economy paradigm, there is a growing interest in transforming WWTPs into "bio-factories" and recovering valuable resources such as nutrients and

energy. Under this paradigm, anaerobic digestion (AD) and the recovery of ammonium and phosphate from digestates and side-streams will be pivotal in the valorisation of organic matter as biogas and fertilizers (Darestani et al., 2017; Rongwong & Goh, 2020).

As a result, new technologies and processes with high selectivity such as ion exchange (IX) (Kurniawan et al., 2006; Wan et al., 2017), its combination with membrane technologies, e.g., ultrafiltration (Hermassi et al., 2017) and membrane contactors (MC) (Hasanoğlu et al., 2010; Licon Bernal et al., 2016; Reig et al., 2021) among others, are being studied for ammonium recovery from several liquid waste streams (e.g., digestates, landfill leachate, industrial waste streams, etc.).

However, IX technology has some limitations including the requirement for a chemical-intensive and time-consuming regeneration process, lower ammonia recovery rates and competence of unwanted ions (Darestani et al., 2017). For example, (Wan et al., 2017) recovered nutrients from liquid supernatant from municipal WWTP excess sludge using natural zeolites (IX) reaching ammonium and phosphate recoveries of 70.5% and 84.3%, respectively after five hours of operation plus another five hours (100% extra time) for the regeneration step. Hermassi et al. 2017, used mixtures of calcium and sodium zeolites for the simultaneous recovery of N-P-K from anaerobic digestion side-streams using a hybrid sorption/filtration system and found an important decrease in the NH_4^+ ion exchange capacity due to the presence of competing ions (any divalent cations) in real waters (Hermassi et al., 2017). The necessity for significant quantities of zeolite material can also be a challenge in IX. For instance, according to a study by (Eskicioglu et al., 2018a) for a medium-sized WWTP (20,000 m^3 d^{-1}) over 8,000 kg of zeolite would be required to treat a side-stream (representing only a 0.5% of the total water input) with an average ammonium concentration of 1.2 g NH_4^+ L^{-1}. As stated by the authors, the expenses related to transporting, maintaining and storing such a substantial amount of zeolite could be prohibitive unless a nearby source is readily accessible.

Among membrane technologies for ammonium recovery, MC stands out for its selectivity. The basis of MC technology is the utilization of a microporous hydrophobic membrane that separate two fluid phases (gas/liquid or liquid/liquid) to promote mass transfer of certain components from one phase to the other while avoiding dispersion (Gabelman & Hwang, 1999; Pabby & Sastre, 2013). MC has been already studied to recover ammonia from wastewater streams in the laboratory (Amaral et al., 2016; García-

González et al., 2015; Pauzan et al., 2021; Reig et al., 2021) and even some medium-scale implementation examples have been reported. For example, Richter et al. 2020 studied the feasibility of implementing a Polypropylene (PP) hollow fiber liquid-liquid membrane contactor (HF-LLMC) stage to treat a centrate water stream of 342 m^3d^{-1} and 0.9 g NH_4^+ L^{-1} in an urban WWTP plant in Münster (Germany) to produce an ammonium sulphate fertilizer solution. The authors reported a recovery efficiency >95% and a concentration factor (CF) calculated as the final NH_4^+ permeate concentration divided by the initial NH_4^+ feed concentration, of 4.1 (i.e., ammonium sulphate solution of 3.69 g NH_4^+ L^{-1}) (Richter et al., 2020).

There are several polymeric MC module configurations, yet the most used ones are hollow fibre modules because of their high packing density and total surface area (Bazhenov et al., 2018). However, these modules are more sensitive to membrane fouling (Darestani et al., 2017). In fact, fouling is reportedly the most challenging drawback of membrane technologies, including MC, and depending on the feed water, pre-treatment might be mandatory. For example, in a previous work (Aguilar-Moreno et al., 2022) we successfully optimized a coagulation/flocculation pre-treatment prior a LLMC module used for the recovery of ammonium from a WWTP centrate stream with moderate fouling potential (i.e., 0.8 g COD L^{-1}). By dosing 30 mg of aluminium sulphate ($Al_2(SO_4)_3$) per litre of centrate, the COD was reduced by 60% while maintaining a relatively high pH (i.e., pH>10) and increasing the ammonium recovery from 8% to 66%.

The combination of the two technologies (IX and MC) can help in this direction since the IX stage not only pre-concentrates the ammonium but also acts as a pre-treatment as ammonium is selectively removed. For example, Sancho et al. 2017 used a LLMC to treat the ammonium-rich regenerated stream from the elution of ammonium-selective zeolites with a 2 g L^{-1} NaOH solution and produced liquid nitrogenous fertilizers. The authors reported removal rates of 95% and final ammonium nitrate and di-ammonium phosphate fertilizer solutions of concentrations ranging 2–5% w N (Sancho et al., 2017). Likewise, Vecino et al. 2019, used MC to obtain a fertilizer product from the regeneration stream of ammonium-selective zeolites. They reported a maximum ammonia recovery of 94% under the following conditions: initial ammonium concentration of 4 g L^{-1}, pH_{feed} of 13.5, feed and acid flow rates of 27 L h^{-1} and two modules in series of 2.8 m^2 each (Vecino et al., 2019).

HF-LLMC are usually fabricated using polymers of the polyolefin family as they are hydrophobic, cheaper to produce, ecologically more sustainable since they can be recycled and have a relatively low environmental footprint, compared to those containing fluor, mechanically and chemically stable (Moradihamedani, 2021; Twarowska-Schmidt & Wlochowicz, 1997; Zhang et al., 2022). They have been mostly produced from polypropylene (PP), polyvinylidene difluoride (PVDF) and polytetrafluoroethylene (PTFE) (Chabanon et al., 2013; Tan et al., 2006; Yu et al., 2021) and with symmetrical membrane structures. A promising (i.e., high hydrophobic nature and good chemical resistance) new polymer chemistry: poly(4-methyl-1-pentene) (PMP) which is being commercialised for degasification of industrial production processes (i.e., O_2(g) in ink production, CO_2(g) in water treatment schemes of the microelectronic and hydrogen production) in gas-liquid (GL) applications, has shown lower water transport and therefore higher selectivity than conventional PP modules (Ignatenko et al., 2020; Z. Yang et al., 2010 (Sheikh et al., 2022)). The PMP polymer has methyl side chains on the surface (Markova et al., 2020) that prevent the formation of hydrogen bridges between the water and the membrane surface generating a very hydrophobic surface. The downside of PMP HF-LLMCs is their low fluxes, consequence of their asymmetric membrane structure containing a thick selective layer (Markova et al., 2020). However, several companies such as Mitsui Chemical Inc. (Japan), Dainippon Ink and Chemicals Co. (Japan) and DuPont Water Solutions (USA) are currently commercialising them under the trademarks TPX, Separel® and Ligasep™, respectively.

While HF-LLMCs have been proposed and tested as an innovative solution for ammonium removal/recovery from liquid streams, there is a need for optimizing their operation in order to maximize the ammonia flux and recovery and characterizing their technical performance to facilitate their industrial implementation (Noriega-Hevia et al., 2021). Furthermore, symmetrical PP hollow fibres are the most used membranes in MC while there are very few references of the use of asymmetrical PMP hollow fibres. Moreover, the previous studies of this new polymer chemistry incorporated into an asymmetric HF membrane, were devoted to studying the performance of MC originally designed for GL applications in liquid-liquid (LL) applications to recover ammonia as liquid fertilizers.

The objective of the present work is to investigate the influence of the feed and acid flow rates combination and the circulation configuration (i.e., counter-current/co-current) on

the performance of a commercial PMP HF-LLMC module (Separel®) for recovering ammonia from simulated industrial wastewaters containing low-levels of dissolved organic matter. Moreover, the experimental results were fitted to a mathematical model to study the transport of ammonia and water through the hydrophobic membrane by calculating the corresponding permeabilities and mass transfer resistances. Thus, the optimization of the MC operation towards the maximum ammonia mass transfer coefficient and the identification of the mass transfer bottlenecks (whether in the feed, membrane or permeate sides) with a mathematical tool were the objectives of the present study.

5.3. Materials and methods

5.3.1. Chemicals and analytical techniques

Artificial feed solutions were prepared with a 30% $NH_{3(l)}$ solution provided by Sigma-Aldrich®,Spain and deionised water in concentrations ranging 6 to 10 g NH_3 L^{-1} simulating those of regeneration zeolites streams (Sancho et al., 2017; Vecino et al., 2019) and certain industrial side-streams like, for example, those of the Solvay process (Trypuć & Białowicz, 2011). The acid stripping solution was prepared by diluting analytical grade sulphuric acid (H_2SO_4, 98%) from Sigma-Aldrich®, Spain in deionised water to a concentration of 0.01M and during the experiment, automatically dosed in concentrated form (H_2SO_4, 98%) to maintain a constant pH. Sulphuric acid was selected based on budget considerations and not on the interest or added value of the final product.

Feed and acid samples were analysed by ion chromatography (IC) (Dionex ICS-1000 and ICS-1100 Thermo-Fisher Scientific, USA) equipped with CS16 and AS23 columns for measuring cations and anions, respectively. The mobile phase was 30 mmol L^{-1} methanesulphonic acid (CH_3SO_3H) for cations and a mixture of 0.8 mmol L^{-1} $NaHCO_3$ and 4.5 mmol L^{-1} Na_2CO_3 for anions. Analytical grade methanesulfonic acid (CH_3SO_3H, 99%), sodium hydrogen carbonate ($NaHCO_3$, 99%) and anhydrous sodium carbonate (Na_2CO_3, 99%) supplied by Sigma-Aldrich (Spain) were used in the analyses. Samples were properly diluted and filtered (0.22 µm) prior to their IC analysis. The pH of the samples was determined using a pH-meter (GLP22 Crison, Spain).

5.3.2. Membrane module

Experiments were carried out with a HF-LLMC Separel® EF-010-Q-60 module. This module is commercialized for degassing liquids and operated by flowing liquid outside the fibers (shell) and vacuuming inside the lumen (i.e., external flow (EF) series). The main characteristics of this module are shown in Table 1.

Table 1. Main characteristics of the Separel® EF-010-Q-60 module. Information provided by Separel, DIC Corporation, Japan (DIC Corporation, 2016; DiC, n.d.)

Type: EF-010-Q-60		
Module size	170 × 430	mm x mm
Number of fibres	72047	-
Effective fibre length	0.16	m
Inner/Outer fibre diameter	135/208	µm
Internal/External membrane area[1]	5.29/6.60	m^2
Fibre bundle diameter	88	mm
Operating temperature	5-40	ºC
Maximum Water pressure	0.5	MPa
Liquid flow rate (shell and lumen side)	100-1500	L h^{-1}

The EF-010-Q-60 module contains thousands of PMP capillary fibres of an asymmetric or heterogeneous structure consisting of a microporous layer and a nonporous layer. The 30–40 µm thick microporous layer contains pores with a diameter of 0.01 to 50 µm, whereas the nonporous layer has pores in the Å range and a thickness of 0.01 to 1 µm (Ono, 1987) (Figure 1).

[1] The membrane area was calculated based on the number of fibres, fibre length and fibre diameters.

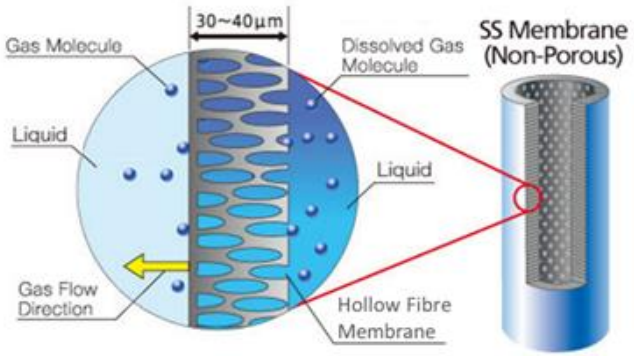

Figure 1. The asymmetric membrane structure of the Separel® EF-010-Q-60 module adapted from (DIC Corporation, 2016; DiC, n.d.).

5.3.3. Experimental set-up

The laboratory set-up used for the experiments is depicted in Figure 2. The module was placed vertically. Feed (Shell) and Acid (Lumen) circulated counter-currently from bottom to top and from top to bottom, respectively, with the exception of experiment of one experiment (180-500-B) during which they circulated co-currently (both from the bottom). All the experiments were performed in batch mode for both circuits. Feed and acid tanks had a capacity of 60 and 28 L respectively (i.e., initial feed/stripping volume ratio of 2.14) and were continuously stirred. In order to avoid the evaporation of $NH_3(g)$ from the feed tank, the recipient was sealed with parafilm. Two peristaltic pumps: Masterflex L/S Easy-load (max. flowrate 600 L h^{-1}) and Ismatec Ecoline VC-380 (max. flowrate 200 L h^{-1}) were used on the feed and acid sides respectively. The set-up was equipped with a pH-meter on the acid side connected to an acid dosing pump (pH/mV Transmitter DO 9785T, Delta OHM) in order to keep the pH below 2.5. Acid consumption, feed pH and ammonium concentration were monitored manually throughout the experiment by taking grab samples and IC analysis. Water flux was difficult to measure experimentally due to the tank volumes and the extremely low water permeabilities of the membrane (i.e., in the order of ml per hour). The water flux data presented in subsequent sections, was calculated theoretically by fitting the experimental data to the mathematical model.

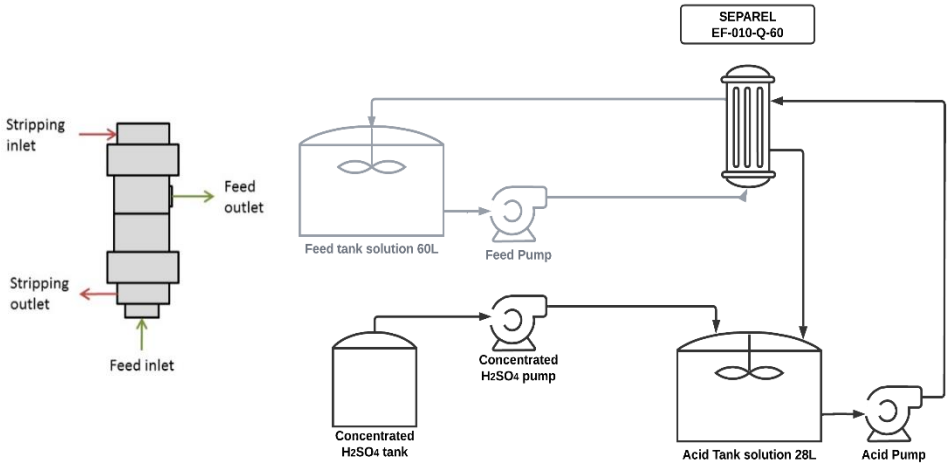

Figure 2. Left, Separel® MC module details on the locations of different in-let and out-let streams. Right, LLMC Experimental set-up used for the ammonia transfer reactions.

5.3.4. Experimental design

In the literature, pH, temperature, and flow rates have been identified as key factors influencing ammonia mass transfer in MCs. Regarding pH, some studies have indicated that increasing the pH beyond 11 has little influence on ammonia transport (Eskicioglu et al., 2018b; Moradihamedani, 2021). Concerning temperature, operating at higher feed temperatures increases the ammonia vapour pressure and promotes mass transfer but it has the same effect in water transport. Besides, temperatures above 40°C are unlikely to significantly enhance mass transfer in many cases (Darestani et al., 2017; Hasanoğlu et al., 2010; Moradihamedani, 2021). Moreover, in the case of the present study, temperature was a limiting factor since the maximum operating temperature of the module is 40ºC (Table 1). Higher flow rates also increase ammonia mass transfer (Hasanoğlu et al., 2010; Reig et al., 2021). Furthermore, recent studies focused on optimizing the economic feasibility of ammonia recovery using HFMC (Rongwong et al., 2022), have pointed out that varying flow rates have the least impact on operating costs compared to the impact of other operational parameters.

Consequently, in the present study, pH, temperature and feed/stripping volume ratio were fixed parameters and only operating flow rates were varied. Six different experiments were carried out using two feed ammonia concentrations (i.e., 6 and 10 g NH_3 L^{-1}) and different feed and acid flow rates combinations (Table 2). Since the objective was to maximize the ammonia transfer, the chosen flow rate combinations were above the values already tested in previous publications (Sheikh et al., 2022) and with increasing

differences between feed and acid flow rates (Reig et al., 2021). The initial pH of the feed solution was adjusted to 11.5 by adding a 0.5 mol L^{-1} NaOH solution. On the acid side, a 0.01 mol L^{-1} H_2SO_4 solution was used at the beginning and a pH of 2.5 was maintained throughout the experiment. Experiments were run until ammonia transfer reached a plateau or the recovery was > 90% and lasted between 10-16 h.

Table 2. Operational parameters of the experimental design.

Experiment	**30-250**	**100-250**	**500-180**	**100-50**	**180-500-A**	**180-500-B**
Feed Initial NH_3 concentration (g L^{-1})	6.8	10	6.3	6.5	6.2	6.1
Feed flowrate (L h^{-1})	30	100	500	100	180	180
Acid flowrate (L h^{-1})	250	250	180	50	500	500
Acid flow-direction	Counter-current	Counter-current	Counter-current	Counter-current	Counter-current	Co-current

5.3.5. Mass transfer modelling in LLMC operations

The ammonia separation in a LLMC using a hydrophobic membrane is usually described as a vapour pressure driven process where only volatiles species (i.e., NH_3(g) and H_2O(v)) are capable of permeating the air-filled membrane pores. When the NH_3(g) crosses the membrane and reaches the acid solution, it gets protonated and forms an ammonium salt (NH_4^+) which is no longer volatile.

In the following sections, a brief description of the mathematical model developed for the evaluation of the experimental results is provided (Sheikh et al., 2022).

Different correlations can be used to account for the mass transfer coefficients in both lumen and shell (X. Yang et al., 2013). For the shell-side, the mass transfer coefficient is calculated using Equation S1.:

$$Sh = 2.15 \cdot Re^{0.42} \cdot Sc^{0.33} \quad \text{(Eq. S1)}$$

Where Sh, Re and Sc are the dimensionless numbers of Sherwood, Reynolds and Schmidt, respectively.

Instead, the mass transfer coefficient in the lumen side (k_{lumen}, m·s^{-1}) is described as:

$$k_{lumen} = 1.62 \cdot \left(\frac{\mathcal{D}^2 \cdot v}{L \cdot d_{t,in}}\right)^{0.33} \quad \text{(Eq. S2)}$$

Where D is the fluid diffusion coefficient (m^2·s^{-1}), v is the flow velocity (m·s^{-1}), L is the effective fibre length (m) and d is the internal fibre diameter (m).

As an initial approach, Equation S2 has been used for the analysis of the experimental results. However, the porous structure in the lumen side defined by Separel module can be wetted by the solution, making necessary to describe the transport as a combination of two resistances: the one of the porous support and the corresponding to the interface of the porous support and the stripping solution.

Additionally, water can be transported across the hollow fibre because of a gradient of water partial pressure between both membrane sides Equation S3.

$$j_W = P_W\left(p^o_{W,f}\gamma_{W,f}x_{W,f} - p^o_{W,a}\gamma_{W,a}x_{W,a}\right) \quad \text{(Eq S3)}$$

Where j_W is the water flux across the membrane (mol/(m^2·s)), $p^o_W$is the water vapour pressure at a given temperature (bar), γ_W is the dimensionless activity coefficient for water and x_W is the molar fraction of water.

The water pressure of water (bar) at a given temperature (K) can be calculated by Antoine's equation Equation S4.:

$$\log_{10}(p^o_W) = A - \frac{B}{T[K] + C} \quad \text{(Eq. S4)}$$

Where A, B and C take the values of 5.40221, 1838.675 and -31.737 for water within the range 273 to 303 K (Technologist et al., 1968).

Different correlations can be found to determine the water activity (a_W, $a_W = \gamma_W\, x_W$). The most known are the Schofield (Lawson & Lloyd, 1997) and Norrish (Barbosa-Cánivas et al., 2007) equations. Due to the lack of correlations for the systems NaOH-NH_3 and NH_4^+-H_2SO_4, it was decided to use Norrish equation (Barbosa-Cánivas et al., 2007) (Equation S5) for both solutions.

$$a_w = x_w \cdot \exp\ (-7.59 \cdot x_{NaCl}^2) \qquad \text{(Eq. S5)}$$

Throughout the text of the present work and whenever possible, the model results have been represented together with the experimental results. More of such comparisons in the form of graphs (Figures 3-4) and a summary table (Table 3) with the RSME (root mean squared errors) and R^2 (coefficient of determination) values for each of the experiments, as indicators of the goodness-of-fit and trend capture of the model respectively. Since most of the obtained R^2 values were above 0.9 and RMSE values were below 0.3, it is considered that the model properly describes both the trends and the performance values obtained experimentally and therefore constitutes a good tool to interpret the system.

Table 3. Root mean squared error (RMSE) and coefficient of determination (R^2) of the mathematical model for the NH_4 permeate concentrations of each experiment.

	NH_4^+	
N. Exp.	**RMSE**	**R^2**
30-250	0.0594	0.993
100-250	0.1204	0.989
500-180	0.034	0.991
100-50	0.0858	0.954
180-500-A	0.0452	0.984
180-500-B	0.0348	0.992

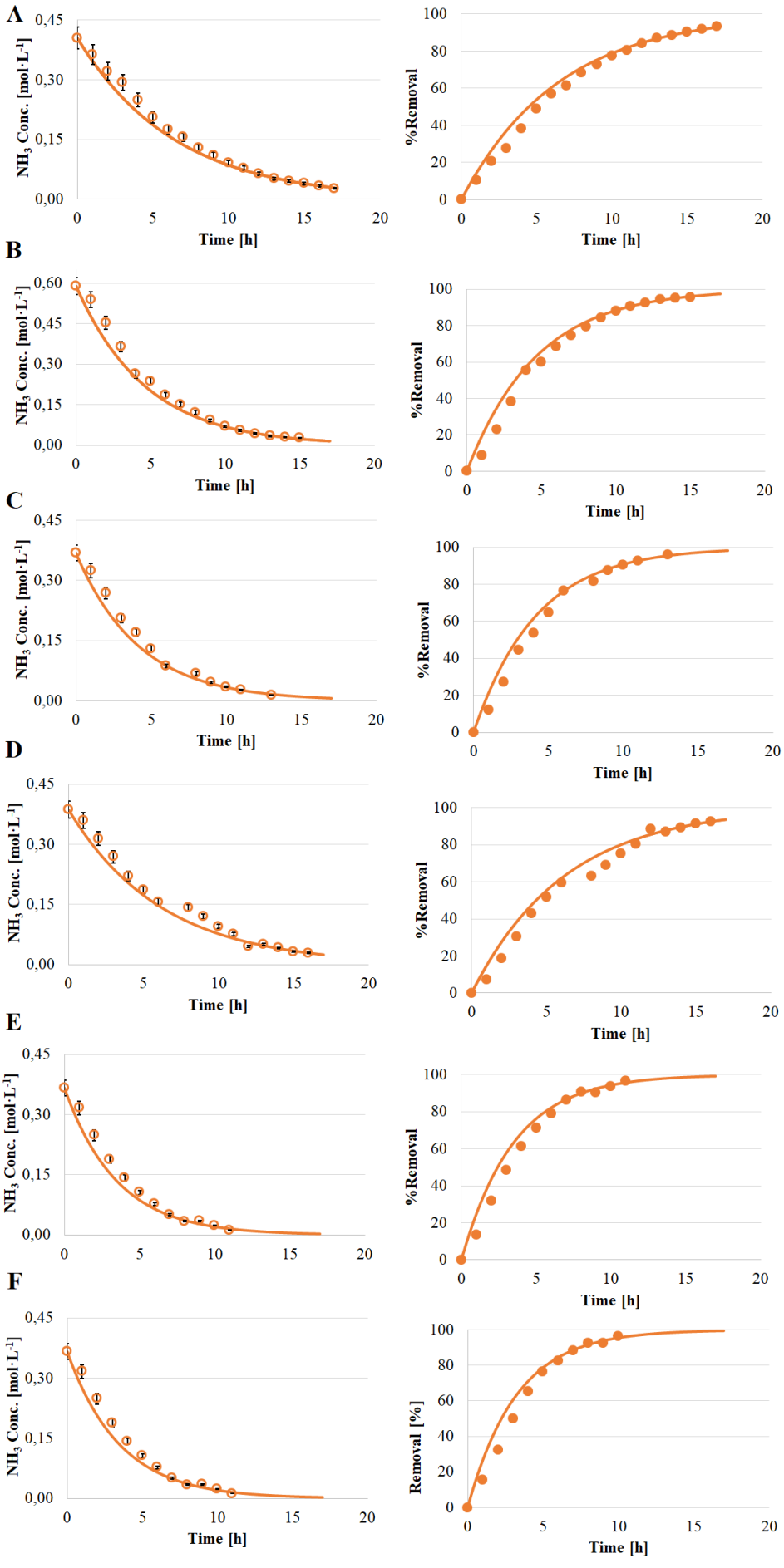
A
B
C
D
E
F
NH3 Conc. [mol·L-1]
%Removal
Removal [%]
Time [h]
0,45
0,30
0,15
0,00
0,60
100
80
60
40
20
0
5
10
15
20

Figure 3. NH_3 concentration (mol L^{-1}) in the feed tank (shell) and percentage of ammonia recovery in the feed tank; (A) Experiment 30-250; (B) Experiment 100-250; (C) Experiment 500-180; (D) Experiment 100-50 (E) Experiment 180-500-A; (F) Experiment 180-500-B**.** Points: experimental data; Lines: model simulation. The bars indicate the absolute errors of the IC measurements. It is observed that the model is in good agreement with the experimental results. The errors bars represent standard deviation (n=3).

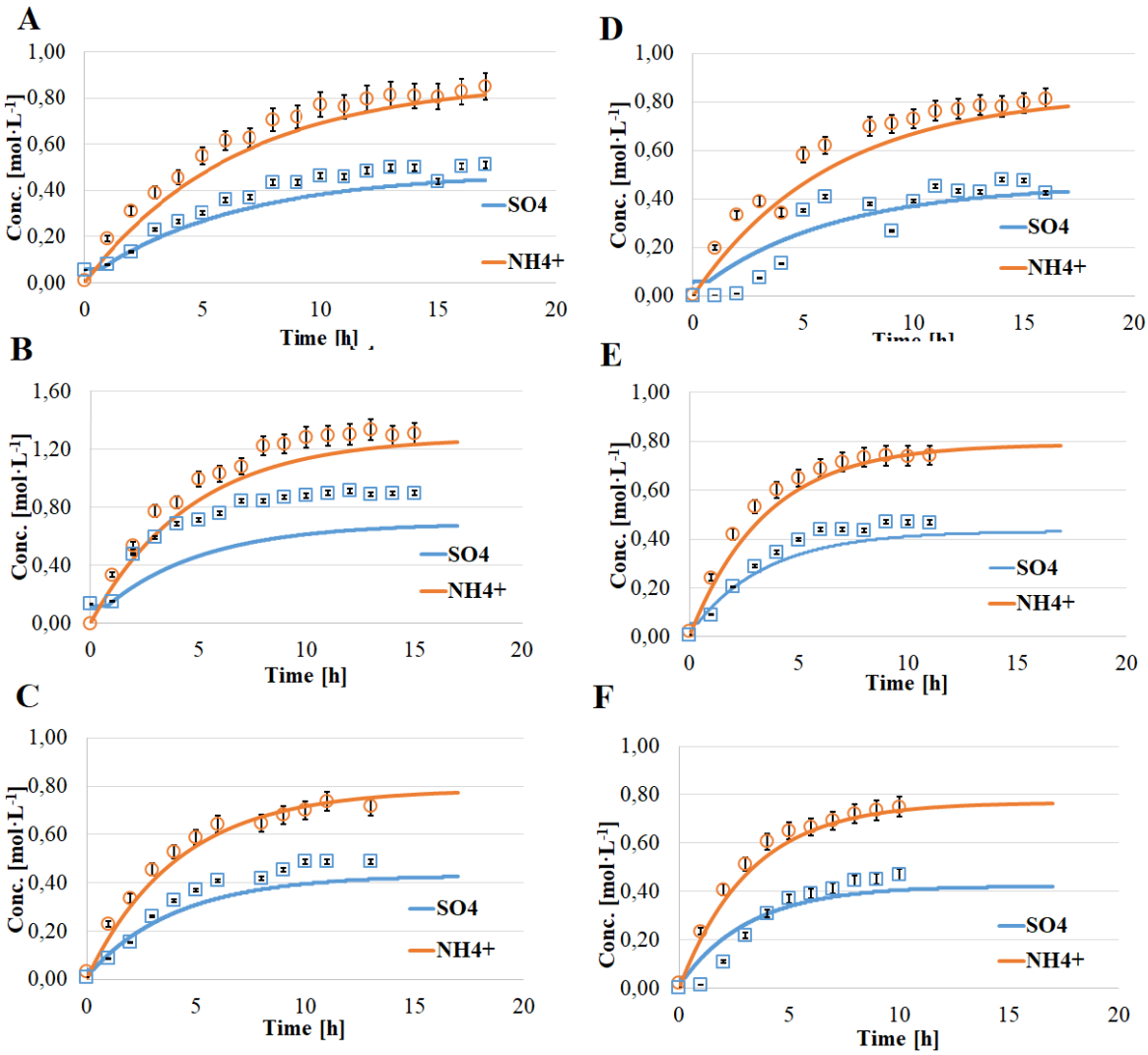

Figure 4. NH_4^+ and SO_4^{2-} concentration (**mol L^{-1}**) in the acid stripping tank (lumen**;** (A) Experiment 30-250; (B) Experiment 100-250; (C) Experiment 500-180; (D) Experiment 100-50 (E) Experiment 180-500-A; (F) Experiment 180-500-B**.** Points: experimental data; Lines: model simulation. The bars indicate the absolute errors associated with the NH_4^+ and SO_4^{2-} IC measurements. It is observed that the model is in good agreement with the experimental results in all the experiments with the exception of the SO_4^{2-} of experiment 100-250 (4.B**).** The errors bars represent standard deviation (n=3).

5.3.5. Ammonia transport

The gaseous transport of ammonia across the membrane can be described as follows (Equation 1) (Licon Bernal et al., 2016):

$$J_{NH_3,m} = \frac{k_{NH_3,m}}{R \cdot T} \cdot \left(p^m_{NH_3,f} - p^m_{NH_3,a}\right) \quad \text{(Eq. 1)}$$

where $J_{NH_3,m}$ is the ammonia flux (mol m^{-2} s^{-1}), $k_{NH_3,m}$ is the membrane ammonia mass transfer coefficient (L m^{-2} s^{-1}), $p^m_{NH_3,f}$ and $p^m_{NH_3,a}$ are the ammonia partial pressures (bar) at the membrane surface of the feed and acid sides, respectively, R is the ideal gas constant (0.083 bar L mol^{-1} K^{-1}) and T is the temperature (K). The ammonia partial pressures ($p^m_{NH_3,f}$ and $p^m_{NH_3,a}$) are calculated based on the ammonia concentrations at the membrane surface (i.e., $c^m_{NH_3,f}$ and $c^m_{NH_3,a}$) using Henry´s law.

The ammonia transport from the feed bulk to the membrane surface and from the membrane surface to the acid bulk can be described using Eq. 2.a and Eq. 2.b, respectively:

$$J_{NH_3,f} = k_{NH_3,f} \cdot \left(c_{NH_3,f} - c^m_{NH_3,f}\right) \quad \text{(Eq. 2.a)}$$

$$J_{NH_3,a} = k_{NH_3,a} \cdot \left(c^m_{NH_3,a} - c_{NH_3,a}\right) \quad \text{(Eq. 2.b)}$$

where c_{NH_3} and $c^m_{NH_3}$ are the ammonia concentrations (mol L^{-1}) in the bulk and at membrane surface and f and a subscripts refer to the feed and acid sides, respectively. $k_{NH_3,f}$ and $k_{NH_3,a}$ (L m^{-2} s^{-1}) are the ammonia mass transfer coefficients from the bulk to the membrane surface of the feed and acid sides, respectively.

Considering that the ammonia transport is conservative (i.e., $J_{NH_3,f} = J_{NH_3,m} = J_{NH_3,a}$), a general expression for the J_{NH_3} can be derived (Equation 3):

$$J_{NH_3} = U_{NH_3} \cdot \left(c_{NH_3,f} - c_{NH_3,a}\right) \quad \text{(Eq. 3)}$$

where U_{NH_3} is an overall ammonia mass transfer coefficient (m s^{-1}), which considers the transport resistances of the feed, membrane and acid sides in series and has been defined according to Equation 4:

$$U_{NH_3} = \frac{1}{\frac{1}{k_{NH_3,f}} + \frac{1}{k_{NH_3,a}} + \frac{R \cdot T}{k_{NH_3,m}}} \quad \text{(Eq. 4)}$$

Different correlations can be used to calculate the mass transfer coefficients (i.e., $k_{NH_3,f}$ and $k_{NH_3,a}$) as a function of the module geometry in the lumen (i.e., acid) and in the shell (i.e., feed). The ones used in this study can be found in (X. Yang et al., 2013) and (Sheikh et al., 2022) and, in general, they are proportional to the velocity in the different channels (shell and lumen).

5.3.6. Experimental determination of the overall ammonia mass transfer coefficient

In scientific literature, the overall mass transfer coefficient (k_{ov} or k_m) is used as a parameter to compare the performance of different membranes and modules (Pauzan et al., 2021; Yu et al., 2021; Zhang et al., 2022). The higher the k_{ov}, the greater the capacity of the membrane to transfer a species through the membrane and therefore the better the performance. The k_{ov} (m^3 m^{-2} s^{-1}) can be calculated experimentally from the total ammonia mass balance in the feed side, as follows (Licon Bernal et al., 2016):

$$\ln\left(\frac{c_{NH3,0}}{c_{NH3,t}}\right) = \frac{k_{ov} \cdot A_m}{V} \cdot t \qquad \text{(Eq. 5)}$$

where $c_{NH3,0}$ and $c_{NH3,t}$ are the NH_3 concentrations in the feed tank at the beginning of the experiment and at time t, respectively, A_m is the membrane area (m^2), V is the feed solution volume (m^3) and t is the time of the experiment (h).

By representing the experimentally measured values of $\ln(c_{NH3,0}/c_{NH3,t})$ versus the time (t) a linear relationship is found which slope is $\frac{k_{ov} \cdot A_m}{V}$ and from which k_{ov} can be calculated. This k_{ov}, as an overall mass transfer coefficient, should be in principle equivalent to U_{NH_3} (Equation 3).

5.3.7. Water transport

Water vapour can be transported across the membrane, provided that a transmembrane water partial pressure gradient exists according to the following equation:

$$J_W = P_W \ (p^o_{W,f} \cdot a_{w,f} - p^o_{W,a} \cdot a_{w,a}) \qquad \text{(Eq. 6)}$$

Where J_W is the water flux (mol m^{-2} s^{-1}), P_W is the water permeability (mol m^{-2} s^{-1} bar^{-1}), p^o_W is the pure water vapour pressure (bar) at a given temperature and calculated via Antoine's equation (Technologist et al., 1968) and a_W is the dimensionless water activity,

calculated using the Norrish equation for NaCl solutions (Barbosa-Cánivas et al., 2007) for the respective sides. Due to the lack of correlations for the NaOH-NH_3 and NH_4^+-H_2SO_4 systems, it was decided to use Norrish equation. The implemented mathematical model aimed to fit the experimental data by adjusting the water and ammonia permeability values (P_W and P_{NH3}, respectively) in order to minimize the RMSE between the model values and the experimental data, namely the measured ammonia concentrations.

5.3.8. Permeate side chemical equilibrium

In order to maintain and enhance the ammonia transport, the NH_3 partial pressure in the stripping side ($p^m_{NH_3,a}$ in Eq. 1) must be kept as low as possible. When the ammonia gas (NH_3) dissolves in water, it behaves like a weak base (reaction 1 in Table 4) consuming the protons from the acid side and increasing the pH. For that reason, the pH in the acid side was maintained below 2.5 by dosing concentrated H_2SO_4 automatically throughout the experiment. Bearing in mind that the second dissociation of the H_2SO_4 is weak, chemical equilibrium reactions must be considered to model the species formed in the acid side. According to this equilibrium, different species, namely: ammonium bisulphate (NH_4HSO_4), ammonium sulphate ($(NH_4)_2SO_4$) or a mixture of both can be found depending on the pH ranges of the stripping solution (Uzkurt Kaljunen et al., 2021). Table 4 collects the equilibrium constants (pK_a) values of the chemical reactions involved in the acid stripping side. Considering that the three species in solution are pH dependant, they must be accounted for in order to model properly the chemical equilibrium of the permeate side, and therefore the acid consumption.

Table 4. Chemical equilibrium reactions that take place in the acidic stripping solution.

Number	Reaction	pK_a **(25ºC)** (Puigdomenech, 2001)
1	$NH_3 + H^+ \rightleftarrows NH_4^+$	9.24
2	$H^+ + SO_4^{2-} \rightleftarrows HSO_4^-$	1.98
3	$NH_3 + H^+ + SO_4^{2-} \rightleftarrows NH_4SO_4^-$	10.36

5.4. Results and discussion

The results of the experiments, named according to the feed and acid flow rate in L h^{-1} as: 30-250 ,100-250, 500-180, 100-50, 180-500-A and 180-500-B, were analysed in terms

of (i) the ammonia recovery and the CF, (ii) the acid consumption, (iii) the ammonia and water transport, (iv) the possible polarization effects induced by the asymmetrical membrane structure and (v) the experimentally calculated and modelled mass transfer coefficients. Letters A and B in the experiments 180-500-A and 180-500-B refer to the acid flow direction (A: co-current and B: counter-current).

5.4.1. Ammonia recovery and CF

The ammonia recovery percentages (measured and simulated) as a function of time for the first four experiments 30-250, 100-250, 500-180 and 100-50 are shown in Figure 5 where dots represent the experimental data and lines the model simulation.

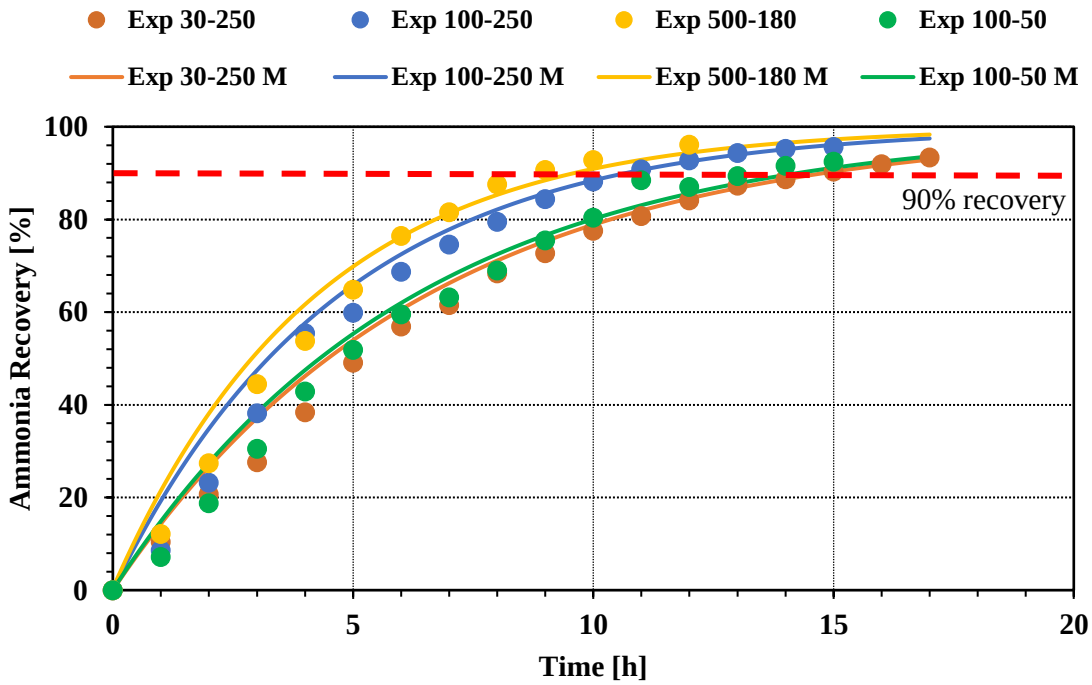

Figure 5. Ammonia recovery (%) as a function of time for experiments 30-250, 100-250, 500-180 and 100-50. Points: experimental data; Lines: model simulation.

The experimental recovery values obtained for all the experiments reached values of 90% after ~15 h (Figure 3). However, two experiments (500-180 and 100-250) were faster (i.e., ~10-11h versus 15h) in reaching 90% recovery than the other two (30-250 and 100-50). In experiment 500-180 the feed concentration decreased from 6.26 g NH_3 L^{-1} to 0.24 g NH_3 L^{-1} after 13h, achieving a recovery of 96% and a CF of 2.1. In experiment 100-250, despite the higher initial concentration (i.e., 10.01 g NH_3 L^{-1}) a recovery and a CF of 96% and 2.3, respectively, were achieved after 15h. On the other hand, during

experiment 30-250, the initial concentration decreased from 6.90 g NH_3 L^{-1} to 0.46 g NH_3 L^{-1} in 17h, which resulted in a recovery of 93% and a CF of 2.1 while in experiment 100-50 the concentration decreased from 6.56 g NH_3 L^{-1} to 0.47 g NH_3 L^{-1} in 16h reaching only a 92.5% recovery and a final CF of 2.2.

Thus, results showed that the relatively higher feed flow rates of experiments 500-180 and 100-250 led to faster recovery rates, while a higher initial concentration had a negligible influence. Regarding the CF, the values for all the experiments are very similar (2.1-2.2) suggesting that the flow rates have a minimal influence and only the feed/stripping volume ratio (i.e., 2.14) is determinant. The higher initial ammonia concentration of experiment 100-250 did lead to a slightly higher CF (i.e., 2.3). However, these minor differences could be attributed to the lack of water flux measurements during the experiments which contribute to the uncertainties in the overall mass balance. Additionally, the higher dilution factors employed for the samples of experiment 100-250 could have introduced additional uncertainties in the extrapolation of the NH_4^+ quadratic calibration curve of the IC measurements. In fact, the calculated absolute errors of the IC measurements associated with the NH_4^+ calibration curves (being the relative mean error in the range of 5.4 - 6.8%) are greater at higher concentrations (see Figures S2-S3 in the appendix).

The experimental results were compared to the literature. For instance, Vecino et al. 2019 using a PP HF-LLMC module (1.44 m^2) and a feed stream of 4 g NH_3 L^{-1} reached a CF of 26 ± 3.3 after 15h of operation. Although the CF was much higher than the results of the present study, the authors reported an ammonium recovery of only a 76%. A 2-stage scheme was proposed by the authors and experiments were extended beyond the 30h, as a result, the recovery was increased to 94%. The higher CF obtained in comparison to our results can be attributed to the higher feed/stripping volume ratio (i.e., 60 versus 2.14). However, assuming no water transport and a 94% recovery, Vecino et al. 2019 should have been able to achieve a CF closer to 60. The CF value obtained (26±3.3) far from 60, meant that water transport occurred and diluted the final product by a factor of 2.3 (Vecino et al., 2019), unlike the current study where the achieved CF was very close or even higher than the used feed/stripping volume ratio (i.e., 2.14) and therefore an almost 100% ammonia selectivity (i.e., negligible water passage) scenario can be assumed.

Shi et al. 2022, evaluated the ammonia recovery from an anaerobic digestate using a 0.165 m^2 PP HFMC module, where a temperature of 60°C and an aeration flow to maintain a high pH (pH > 8.1) on the feed side were applied (Shi et al., 2022). Authors reported that 82% of the ammonia was recovered from an initial concentration of 3.8 g NH_4^+ L^{-1} after only 6h of operation. Temperature accelerated the ammonia transfer but also enhanced the water transport which was in the range of 0.09 g h^{-1} m^{-2} and limited the CF to a value of around 8.9. In the 500-180 experiment, similar recovery values were achieved after 6h, but with the significant difference that the 500-180 experiment was operated at room temperature and a negligible water transport can be assumed.

Reig et al. 2021 also studied the influence of flow rate (16.0 - 46.2 L h^{-1}) on ammonium recovery using a PP HFMC (1.44 m^2). Authors found that lower flow rates entailed lower recoveries and observed that the highest recovery values were obtained when at least one of the two flowrates (e.g., stripping acid or feed) was the highest value tested (Reig et al., 2021), like in the present study. However, they also reported CF values of 20-29 working at a feed/stripping volume ratio of 120 which pointed towards an important water passage. Likewise, Hasanoğlu et al. 2010, concluded that increasing the flow rate of both streams (47 - 120 L h^{-1}) reduced the mass transfer resistance due to the boundary layer effect and increased the recovery values (Hasanoğlu et al., 2010).

In all the experiments, a feed pH decrease with time was measured (Figure 6). Because of the transport of NH_3 from the feed to the stripping side, the equilibrium NH_3/NH_4^+ was shifted to the deprotonation of NH_4^+ (reaction 1 in Table 3) which decreased the feed pH from 11.8 (max value) to 9.9 (minimum value in Experiment 100-50), but in all cases it remained higher than the ammonia pK_a (9.33 at 25°C) making NH_3(g) the dominant species in the feed. Very similar results were obtained and reported previously (Aguilar-Moreno et al., 2022).

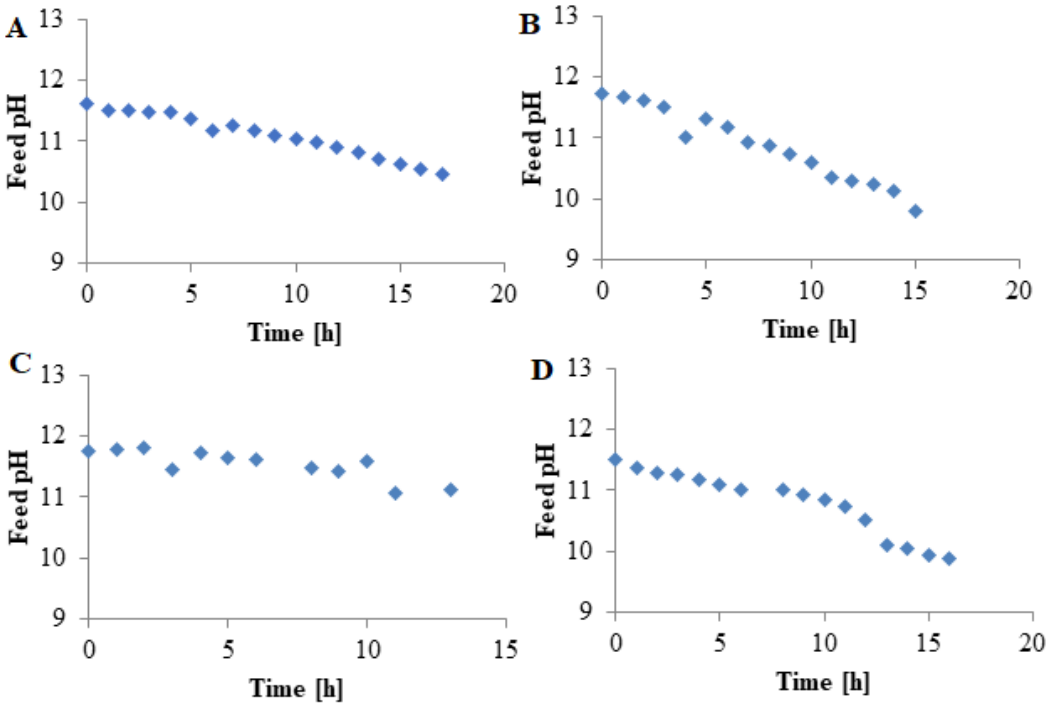

Figure 6. Experimental data of the evolution of pH in the feed tank; (A) Experiment 30-250; (B) Experiment 100-250; (C) Experiment 500-180; (D) Experiment 100-50.

Similarly, Jang et al. 2022 experimented with ammonia recovery at different concentrations and pH values from 9-12 using a PP-HFMC module and concluded that increasing the pH resulted in higher removal percentages. They reported values of 20% removal at a pH of 9, which later increased to 50% at a pH of 12, concluding that increasing the initial pH above 10 resulted in a slight improvement of the removal (Jang et al., 2022).

5.4.2. Acid consumption in the permeate side

As explained before, because of the transfer of NH_3 to the acid side and the subsequent conversion of NH_3 into NH_4^+, H^+ was consumed and so 98% concentrated H_2SO_4 was added to maintain the pH < 2.5 and ensure the lowest ammonia vapour pressure on the stripping side. According to this, each experiment needed different acid dosing rates, but the total amount of acid was very similar and proportional to the total recovered ammonia. For instance, during experiments 30-250, 500-180 and 100-50 a total of 921.8, 997.8 and 909.8 g H_2SO_4 were correspondingly added while for experiment 100-250 (36% higher NH_4^+ feed concentration) approximately a 27% more acid (i.e., 1,287.5 g) was used.

The average flow rate of the acid dosing pump was in the range of 30-47 ml h^{-1} and the average total added acid volume per experiment was around 540 ml. Considering that the permeate tank volume was 28 l the total acid addition is less than a 2% volume increase, therefore barely affecting the feed/stripping volume ratio.

Evolution of the sulphate (SO_4^{2-}) and ammonium (NH_4^+) molar concentrations in the acid side were also measured and simulated according to the chemical equilibrium described by the reactions in Table 3. It was found that for experiments 30-250, 500-180 and 100-50 the average value of the NH_4^+/SO_4^{2-} molar concentration ratio was around 1.7:1, which is between the ammonium sulphate ($(NH_4)_2SO_4$) and ammonium bisulphate (NH_4HSO_4) ratios, 2:1 and 1:1, respectively.

Further analysis with the speciation software Hydra/Medusa developed by Puigdomench 2001, (Figure 7***)*** shows that at the operating pH of 2.5, around a 74% of the sulphuric acid is dissociated in the form of SO_4^{2-} while the remaining 26% stays as HSO_4^- which matches well with the NH_4^+/SO_4^{2-} molar concentration ratio measured (Uzkurt Kaljunen et al., 2021). The only exception is experiment 100-250, where a lower ratio was measured (i.e., 1.4) although the acid pH (i.e., 2.5) was the same. However, it is possible that the high acid concentrations reached in this particular experiment and the corresponding higher dilution factor needed for the IC measurements introduced more uncertainties in the measurements. The calculated mean relative error for the SO_4^{2-} IC measurements was in the range of 1.8-2.8% (Figure S3).

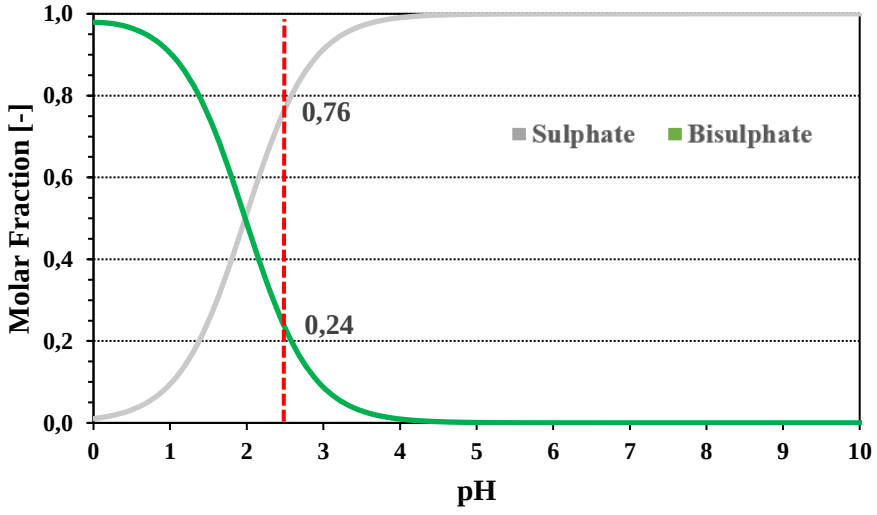

Figure 7. Dissociation of the sulfuric acid and corresponding sulphate (SO_4^{2-}) bisulphate (HSO_4^-) molar fractions as a function of pH simulated with the Hydra/Medusa speciation software (Puigdomenech, 2001).

5.4.3. Ammonia and water transport

By means of the mathematical model, the ammonia and water fluxes (g $h^{-1}m^{-2}$) as a function of time could be simulated and have been represented (dashed lines) along with the experimentally measured ammonia fluxes (points) in figures 8a and 8b, respectively. For the sake of clarity, not all experimental values have been represented in the graph and only those of experiments 500-180 are included. Additional figures showing the accuracy of the model in fitting the experimentally measured ammonia concentrations in the feed and permeate for each experiment can be found in the appendix (Figures 3 and 4).

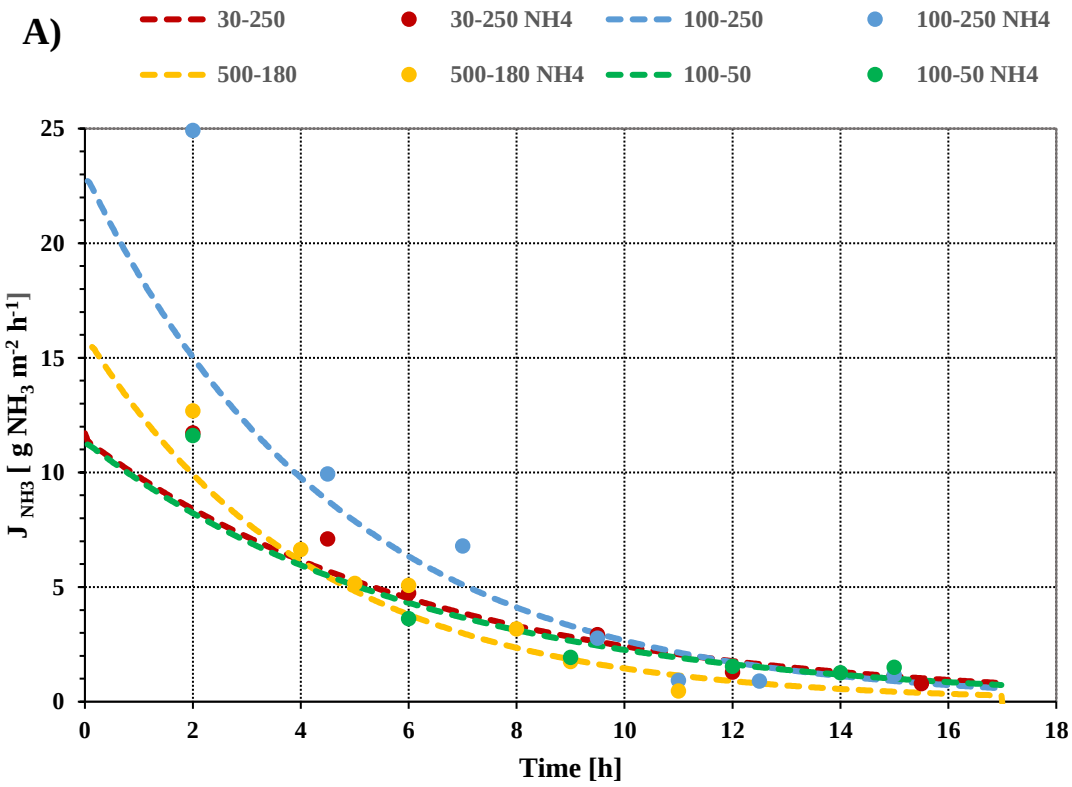

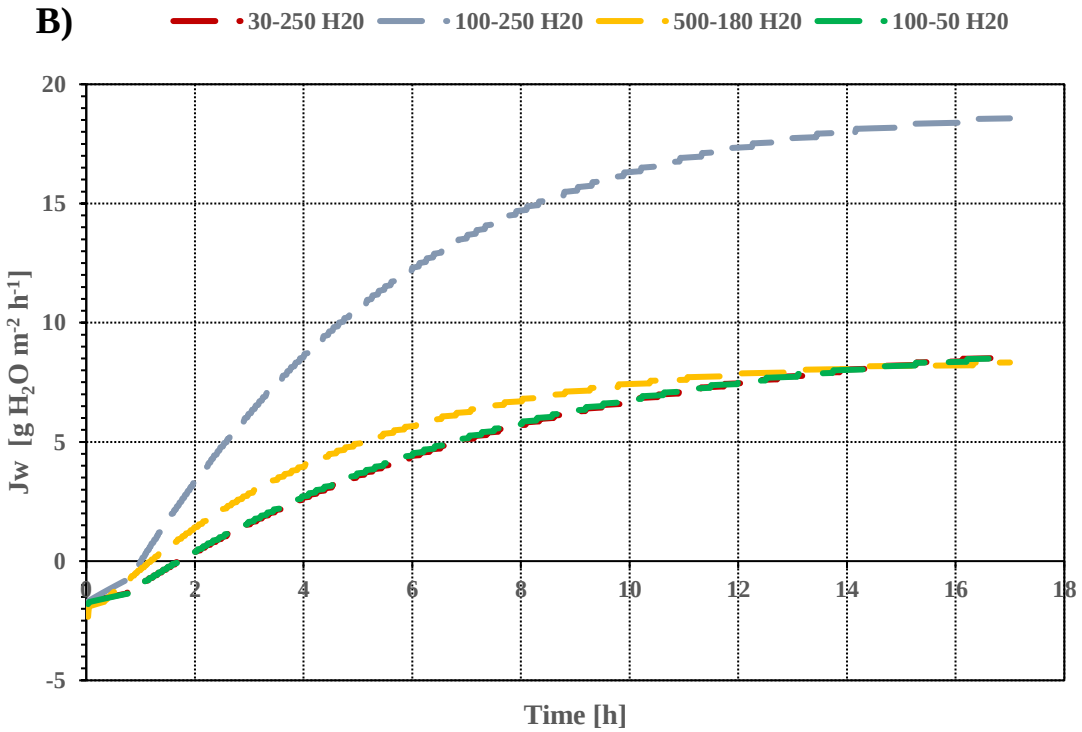

Figure 8. Results of experiments 30-250; 100-250; 500-180 and 100-50: A) ammonia flux over time. Experimental results (dots) and simulated results (lines). B) Simulated water flux over time.

The ammonia flux decreased more drastically during the first 6-7 hours, and thereafter remained relatively constant for all experiments (< 5 g NH_3 h^{-1} m^{-2}). Initial ammonia fluxes of experiment 100-250 were higher in comparison to the rest of the experiments due to the initial higher NH_3 concentration (i.e., 10 g L^{-1} versus 6 g L^{-1}). Comparing the different experiments, the results showed that for this particular module, low flowrates (i.e., < 100 l h^{-1}) on any side, caused a high ammonia transfer resistance. As flow rates decreased, the resistance of the films formed in the surroundings of the membrane surface increased, causing a low bulk-to-membrane mass transfer rate (Ahn et al., 2011) and affecting not only the ammonia flux but also the water flux.

Regarding the model goodness-of-fit, the error is higher in the first hours which is attributed to the also bigger error of the IC measurements at higher ammonia concentrations (see Figures 3 and 4 in the secction 5.3.5.). The purpose of this work was not to validate an already published model (Sheikh et al., 2023), but to utilize it for studying the membrane permeability and mass transfer resistance regime of this specific HF-LLMC module. Despite not having an excellent goodness-of-fit (RMSE), the model's capacity to describe trends (R^2) is very good. Hence, it remains a valuable tool for studying mass transfer phenomena in the module.

Additionally, the effect of a higher feed ammonia concentration of experiment 100-250 was an expectedly higher ammonia flux but a rather counter-intuitive higher water flux. However, this could be explained by a comparatively higher osmotic distillation (OD) effect due to higher NH_4^+ and SO_4^{2-} concentrations in the acid side than in the other experiments. According to Darestani et al. 2017, OD facilitates the transfer of water vapor across the hydrophobic membrane of an MC, promoting its movement from one side to the other (Darestani et al., 2017). The direction of this transfer is determined by the relative concentrations of acid on the strip side and soluted species on the feed side. This explains why the initial water fluxes of all the experiments in Figure 4b were negative, indicating a net water flux from the acid side to the feed side and possibly the reason why the reached CFs were greater than the feed/permeate volume ratio. At the beginning of the experiment, the ionic concentration on the feed side was significantly higher than on the acid side thus creating a water vapour pressure gradient towards the feed. As the ammonium was transferred to the stripping side, the water vapour pressure on the feed side gradually increased while that on the acid side decreased until the gradient was reversed (i.e., towards the acid) causing the water vapour to evaporate from the feed. This phenomenon can limit the maximum ammonia concentration and CF that can be reached in the stripping side with time and increasing ammonia recovery %

Noteworthy, the simulations showed a relatively lower ammonia flux increase compared to the water flux increase when the initial ammonia feed concentration was higher. For example, comparing experiment 500-180 to experiment 100-250 (i.e., initial ammonia feed concentration of 6.3 g L^{-1} versus 10 g L^{-1}) the model showed a 53% higher ammonia flux as opposed to a 225% higher water flux.

Lastly, the mathematical model was used to calculate and compare the membrane average permeabilities, expressed in L h^{-1} m^{-2} bar^{-1} and at NTP conditions (i.e., 1 bar and 25 °C temperature) for water (P_w in equation 5) and ammonia (P_{NH3}) and for each of the experiments (Figure 9).

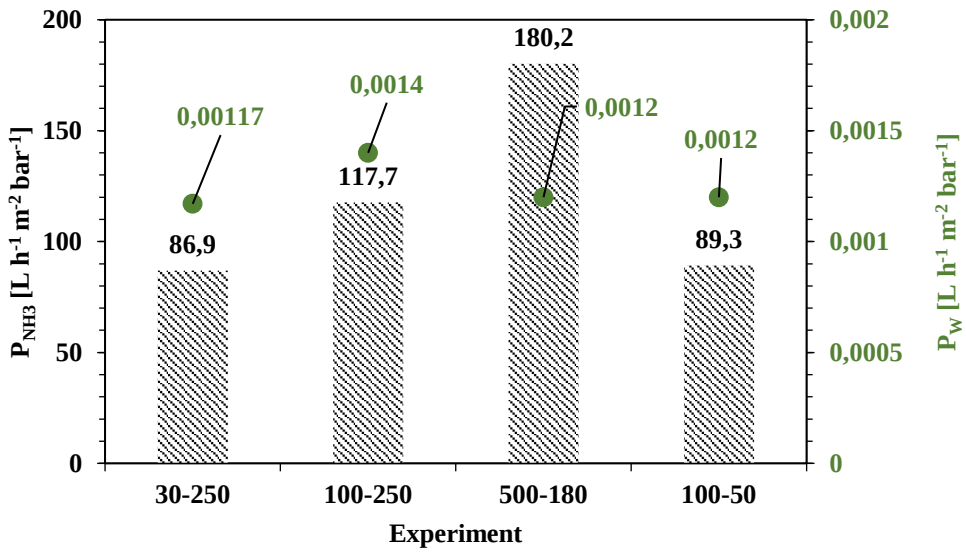

Figure 9. Membrane permeabilities for ammonia (P_{NH3}) and water (P_w), modelled mathematically at NTP conditions (i.e., 1 bar and 25 °C temperature) for each experiment.

The values obtained for P_{NH3} were 4 to 5 orders of magnitude higher than those of P_w, supporting the hypothesis of a highly selective membrane towards ammonia. Regarding the absolute P_w values (in the order of 10^{-4} L h^{-1} m^{-2} bar^{-1}) they were extremely low if compared, for example, to those of similar hydrophobic membranes used in membrane distillation desalination reporting values in the order of 10 or 10^2 L h^{-1} m^{-2} bar^{-1} (Summers et al., 2012). Additionally, the fact that the P_w was practically constant (i.e., average value of 1.29 ± 0.105 $\cdot 10^{-3}$ L h^{-1} m^{-2} bar^{-1}) for all the experiments, supports the OD hypothesis for the relatively higher water flux (J_w) in experiment 100-250 (at higher initial ammonia feed concentration and resulting higher dissolved species concentration in the permeate side) according to Eq. 5. In any case, this membrane seems to exert a high resistance to water transport and therefore very low J_w even at higher permeate concentrations can be expected.

Next, according to the model, P_{NH3} values varied with the different flowrate combinations and ranged from 86.9 L h^{-1} m^{-2} bar^{-1} in experiment 30-250 to the highest value (i.e., 180.2 L h^{-1} m^{-2} bar^{-1}) for experiment 500-180. These results are in fact counterintuitive, since the membrane permeability is an intrinsic property and should remain constant unless structural alterations (i.e., deformation, compaction, etc.) occur (Laguntsov & Karaseva, 2019). However, the seeming variations in the calculated P_{NH3} values in this research can be attributed to two aspects. First, an uneven distribution of flow inside the membrane module during operation at different flowrates can result in reduced effective membrane

areas due to the presence of dead zones, bypassing and channelling effects (Noda et al., 1979; X. Yang et al., 2013; Zheng et al., 2003). Second, the methodology employed to solve the mathematical model, which iteratively adjusts and computes the system parameters such as P_{NH3} based on experimental results and a set of fixed variables, including the membrane area (Table 1). As a result, a probable misestimation of the effective membrane area by the model could have underestimated/overestimated the experimental flux results and hence, the different predicted P_{NH3} values. In the case of water, because the P_w is already so limited, the membrane resistance is dominant and a better flow distribution would have a minimal effect in the calculations, in addition, there were no experimental water flux values for the model to fit.

However, a second hypothesis that could not be ruled out, was a possible polarization induction due to the asymmetry of the membrane structure (Alkhudhiri et al., 2012). Because of this second hypothesis, additional experiments were performed and are discussed in the next section.

5.4.4. Asymmetrical membrane structure related effects

Two additional experiments were performed: experiment 180-500-A to be compared with the results of experiment 500-180 and evaluate if the asymmetrical membrane structure induced polarisation at the lumen side (Alkhudhiri et al., 2012) and experiment 180-500-B, performed in co-current circulation to be compared with experiment 180-500-A (done counter-currently) and verify if a better performance was achieved working in this configuration. Results are shown in figures 6a and 6b (points: experimental data, lines: model simulation) and their corresponding P_w and P_{NH3} calculated values are shown in table 4.

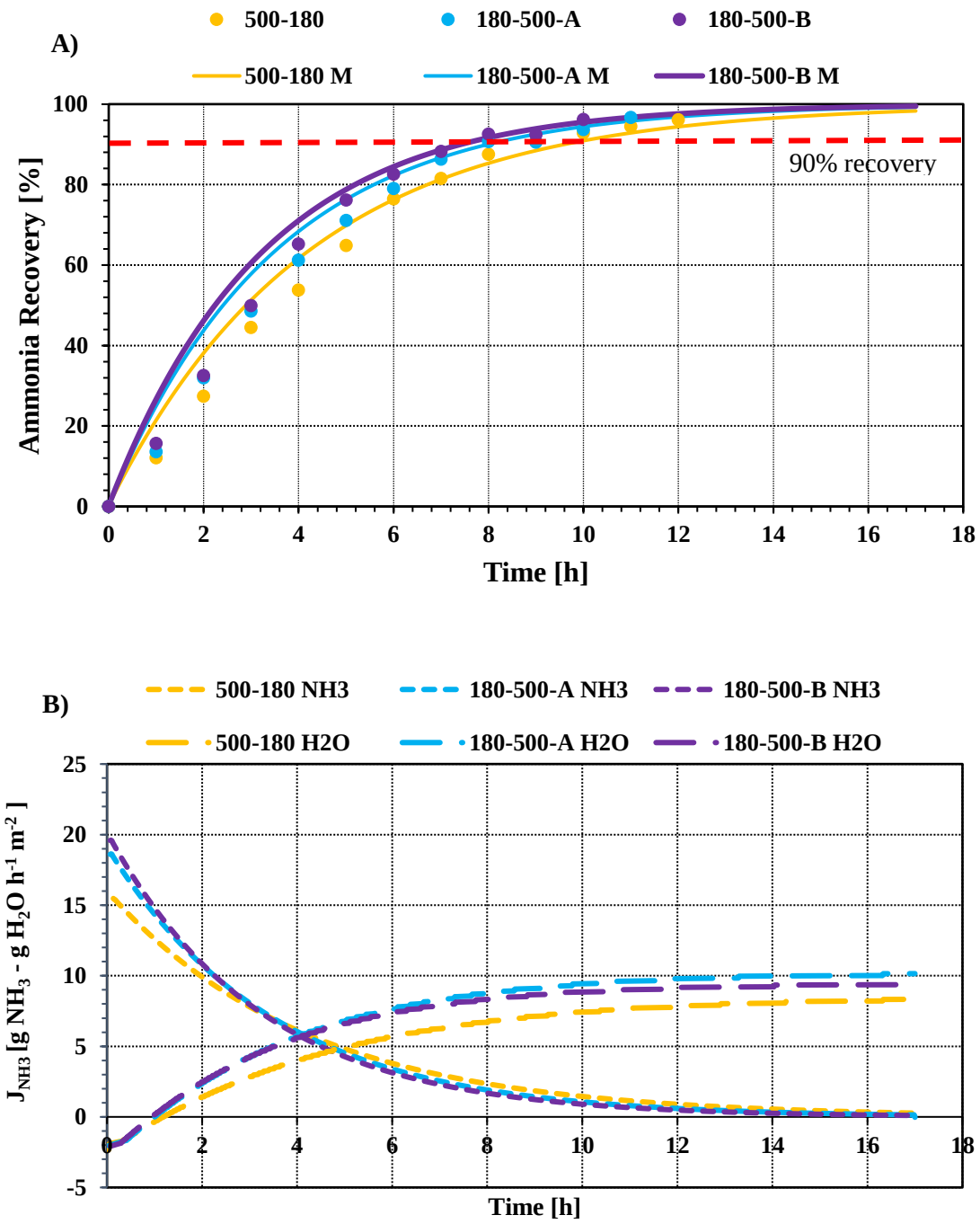

Figure 10. Comparison between experiments 500-180, 180-500-A and 180-500-B in terms of A) ammonia % removal and B) theoretical ammonia (J_{NH3}) and water (J_w) fluxes. Points: experimental data; Lines: model simulation.

In experiment 180-500-A the ammonia concentration in the feed side decreased from 6.20 g NH_3 L^{-1} to 0.20 g NH_3 L^{-1} (i.e., 97% recovery) after 11h (Figure 10a). The feed pH shifted from 11.5 to 10.7 and a CF of 2.2 was reached. A total of 854 g of H_2SO_4 were added and the final NH_4^+/SO_4^{2-} molar concentration ratio was around 1.6. In comparison

to experiment 500-180, ammonia recovery and therefore ammonia transfer were faster (e.g., in experiment 500-180 a recovery of 96% was registered after 13h) but not significantly. The results of experiment 180-500-B are also shown in Figure 10a. In this case, the feed decreased from 6.10 g NH_3 L^{-1} to 0.22 g NH_3 L^{-1} (i.e., 96% recovery) after 10h, the feed pH went down from 11.7 to 11.5 and a CF of 2.2 was reached. A total of 952 g of H_2SO_4 were added and the final NH_4^+/SO_4^{2-} molar concentration ratio was also around 1.6. In comparison to experiment 180-500-A, the ammonia recovery rate was again, very similar.

In terms of ammonia flux (Figure 10b), the highest maximum flux was measured in experiment 180-500-B (i.e., 19.6 g NH_3 h^{-1} m^{-2}) which was very similar to that of experiment 180-500-A (i.e., 18.6 g NH_3 h^{-1} m^{-2}) and both were comparatively higher than that of experiment 500-180 (i.e., 15.4 g NH_3 h^{-1} m^{-2}) but only in the beginning of the experiment, after 2-3 h the ammonia fluxes were practically the same for the three experiments according to the model.

Table 5 shows the simulated P_w and P_{NH3} for the three experiments. Again, the P_{NH3} values were very similar for the three experiments (i.e., average value of 175.15 ± 6.8 L h^{-1} m^{-2} Pa^{-1}) supporting the idea that a polarization effect due to the asymmetry of the polymeric membrane was not necessarily happening under these working conditions. Regarding co-current versus counter current operation, in light of these results, a similar conclusion can be reached since no significant differences were found for experiments 180-500-A and 180-500-B.

Table 5. Membrane permeabilities to water (P_w) and ammonia (P_{NH3}) calculated via the mathematical model for experiments 500-180, 180-500-A and 180-500-B.

Experiment	P_w **[L h^{-1} m^{-2} Pa^{-1}]**	P_{NH3} **[L h^{-1} m^{-2} Pa^{-1}]**
500-180	$1.2 \cdot 10^{-3}$	180.2
180-500-A	$1.4 \cdot 10^{-3}$	165.5
180-500-B	$1.4 \cdot 10^{-3}$	179.8

5.4.5. Mass transfer coefficient and resistance regime

In the MC literature, the k_{ov} is generally accepted as an overall mass transfer coefficient that collectively accounts for the mass transfer phenomena in the feed, membrane and

acid sides and therefore, it would be expected to be equivalent to U_{NH_3}. It is also the most used parameter to compare the performance of different MC membranes, modules and processes (Lauterböck et al., 2012; Moradihamedani, 2021; Tan et al., 2006; Uzkurt Kaljunen et al., 2021; Vecino et al., 2019; Yu et al., 2021). Table 6 summarizes the k_{ov} values for all the performed experiments calculated as described in section 3.1. (Figure 11) and the modelled U_{NH_3}, $k_{NH3,f}$, $k_{NH3,m}$ and $k_{NH3,a}$ values, according to the mathematical model and expressed in m h^{-1}.

Table 6. Experimentally calculated k_{ov} values referred to the internal membrane area (Table 1) and modelled U_{NH_3}, $k_{NH3,f}$, $k_{NH3,m}$ and $k_{NH3,a}$ values for each experiment.

Experiment	k_{ov} (m s^{-1})	U_{NH_3} (m s^{-1})	$k_{NH3,f}$ (m s^{-1})	$k_{NH3,m}$ (m s^{-1})	$k_{NH3,a}$ (m s^{-1})
30-250	(4.56±0.06) $\cdot 10^{-7}$	$1.99 \cdot 10^{-8}$	$7.5 \cdot 10^{-5}$	$1.64 \cdot 10^{-10}$	$1.76 \cdot 10^{-6}$
100-250	(6.28±0.08) $\cdot 10^{-7}$	$7.39 \cdot 10^{-8}$	$1.25 \cdot 10^{-4}$	$2.21 \cdot 10^{-10}$	$1.76 \cdot 10^{-6}$
500-180	(7.39±0.11) $\cdot 10^{-7}$	$1.10 \cdot 10^{-7}$	$2.47 \cdot 10^{-4}$	$3.37 \cdot 10^{-10}$	$1.58 \cdot 10^{-6}$
100-50	(4.61±0.19) $\cdot 10^{-7}$	$5.61 \cdot 10^{-8}$	$9.44 \cdot 10^{-5}$	$1.68 \cdot 10^{-10}$	$1.30 \cdot 10^{-6}$
180-500-A	(8.33±0.22) $\cdot 10^{-7}$	$1.03 \cdot 10^{-7}$	$1.61 \cdot 10^{-4}$	$3.12 \cdot 10^{-10}$	$2.22 \cdot 10^{-7}$
180-500-B	(9.75±0.26) $\cdot 10^{-7}$	$1.11 \cdot 10^{-7}$	$1.62 \cdot 10^{-4}$	$3.37 \cdot 10^{-10}$	$2.22 \cdot 10^{-7}$

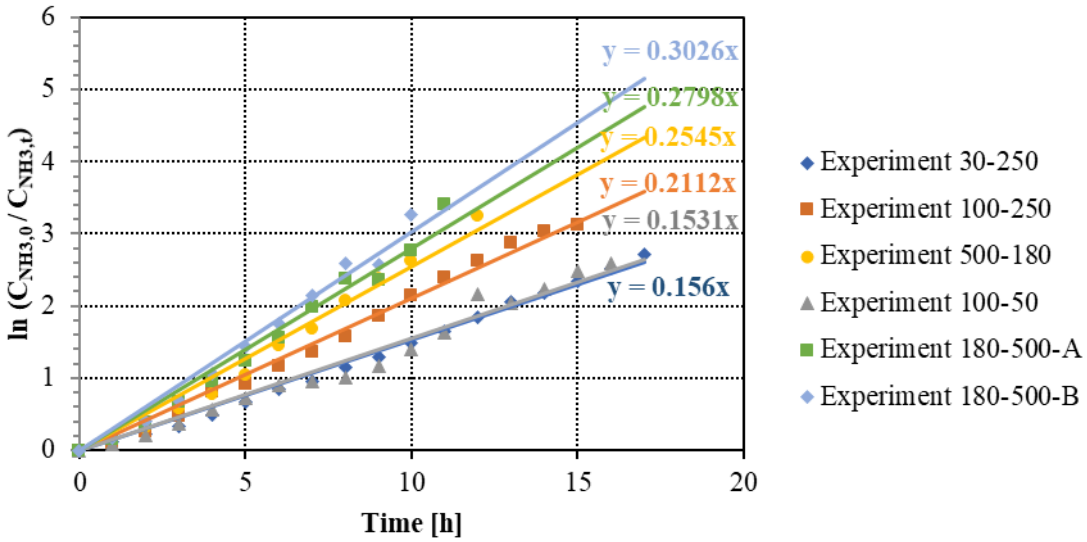

Figure 11. Representation of the natural logarithm $\ln(c_{NH3,0}/c_{NH3,t})$ versus the time (t) a linear relationship is found which slope is $\frac{k_{ov} \cdot A_m}{V}$ and from which k_{ov} is calculated**.** Points: experimental data; lines: linear fit to eq. 1.

As expected, the highest k_{ov} values corresponded to the experiments performed at higher flow rates and amongst them, experiment 180-500-B (i.e., co-current configuration configuration) with a k_{ov} of 3.51±0.10 $\cdot 10^{-3}$ m h^{-1} was the highest. As the flow rates increased, the thickness of the respective boundary layers decreased and their mass transfer resistances became lower, resulting in an overall improvement of the k_{ov} (Moradihamedani, 2021). On the other hand, experiment 100-250, whose initial ammonia feed concentration was higher (i.e., 10 g l^{-1}) and having showed higher ammonia fluxes than the rest of the experiments, did not exhibited a comparatively higher k_{ov} value, in fact it was among the lowest (i.e., 2.26 ± 0.03$\cdot 10^{-3}$ m h^{-1}). This is in principle, consistent with other authors results (Lauterböck et al., 2012; Uzkurt Kaljunen et al., 2021), who reported decreasing k_{ov} values with higher initial ammonia feed concentrations. Conversely, other studies (Tan et al., 2006) support the opposite hypothesis and conclude that the k_{ov} is in fact independent of the initial concentration. In any case, it must be pointed out that the feed and acid flow rates combination in experiment 100-250 was in the lower range.

When compared to other values reported in literature, these k_{ov} values are higher to those reported by Uzkurt Kaljunen et al. 2021 who used a PTFE module of 10 mm diameter membrane fibres (i.e., 0.612$\cdot 10^{-3}$ and 0.36$\cdot 10^{-3}$ m h^{-1} working with 0.75 and 3 g L^{-1} NH_3) (Uzkurt Kaljunen et al., 2021) but very similar to those reported by (Reig et al., 2021) (i.e., 2.05 - 3.96 $\cdot 10^{-3}$ m h^{-1}) and (Vecino et al., 2019) (i.e., 2.3 - 3.1 $\cdot 10^{-3}$ m h^{-1}) working with a 1.4 m^2 PP Liqui-Cel® Membrane Contactor X-50 and ammonia feed streams in the range of 4-4.5 g NH_3 L^{-1}. Sheikh et al. 2022, using the same membrane module as in the present study and 5 g NH_3 L^{-1} in the feed, reported k_{ov} values between 1.8$\cdot 10^{-4}$ and 1.04$\cdot 10^{-3}$ m h^{-1} (i.e., below the lowest k_{ov} obtained here). Nevertheless, they worked at much lower flow rates (i.e., 27 L h^{-1}) and noted a significant reduction in the k_{ov} values when the feed/acid volume ratio was reduced from 60 to 10 (Sheikh et al., 2022).

Compared to other novel polymer chemistries, such as Nafion, which is claimed to be an ammonia selective membrane with high flux (Tricoli & Cussler, 1995), Yu et al. 2021, have recently evaluated the effect of different operational parameters in the k_{ov} of a new Nafion-PFTE HF membrane. By maintaining a constant flow velocity of 0.037 m s^{-1} (the maximum flow velocity in the present study was 1.21 m s^{-1}) and an initial concentration

of 0.1 g NH_3 L^{-1} at a pH 12, the authors reported k_{ov} values of $1.2 \cdot 10^{-2}$ m h^{-1}, one order of magnitude higher that the ones obtained in this study (Yu et al., 2021). However, Yu et al. operated the HF system quite differently since the feed was circulated through the lumen side and the fibre bundle was simply immersed in a stirred beaker with the receiving solution.

As discussed earlier in the introduction section, HFMC have been already tested at pilot scale. At pilot or even industrial scale the ideal operation is not batch but continuous flow or open-loop configuration. In this direction, Licon et al. 2015, evaluated the removal of ammonia traces from water used for hydrogen production by electrolysis, operating at a feed flow rate between 10 and 82 L h^{-1} in open loop configuration. The authors obtained an ammonia removal rate of 78% for a single step process and from an initial concentration of 15 mg NH_3 L^{-1} but reported a k_{ov} value of 1.47 m h^{-1}. In the end, they calculated that a total of three modules in series were needed to reach a 95% removal (Licon et al., 2015).

Regarding the U_{NH_3} values, they followed the same trend as the k_{ov} but they differ by an order of magnitude. As mentioned before, it is generally accepted that the k_{ov} represents the overall mass transfer coefficient, however, as pointed out by Wang L. K. et al. 1993, the k_{ov} can be used as the overall mass transfer coefficient only if no mass transfer resistance across the membrane and the stripping side exists (Wang & Cussler, 1993), which is not the case in LL applications. In fact, when comparing the different transport resistances calculated via the mathematical model (i.e., $k_{NH3,f}$, $k_{NH3,m}$ and $k_{NH3,a}$ in Table 5) the system seems to be dominated primarily by the $k_{NH3,m}$ (i.e., membrane resistance regime) which is in agreement with the semi volatile nature of the ammonia (i.e., Henry constant between 10^{-4} and $3 \cdot 10^{3}$ Pa L mol^{-1}) (S. Lee & Straub, 2022) and secondly by the $k_{NH3,a}$ which is often considered as a minor limiting factor in MC literature.

The fact that this particular MC has been design for gas-liquid (GL) applications where the gas flows in the lumen side (i.e., acid side in our application) and where negligible resistances on this side and across the membrane are often found (Wang & Cussler, 1993), points out the need for further lumen side flow conditions optimization (i.e., flowrates, fiber/module geometry) if used in LL configuration. Regarding the different $k_{NH_3,m}$ values obtained via modelling (Table 5), just like the P_{NH_3} values, these should be

independent of the flow conditions (i.e., constant for all the experiments) and yet the mathematical model calculated different values. A possible explanation for these results has been already provided in section 4.3.

Finally, the maximum J_{NH3} (at time = 0h in graphs 4a and 6b) versus the calculated k_{ov} and U_{NH_3}values (Table 5) has been plotted in Figure 7. As previously mentioned, the maximum ammonia flux does depend on the initial concentration, for this reason, the maximum J_{NH3} has been normalized by the initial ammonia concentration.

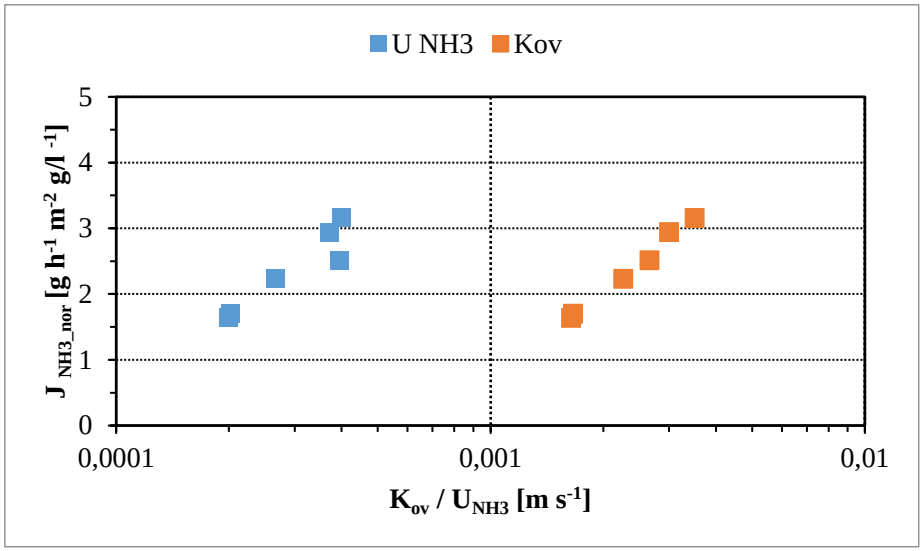

Figure 12. Maximum J_{NH3} (at time = 0h in graphs 12A and 12B) and normalized by the initial ammonia feed concentration in g L^{-1} versus k_{ov} and U_{NH3} calculated for all the experiments.

Figure 12 shows a steady increase of the J_{NH3} with increasing k_{ov} or U_{NH3}. Thus, it suggests that even further improvements can be made to enhance the module's performance in terms of ammonia flux. In view of the mass transfers coefficients calculated in Table 5 further operational improvements should be focussed on the acid/stripping side.

5.5. Conclusions

In this study PMP LL-HF asymmetric MC membrane has been tested and proved as a promising technology for the selective recovery and concentration of ammonia from rather diluted waste streams.

All experiments performed in this study reached recovery values above 90% after 15h. The results showed that increasing the flowrate (experiments 500-180; 180-500-A and 180-500-B) decreased the recovery time, while the initial concentration had a minimal influence (experiment 100-250). Likewise, the CF values obtained (i.e., 2.1-2.2) were also independent from the flow rate combinations and rather determined by the feed/stripping volume ratio (i.e. 2.14). Regarding which species were formed on the acid side, the mean value of the measured NH_4^+/ SO_4^{-2} molar ratio was 1.7:1 in most experiments, agreeing with the acid dissociating analysis of the Hydra/Medusa speciation software and confirming that the operating acid pH determined the ammonium salts fractions.

It was observed that for this module, low flowrate values (i.e., <100 L h^{-1}) on either side reduced greatly the ammonia mass transfer rate due to a combination of a greater boundary layer effect and a poorer flow distribution. Highest ammonia flux was that of experiment 100-250 due to the higher initial ammonia concentration. But also, and according to the model, the higher ammonia initial concentration and the consequent final dissolved species in the permeate side led to the highest water flux (i.e., 18.6 g H_2O h^{-1} m^{-2}) attributed to a larger OD effect.

The mathematical model was used for determining and comparing the NH_3 and H_2O membrane permeabilities of the module. It was confirmed that the membrane used in this study was highly selective towards ammonia with a P_{NH3} between 86.9 and 180.2 L h^{-1} m^{-2} bar^{-1} and an average P_w of 1.29 ± 0.105 ·10^{-3} L h^{-1} m^{-2} bar^{-1}. Additionally, the similar ammonia flux and P_{NH3} values of experiments 500-180, 180-500-A and 180-500B, supported the idea that a polarization effect due to the asymmetry of the polymeric membrane is not necessarily happening under these working conditions or is negligibly small.

The highest k_{ov} value experimentally obtained was 3.51±0.10·10^{-3} m h^{-1} (experiment 180-500-B) which was in the upper range of the HF-LLMC literature. However, it was proven that the k_{ov} might not be the most appropriate parameter to compare different MC modules operating in LL mode and particularly inadequate in capturing the influence of the acid side parameters. Finally, a deeper analysis of the mass transfer resistances on each of the channels showed further potential improvement on the acid side hydrodynamics.

5.6. References

Aguilar-Moreno, M., Vinardell, S., Reig, M., Vecino, X., Valderrama, C., & Cortina, J. L. (2022). Impact of Sidestream Pre-Treatment on Ammonia Recovery by Membrane Contactors: Experimental and Economic Evaluation. *Membranes*, *12*(12). https://doi.org/10.3390/membranes12121251

Ahn, Y. T., Hwang, Y. H., & Shin, H. S. (2011). Application of PTFE membrane for ammonia removal in a membrane contactor. *Water Science and Technology*, *63*(12), 2944–2948. https://doi.org/10.2166/wst.2011.141

Alkhudhiri, A., Darwish, N., & Hilal, N. (2012). Membrane distillation: A comprehensive review. *Desalination*, *287*, 2–18. https://doi.org/10.1016/j.desal.2011.08.027

Amaral, M. C., Magalhães, N. C., Moravia, W. G., & Ferreira, C. D. (2016). Ammonia recovery from landfill leachate using hydrophobic membrane contactors. *Water Science and Technology*, *74*(9), 2177–2184. https://doi.org/10.2166/wst.2016.375

Bazhenov, S. D., Bildyukevich, A. V., & Volkov, A. V. (2018). Gas-liquid hollow fiber membrane contactors for different applications. *Fibers*, *6*(4). https://doi.org/10.3390/fib6040076

Beckinghausen, A., Odlare, M., Thorin, E., & Schwede, S. (2020). From removal to recovery: An evaluation of nitrogen recovery techniques from wastewater. *Applied Energy*, *263*(February), 114616. https://doi.org/10.1016/j.apenergy.2020.114616

Chabanon, E., Roizard, D., & Favre, E. (2013). Modeling strategies of membrane contactors for post-combustion carbon capture: A critical comparative study. *Chemical Engineering Science*, *87*, 393–407. https://doi.org/10.1016/j.ces.2012.09.011

Chagas, G. O., Coelho, L. C., Darvish, M., & Renaud, J. (2023). Modeling and solving the waste valorization production and distribution scheduling problem. *European Journal of Operational Research*, *306*(1), 400–417. https://doi.org/10.1016/j.ejor.2022.06.036

Darestani, M., Haigh, V., Couperthwaite, S. J., Millar, G. J., & Nghiem, L. D. (2017). Hollow fibre membrane contactors for ammonia recovery: Current status and future developments. *Journal of Environmental Chemical Engineering*, *5*(2), 1349–1359.

https://doi.org/10.1016/j.jece.2017.02.016

Deng, Z., van Linden, N., Guillen, E., Spanjers, H., & van Lier, J. B. (2021). Recovery and applications of ammoniacal nitrogen from nitrogen-loaded residual streams: A review. *Journal of Environmental Management*, *295*, 113096. https://doi.org/10.1016/j.jenvman.2021.113096

DIC Corporation. (2016). *Instruction Manual for SEPAREL PF Modules*. 1–22.

DiC, S. (n.d.). *Dic_Separel.Pdf*.

Eskicioglu, C., Galvagno, G., & Cimon, C. (2018a). Approaches and processes for ammonia removal from side-streams of municipal effluent treatment plants. *Bioresource Technology*, *268*(May), 797–810. https://doi.org/10.1016/j.biortech.2018.07.020

Eskicioglu, C., Galvagno, G., & Cimon, C. (2018b). Approaches and processes for ammonia removal from side-streams of municipal effluent treatment plants. *Bioresource Technology*, *268*(May), 797–810. https://doi.org/10.1016/j.biortech.2018.07.020

Gabelman, A., & Hwang, S. T. (1999). Hollow fiber membrane contactors. *Journal of Membrane Science*, *159*(1–2), 61–106. https://doi.org/10.1016/S0376-7388(99)00040-X

García-González, M. C., Vanotti, M. B., & Szogi, A. A. (2015). Recovery of ammonia from swine manure using gas-permeable membranes: Effect of aeration. *Journal of Environmental Management*, *152*, 19–26. https://doi.org/10.1016/j.jenvman.2015.01.013

González Montiel, J. M. (2008). Acetato de etilo en la Industria. *Journal of Chemical Information and Modeling*, *53*(9), 287.

Hasanoğlu, A., Romero, J., Pérez, B., & Plaza, A. (2010). Ammonia removal from wastewater streams through membrane contactors: Experimental and theoretical analysis of operation parameters and configuration. *Chemical Engineering Journal*, *160*(2), 530–537. https://doi.org/10.1016/j.cej.2010.03.064

Hermassi, M., Valderrama, C., Gibert, O., Moreno, N., Querol, X., Batis, N. H., & Cortina, J. L. (2017). Recovery of nutrients (N-P-K) from potassium-rich sludge

anaerobic digestion side-streams by integration of a hybrid sorption-membrane ultrafiltration process: Use of powder reactive sorbents as nutrient carriers. *Science of the Total Environment*, *599–600*, 422–430. https://doi.org/10.1016/j.scitotenv.2017.04.140

Ignatenko, V. Y., Anokhina, T. S., Ilyin, S. O., Kostyuk, A. V., Bakhtin, D. S., Antonov, S. V., & Volkov, A. V. (2020). Fabrication of microfiltration membranes from polyisobutylene/polymethylpentene blends. *Polymer International*, *69*(2), 165–172. https://doi.org/10.1002/pi.5932

Jang, D., Tran, T. N., Ko, K., Park, D., Park, S., & Kang, S. (2022). Parametric studies during the removal of ammonia by membrane contactor with various stripping solutions. *Chemosphere*, *309*(P1), 136648. https://doi.org/10.1016/j.chemosphere.2022.136648

Kurniawan, T. A., Lo, W. H., & Chan, G. Y. S. (2006). Physico-chemical treatments for removal of recalcitrant contaminants from landfill leachate. *Journal of Hazardous Materials*, *129*(1–3), 80–100. https://doi.org/10.1016/j.jhazmat.2005.08.010

Laguntsov, N. I., & Karaseva, M. D. (2019). Pressure effect at permeability and deformation of the hollow fiber membrane gas separation module. *Journal of Physics: Conference Series*, *1189*(1). https://doi.org/10.1088/1742-6596/1189/1/012028

Lauterböck, B., Ortner, M., Haider, R., & Fuchs, W. (2012). Counteracting ammonia inhibition in anaerobic digestion by removal with a hollow fiber membrane contactor. *Water Research*, *46*(15), 4861–4869. https://doi.org/10.1016/j.watres.2012.05.022

Lawson, K. W., & Lloyd, D. R. (1997). Membrane distillation. *Journal of Membrane Science*, *124*(1), 1–25. https://doi.org/10.1016/S0376-7388(96)00236-0

Ledezma, P., Kuntke, P., Buisman, C. J. N., Keller, J., & Freguia, S. (2015). Source-separated urine opens golden opportunities for microbial electrochemical technologies. *Trends in Biotechnology*, *33*(4), 214–220. https://doi.org/10.1016/j.tibtech.2015.01.007

Lee, S., & Straub, A. P. (2022). Analysis of Volatile and Semivolatile Organic Compound

Transport in Membrane Distillation Modules. *ACS ES and T Engineering*, *2*(7), 1188–1199. https://doi.org/10.1021/acsestengg.1c00432

Lee, W., An, S., & Choi, Y. (2021). Ammonia harvesting via membrane gas extraction at moderately alkaline pH: A step toward net-profitable nitrogen recovery from domestic wastewater. *Chemical Engineering Journal*, *405*(May 2020), 126662. https://doi.org/10.1016/j.cej.2020.126662

Licon Bernal, E. E., Maya, C., Valderrama, C., & Cortina, J. L. (2016). Valorization of ammonia concentrates from treated urban wastewater using liquid-liquid membrane contactors. *Chemical Engineering Journal*, *302*, 641–649. https://doi.org/10.1016/j.cej.2016.05.094

Licon, E., Reig, M., Villanova, P., Valderrama, C., Gibert, O., & Cortina, J. L. (2015). Ammonium removal by liquid–liquid membrane contactors in water purification process for hydrogen production. *Desalination and Water Treatment*, *56*(13), 3607–3616. https://doi.org/10.1080/19443994.2014.974216

Markova, S. Y., Gries, T., & Teplyakov, V. V. (2020). Poly(4-methyl-1-pentene) as a semicrystalline polymeric matrix for gas separating membranes. *Journal of Membrane Science*, *598*(December 2019). https://doi.org/10.1016/j.memsci.2019.117754

Matassa, S., Batstone, D. J., Hülsen, T., Schnoor, J., & Verstraete, W. (2015). Can direct conversion of used nitrogen to new feed and protein help feed the world? *Environmental Science and Technology*, *49*(9), 5247–5254. https://doi.org/10.1021/es505432w

Mayor, Á., Beltran, E., Cortina, J. L., & Valderrama, C. (2023). Nitrogen flow analysis in Spain: Perspectives to increase sustainability. *Science of the Total Environment*, *858*(March 2022), 10–14. https://doi.org/10.1016/j.scitotenv.2022.160117

Moradihamedani, P. (2021). Recent developments in membrane technology for the elimination of ammonia from wastewater: A review. *Polymer Bulletin*, *78*(9), 5399–5425. https://doi.org/10.1007/s00289-020-03386-y

Noda, I., Brown-West, D. G., & Gryte, C. C. (1979). Effect of flow maldistribution on hollow fiber dialysis - experimental studies. *Journal of Membrane Science*, *5*(C),

209–225. https://doi.org/10.1016/S0376-7388(00)80449-4

Noriega-Hevia, G., Serralta, J., Seco, A., & Ferrer, J. (2021). Economic analysis of the scale-up and implantation of a hollow fibre membrane contactor plant for nitrogen recovery in a full-scale wastewater treatment plant. *Separation and Purification Technology*, *275*(June), 119128. https://doi.org/10.1016/j.seppur.2021.119128

Nowak, O. (2003). Benchmarks for the energy demand of nutrient removal plants. *Water Science and Technology*, *47*(12), 125–132. https://doi.org/10.2166/wst.2003.0637

Ono, Y. (1987). *United States Patent (19). 19*.

Pabby, A. K., & Sastre, A. M. (2013). State-of-the-art review on hollow fibre contactor technology and membrane-based extraction processes. *Journal of Membrane Science*, *430*, 263–303. https://doi.org/10.1016/j.memsci.2012.11.060

Pauzan, M. A. B., Hubadillah, S. K., Mohamad Kamal, S. N. E. A., Othman, M. H. D., Puteh, M. H., Kurniawan, T. A., Abu Bakar, S., Abdullah, H., Jamalludin, M. R., Naim, R., & Sheikh Abdul Kadir, S. H. (2021). Novel ceramic hollow fibre membranes contactor derived from kaolin and zirconia for ammonia removal and recovery from synthetic ammonia. *Journal of Membrane Science*, *638*(April), 119707. https://doi.org/10.1016/j.memsci.2021.119707

PotashCorp. (2014). Overview of PotashCorp and Its Industry. *Overview of PotashCorp and Its Industry*.

Razon, L. F. (2018). Reactive nitrogen: A perspective on its global impact and prospects for its sustainable production. *Sustainable Production and Consumption*, *15*, 35–48. https://doi.org/10.1016/j.spc.2018.04.003

Reig, M., Vecino, X., Gibert, O., Valderrama, C., & Cortina, J. L. (2021). Study of the operational parameters in the hollow fibre liquid-liquid membrane contactors process for ammonia valorisation as liquid fertiliser. *Separation and Purification Technology*, *255*(July 2020), 117768. https://doi.org/10.1016/j.seppur.2020.117768

Richter, L., Wichern, M., Grömping, M., Robecke, U., & Haberkamp, J. (2020). Ammonium recovery from process water of digested sludge dewatering by membrane contactors. *Water Practice and Technology*, *15*(1), 84–91. https://doi.org/10.2166/wpt.2020.002

Rongwong, W., Bae, T. H., & Jiraratananon, R. (2022). Economic optimization of hollow fiber membrane contactors for ammonia nitrogen recovery from anaerobic digestion effluents. *Journal of Environmental Chemical Engineering*, *10*(6), 108631. https://doi.org/10.1016/j.jece.2022.108631

Rongwong, W., & Goh, K. (2020). Resource recovery from industrial wastewaters by hydrophobic membrane contactors: A review. *Journal of Environmental Chemical Engineering*, *8*(5), 104242. https://doi.org/10.1016/j.jece.2020.104242

Sancho, I., Licon, E., Valderrama, C., de Arespacochaga, N., López-Palau, S., & Cortina, J. L. (2017). Recovery of ammonia from domestic wastewater effluents as liquid fertilizers by integration of natural zeolites and hollow fibre membrane contactors. *Science of the Total Environment*, *584–585*, 244–251. https://doi.org/10.1016/j.scitotenv.2017.01.123

Sheikh, M., Lopez, J., Reig, M., Vecino, X., Rezakazemi, M., Valderrama, C. A., & Cortina, J. L. (2023). Ammonia recovery from municipal wastewater using hybrid NaOH closed-loop membrane contactor and ion exchange system. *Chemical Engineering Journal*, *465*(December 2022), 142859. https://doi.org/10.1016/j.cej.2023.142859

Sheikh, M., Reig, M., Vecino, X., Lopez, J., Rezakazemi, M., Valderrama, C. A., & Cortina, J. L. (2022). Liquid–Liquid membrane contactors incorporating surface skin asymmetric hollow fibres of poly(4-methyl-1-pentene) for ammonium recovery as liquid fertilisers. *Separation and Purification Technology*, *283*, 120212. https://doi.org/10.1016/j.seppur.2021.120212

Shi, M., Zeng, X., Xiao, M., He, Q., & Yan, S. (2022). Ammonia recovery from anaerobic digestion effluent by aeration-assisted membrane contactor. *Chemical Engineering Research and Design*, *188*, 954–963. https://doi.org/10.1016/j.cherd.2022.10.036

Summers, E. K., Arafat, H. A., & Lienhard V, J. H. (2012). Energy efficiency comparison of single-stage membrane distillation (MD) desalination cycles in different configurations. *Desalination*, *290*, 54–66. https://doi.org/10.1016/j.desal.2012.01.004

Tan, X., Tan, S. P., Teo, W. K., & Li, K. (2006). Polyvinylidene fluoride (PVDF) hollow fibre membranes for ammonia removal from water. *Journal of Membrane Science*,

271(1–2), 59–68. https://doi.org/10.1016/j.memsci.2005.06.057

Technologist, S., Bridgeman, O. C., Aldrich, E. W., & Vapor, A. N. (1968). *N A S A Trainee . Momenclature , Journal of Heat Transfer Copyright © 1968 by ASME Transactions of the ASME*.

Tricoli, V., & Cussler, E. L. (1995). Ammonia selective hollow fibers. *Journal of Membrane Science*, *104*(1–2), 19–26. https://doi.org/10.1016/0376-7388(94)00208-G

Trypuć, M., & Białowicz, K. (2011). CaCO3 production using liquid waste from Solvay method. *Journal of Cleaner Production*, *19*(6–7), 751–756. https://doi.org/10.1016/j.jclepro.2010.11.009

Twarowska-Schmidt, K., & Wlochowicz, A. (1997). Melt-spun asymmetric poly(4-methyl-1-pentene) hollow fibre membranes. *Journal of Membrane Science*, *137*(1–2), 55–61. https://doi.org/10.1016/S0376-7388(97)00180-4

Uzkurt Kaljunen, J., Al-Juboori, R. A., Mikola, A., Righetto, I., & Konola, I. (2021). Newly developed membrane contactor-based N and P recovery process: Pilot-scale field experiments and cost analysis. *Journal of Cleaner Production*, *281*, 125288. https://doi.org/10.1016/j.jclepro.2020.125288

Vecino, X., Reig, M., Bhushan, B., Gibert, O., Valderrama, C., & Cortina, J. L. (2019). Liquid fertilizer production by ammonia recovery from treated ammonia-rich regenerated streams using liquid-liquid membrane contactors. *Chemical Engineering Journal*, *360*(December 2018), 890–899. https://doi.org/10.1016/j.cej.2018.12.004

Vineyard, D., Hicks, A., Karthikeyan, K. G., & Barak, P. (2020). Economic analysis of electrodialysis, denitrification, and anammox for nitrogen removal in municipal wastewater treatment. *Journal of Cleaner Production*, *262*, 121145. https://doi.org/10.1016/j.jclepro.2020.121145

Wan, C., Ding, S., Zhang, C., Tan, X., Zou, W., Liu, X., & Yang, X. (2017). Simultaneous recovery of nitrogen and phosphorus from sludge fermentation liquid by zeolite adsorption: Mechanism and application. *Separation and Purification Technology*, *180*, 1–12. https://doi.org/10.1016/j.seppur.2017.02.031

Wang, K. L., & Cussler, E. L. (1993). Baffled membrane modules made with hollow fiber fabric. *Journal of Membrane Science*, *85*(3), 265–278. https://doi.org/10.1016/0376-7388(93)85280-A

Xie, M., Shon, H. K., Gray, S. R., & Elimelech, M. (2016). Membrane-based processes for wastewater nutrient recovery: Technology, challenges, and future direction. *Water Research*, *89*, 210–221. https://doi.org/10.1016/j.watres.2015.11.045

Yang, X., Wang, R., Fane, A. G., Tang, C. Y., & Wenten, I. G. (2013). Membrane module design and dynamic shear-induced techniques to enhance liquid separation by hollow fiber modules: A review. *Desalination and Water Treatment*, *51*(16–18), 3604–3627. https://doi.org/10.1080/19443994.2012.751146

Yang, Z., Peng, H., Wang, W., & Liu, T. (2010). Crystallization behavior of poly(ε-caprolactone)/layered double hydroxide nanocomposites. *Journal of Applied Polymer Science*, *116*(5), 2658–2667. https://doi.org/10.1002/app

Yu, S., Qin, Y., Zhao, Q., Li, M., Yu, H., Kang, G., & Cao, Y. (2021). Nafion-PTFE hollow fiber composite membranes for ammonia removal and recovery using an aqueous-organic membrane contactor. *Separation and Purification Technology*, *271*(April), 118856. https://doi.org/10.1016/j.seppur.2021.118856

Zhang, T. Q., Jia, Z. Q., Peng, W., Li, S., & Wen, J. (2022). Preparation of 4-methyl-1-pentene membranes via non-solvent induced phase separation (NIPS). *European Polymer Journal*, *178*(August), 111480. https://doi.org/10.1016/j.eurpolymj.2022.111480

Zheng, J., Xu, Y., & Xu, Z. (2003). Flow distribution in a randomly packed hollow fiber membrane module. *Journal of Membrane Science*, *211*(2), 263–269. https://doi.org/10.1016/S0376-7388(02)00426-X

CHAPTER 6

Conclusions

In the context of the present research, three rigorous studies have been conducted to evaluate various strategies for the selective recovery of nitrogen and ammonia from different streams and effluents. The results obtained across the presented studies provide a exhaustive and detailed insight into the inherent capabilities and limitations associated with the technologies considered in the study. Additionally, key operational conditions influencing the performance of these strategies were thoroughly analyzed.

This study not only addresses the effectiveness of the technologies considered but also delves into understanding the operational factors impacting their performance. The findings not only contribute valuable insights to current knowledge in the field but also provide a solid foundation for the design and implementation of nitrogen and ammonia recovery systems in diverse contexts and different effluents.

The initial part of the study was focused on nitrogen recovery from the sidestream of anaerobic digestion centrate, it was identified that the dosing of aluminum sulphate at a concentration of 30 mg of Al^{+}·L-1emerged as the most efficient coagulation strategy. This discovery underscores the importance of carefully selecting coagulant agents to maximize effectiveness in solids precipitation and unwanted compound removal. The proper choice of these agents significantly contributes to optimizing the process performance in terms of nitrogen recovery.

Additionally, it was observed that pre-treatment through aeration represented a crucial role in the overall process. This stage proved effective in reducing bicarbonate (HCO_3^-) content by up to 51%, significantly enhancing the overall process efficiency. Decreasing bicarbonate content is crucial as this compound can interfere with the effectiveness of subsequent treatment membrane stages and impact the quality of the final product.

The implementation of a membrane contactor in a later stage resulted in a successful recovery of 67% of total ammonia nitrogen (TAN), with a notable concentration factor of 3.8 in the acidic stripping solution. This membrane stage proves to be a crucial component in the overall strategy, indicating that the combination of coagulation/flocculation, aeration, and membrane processes can be economically competitive for nitrogen recovery from waste streams. This approach not only

demonstrates effectiveness in terms of performance but also highlights its potential industrial-scale applicability.

The synergy of initial coagulation/flocculation, followed by aeration and the membrane stage, has proven to be a comprehensive and efficient approach to nitrogen recovery. The membrane phase, in particular, has allowed for notable concentration levels, significantly enhancing the overall process efficiency. This result suggests not only higher nitrogen recovery performance but also the economic feasibility of this strategy, emphasizing its potential for large-scale implementation in industrial settings.

The combination of these advanced techniques offers a promising perspective for addressing challenges associated with nitrogen recovery from wastewater streams. The achieved efficiency and concentration factor underscore the technical and economic viability of this strategy, suggesting the beginning of a path toward practical industrial implementation. These results contribute not only to scientific knowledge in the field but also provide a solid foundation for the application of sustainable technologies such as membrane contactor in the treatment and utilization of anaerobic digestion centrate streams, highlighting the transformative potential of this strategy in resource management on an industrial scale.

In the second phase of the research, focusing on the operation of Liquid-Liquid Hollow Fiber Membrane Contactors (LL-HFMC) for ammonia recovery, thorough explorations of various operational conditions impacting process efficiency were conducted. A notable finding was the strategic importance of switching the acidic solution between different process steps, leading to substantial improvements exceeding 20% in ammonia removal efficiency. The observation suggests that optimizing this specific parameter can result in substantial overall system efficiency improvements. These results offer valuable insights into how strategic adjustments in operational conditions, particularly regarding the solutions used, can have a significantly positive impact on the efficiency of the ammonia recovery process. This detailed focus on solution management could be key to maximizing the effectiveness and sustainability of such processes.

Furthermore, It was observed that LL-HFMC systems demonstrated efficacy for both sidestream and mainstream applications, providing flexibility in selecting the ammonia source based on specific process objectives. LL-HFMC emerged as a versatile technique capable of addressing both low and high initial feed concentrations of ammonia in

wastewater, highlighting its potential application in various conditions and types of effluents.

In the third phase of the research, a comprehensive evaluation of the performance of an asymmetric PMP LL-HFMC membrane for ammonia recovery from industrial synthetic streams with concentrations of 5-10 $g \cdot L^{-1}$ of NH_3 was conducted. The results indicated notable selectivity toward ammonia, achieving recovery values exceeding 90% after 15 hours of operation. The independence from the initial ammonia concentration and the membrane's robustness to variations in flow highlighted its potential for practical application in varied conditions.

The membrane asymmetry did not reveal significant effects under the evaluated working conditions, conclusively supporting its effectiveness in the selective recovery of ammonia.

The use of the mathematical model not only contributed to a deeper understanding of the involved mechanisms but also provided quantitative confirmation of the membrane's outstanding selectivity toward ammonia. Overall, these findings support the suitability and reliability of the asymmetric PMP LL-HFMC membrane in the selective recovery of ammonia, opening promising perspectives for its application in various industrial contexts.

In conclusion, this thesis has provided a comprehensive insight into nitrogen and ammonia recovery strategies, emphasizing the importance of specific operational conditions in the performance of evaluated technologies. The combination of coagulation/flocculation, aeration, and membrane contactor has shown promise for nitrogen recovery, while LL-HFMC and asymmetric PMP LL-HFMC membrane have proven effective in the selective recovery of ammonia from a variety of streams and conditions.

Future directions and prospects

It is crucial to recognize that significant challenges persist on the path towards sustainable and scalable nutrient recovery in wastewater treatment plants. Several factors stand out as obstacles to achieving this goal. Firstly, the diversity in the composition and characteristics of wastewater complicates the implementation of a standardized approach.

It is necessary to have a methodology for characterizing these streams and the available technologies. Depending on the nature of the stream, pre-treatment may be required before passing through membrane contactors. The current lack of standardization makes it difficult to compare studies, thus limiting research capacity.

Secondly, membrane fouling remains a significant obstacle to its large-scale application. In most cases, fouling interrupts continuous operation, requiring frequent cleaning stages. Although these cleanings can be carried out with varying degrees of effectiveness, they remain a significant inconvenience for large-scale implementation.

Thirdly, the selectivity of current membranes continues to be a challenge. Despite advances in the development of new polymeric materials, selectivity remains problematic. While nutrient recovery such as nitrogen can be achieved with high yields, selectivity often does not allow for obtaining a sufficiently concentrated stream, limiting the production of pure products such as fertilizers.

In summary, these challenges, in my opinion, represent the major obstacles to the future of membrane contactors in nutrient recovery, such as nitrogen, in wastewater treatment.